eman ta zabal zazu

Universidad del País Vasco

Euskal Herriko Unibertsitatea

# Studying the role of E2F1 and E2F2 in the metabolism of nucleotides: therapeutic implications for the treatment of prostate cancer

PhD Thesis

Mohaddase Hamidi

*2022*

Supervisors

Ana María Zubiaga Elordieta

Ainhoa Iglesias Ara

This work was funded by a Predoctoral Fellowship from AECC (Asociación Española Contra el Cáncer) and by an aid from the Vice-rectorate for Innovation, Social Commitment and Cultural Action of the UPV/EHU to Mohaddase Hamidi, and by Research Grants awarded by the Spanish Ministry of Science and Innovation (SAF2015-67562-R, RTI2018-097497-B-I00, RED2018-102723-T) and by the Basque Government, Department of Industry (KK-2017/00084) and Department of Education, University and Research (IT634-13, IT1257-19).

## Acknowledgements

A doctoral thesis is never the work of a single person therefore; I would like to thank all the people who have helped me during the preparation of this work.

Firstly, I would like to express my sincere gratitude to my advisor Prof. Ana Zubiaga for the continuous support of my Ph.D study and related research, for her patience, motivation, and immense knowledge. Her guidance helped me in all the time of research and writing of this thesis. I could not have imagined having a better advisor and mentor for my Ph.D study.

I would like to thank to my co supervisor, Dr. Ainhoa Iglesias, for your patience, guidance, and support. I have benefited greatly from your wealth of knowledge and meticulous editing. I am extremely grateful that you took me on as a student and continued to have faith in me over the years.

I would like to express my gratitude to Dr. Marta Macho. Your kind generosity meant a lot to me, because it enabled me to initiate the first steps in my doctoral training.

I am fortunate to have been a part of the AZ group. I would like to thank Dr. Asier Fullaondo for his valuable suggestions and advise during our lab meetings.

Thank you to my labmates (Ireia, Jon, Aintzane, Jone, Larraitz, Endika, Gartze, Bea, Alejandro, Ainhoa, Ekaitz) for their pleasant working atmosphere, friendship, encouraging and motivating guidance and support.

Last but not the least, Thank you to my parents, for your unconditional, unequivocal, and loving support. You have always stood behind me, and this was no exception. Mom, thank you for fielding a ridiculous number of phone calls, for calming me down, and for proofreading anytime, anywhere. Dad, thank you for all of your love and for always reminding me of the end goal. My accomplishments and success are because they believed in me. Deepest thanks to my siblings, for always being there for me, and are always supportive of my adventure.

# Resumen

El cáncer comprende un grupo de enfermedades en las que las células proliferan de forma continua y excesiva. La proliferación celular está estrictamente regulada por múltiples mecanismos de control del ciclo celular que aseguran la producción de dos células hijas genéticamente idénticas, y los factores de transcripción E2F (E2F1-8) son reguladores clave en este proceso. Así, la activación de la red transcripcional dependiente de E2F está estrechamente relacionada con la entrada y progresión en la fase S, dado que estos factores controlan la expresión de una multitud de genes que codifican proteínas clave involucradas en la replicación del ADN y biosíntesis de nucleótidos, así como en la progresión del ciclo celular (Dyson, 1998). La actividad de E2F durante la fase S también asegura que las células no entren prematuramente en la mitosis al restringir la activación de la CDK mitótica. De acuerdo con el modelo clásico de regulación del ciclo celular, durante la fase G1 temprana, la proteína Retinoblastoma (RB) se une a E2F y mantiene inactiva la transcripción dependiente de E2F. La fosforilación de RB en G1, mediada por los complejos ciclina/CDK, conduce a su inactivación y la consiguiente inducción de la transcripción dependiente de E2F (Nevins, 2001). Mi trabajo de tesis doctoral se ha centrado en el estudio del mecanismo de acción en células normales y tumorales de dos miembros de la familia, E2F1 y E2F2.

Los estudios de nuestro grupo y otros han demostrado que E2F1 y E2F2 pueden jugar un papel tanto oncogénico como oncosupresor, dependiendo del contexto celular. La inactivación de estos dos factores por recombinación homóloga en ratones conduce a una replicación inapropiada de ADN asociada a la sobreexpresión de genes diana E2F implicados en la síntesis de ADN. Este fenotipo aberrante promueve daño en el DNA y una apoptosis masiva dependiente de p53, lo que sugiere un papel supresor para estos factores E2F (Iglesias-Ara et al., 2010; Iglesias-Ara et al., 2015). El mecanismo subyacente al aumento del daño en el ADN tras la pérdida de E2F1 y E2F2 aún no se ha resuelto. En esta tesis doctoral se ha trabajado con la hipótesis de que el consumo de nucleósidos debido a la replicación excesiva del ADN en las células DKO podría ser responsable de la activación de la respuesta al daño del ADN, de manera similar a lo que se ha demostrado en situaciones de estrés replicativo inducido por oncogenes (Bester et al., 2011; Burrell et al., 2013; Mannava et al., 2013). En nuestro caso, dado que la transcripción de enzimas clave en la biosíntesis y el reciclaje de nucleósidos está bajo el control de factores E2F, la pérdida de E2F1/2 reduciría las reservas de nucleótidos y, por lo tanto, agravaría el estrés replicativo.

Por otra parte, la actividad incrementada de los factores E2F se ha asociado con su papel oncogénico. De hecho, la actividad aberrante de E2F se considera un sello distintivo de una gran cantidad de tumores, debido a mutaciones que ocurren

comúnmente en la vía que controla su función (pérdida de función de *RB1* o *CDKN2A*, ganancia de función de *CCND1*, entre otros) (Dimova & Dyson, 2005). Así, la expresión de E2F y/o la elevada expresión de las dianas de E2F se han relacionado con un mal pronóstico (Kent et al., 2016, 2017; Lan et al., 2018). Sin embargo, queda por resolver si los E2F son los promotores de la tumorigénesis o si la elevada expresión de E2F refleja simplemente la naturaleza altamente proliferativa de los tumores agresivos.

En el caso del cáncer de próstata, se ha descrito que el aumento de la expresión de E2F1 está asociado con el crecimiento tumoral y la supervivencia celular del cáncer de próstata (PCa) (Ren et al., 2014). Sin embargo, su mecanismo de acción en PCa no se ha dilucidado, y poco se sabe sobre el papel de E2F en la reprogramación metabólica que tiene lugar en este tipo de cáncer. Una mejor comprensión de esta vía podría ayudar a definir si E2F promueve la resistencia de las células PCa a la quimioterapia y qué dianas de E2F son mediadores clave de resistencia en este tipo de cáncer.

**Metabolismo de nucleótidos regulado por los factores E2F *in vivo* y su relevancia**

En esta tesis se ha estudiado si la respuesta al daño del ADN observada tras la inactivación de E2f1 y E2f2 (DKO) *in vivo* podría ser el resultado de alguna deficiencia de nucleótidos que provocaría estrés replicativo. Se analizó la expresión de genes diana de E2F implicados tanto en la vía *de novo* como en la vía de rescate de biosíntesis de nucleótidos. Curiosamente, los niveles de expresión de genes que codifican proteínas clave de la vía de rescate, a saber, *Tk1*, *Tk2* y *Dck*, se encontraron significativamente reprimidos en células knockout para E2f1/E2f2 en comparación con las células WT. Estos resultados sugieren que E2f1/E2f2 podrían estar controlando los pools de nucleótidos celulares a través de la vía de rescate, mediante la regulación de la expresión de *Tk1, Tk2* y *Dck*.

A continuación, nos preguntamos si el aumento en la síntesis de nucleótidos en ratones DKO podría aliviar el estrés replicativo y prevenir la apoptosis y atrofia tisular. El grupo de Fernández-Capetillo ha demostrado en un modelo de ratón mutante ATR-hipomorfo que presenta altos niveles de estrés replicativo, que un aumento en la dosis del gen *Rrm2* (subunidad regulatoria de la ribonucleótido reductasa RNR) potencia la síntesis de nucleótidos y prolonga la supervivencia de estos ratones (Lopez-Contreras et al., 2015). Para verificar esta posibilidad en nuestros ratones, introdujimos un alelo adicional de *Rrm2* (*Rrm2*$^{TG}$) en ratones *E2f1/E2f2* DKO. Sin embargo, un alelo *Rrm2* adicional en ratones DKO no rescató la baja tasa de supervivencia, la hiperglucemia y la atrofia pancreática de los ratones *E2f1/E2f2* DKO.

Una posibilidad que podría explicar la incapacidad para revertir el fenotipo aberrante en ratones *E2f1*$^{-/-}$;*E2f2*$^{-/-}$;*Rrm2*$^{TG}$ es que estos animales podrían tener una deficiencia en los precursores de ribonucleótidos, es decir, los sustratos de RNR, de modo que la producción de nucleótidos estaría bloqueada aguas arriba de RNR en nuestro modelo de ratón. Efectivamente, la administración de un cóctel de nucleósidos a ratones DKO dio lugar a una reducción sustancial en los niveles de marcadores de estrés replicativo y apoptosis (γ-H2AX, p53 y Bax) en muestras pancreáticas derivadas de ratones DKO en comparación a muestras DKO no tratadas, y mostró unos niveles similares a los de ratones WT. Por lo tanto, la suplementación de ratones DKO con el conjunto completo de productos finales de la biosíntesis de nucleótidos pudo prevenir el daño al ADN y la apoptosis. Nuestros hallazgos están en línea con los de Kerem y colaboradores, quienes han demostrado que el estrés replicativo provocado por los oncogenes, que es una consecuencia de la deficiencia de nucleótidos, puede restaurarse mediante nucleósidos suministrados exógenamente (Bester et al., 2011). En conjunto, el rescate fenotípico observado desencadenado por la adición de nucleósidos sugiere que la activación de la respuesta al daño del ADN y la atrofia tisular dependiente de p53 en ratones que carecen de E2f1 y E2f2 podrían ser el resultado de un agotamiento prematuro de nucleótidos, y muestra a E2F como un regulador crítico de las reservas de nucleósidos celulares. Además, el hecho de que la expresión de *Tk1* y *Dck* sea reducida en el páncreas DKO apunta hacia un mecanismo guiado por un eje E2F-Tk1/Dck para promover la producción de nucleótidos en el páncreas.

**Relevancia del metabolismo nucleotídico regulado por E2F1/E2F2 en cáncer de próstata**

Nuestro siguiente objetivo fue estudiar la relevancia del metabolismo de nucleótidos regulado por E2F en cáncer. Utilizando cBioportal y KM-plotter encontramos una correlación inversa entre la supervivencia libre de enfermedad y la expresión de los genes *E2F1* y *E2F2*, así como sus genes diana *TK1, DCK* y *TYMS*. Es decir, la alta expresión de estos genes se correlacionó significativamente con un peor pronóstico en varios cánceres, incluido el de próstata (PCa). La correlación negativa entre la expresión de estos genes y el grado de malignidad pudo corroborarse así mismo en líneas celulares de cáncer de próstata, a saber, LNCaP, DU145 y PC3. Además, la línea celular PCa más maligna, PC3, mostró los niveles de expresión génica diferencial más altos para la mayoría de estos genes.

Trabajos anteriores ya han indicado que la expresión elevada de E2F1 podría contribuir a la progresión del PCa (Davis et al., 2006; Libertini et al., 2006). Sin embargo, estos estudios no abordaron la relevancia de E2F en la regulación de la biosíntesis de

nucleótidos y su implicación en la malignización del cáncer de próstata. Para abordar estos estudios se analizó la expresión génica a nivel de RNA y de proteína en líneas celulares de PCa sometidas a silenciamiento individual y combinado de E2F1 y E2F2 con siRNA específicos. Estos experimentos mostraron que el silenciamiento individual de E2F1 y E2F2, y en mayor medida el silenciamiento combinado, reduce significativamente los niveles de expresión de *TK1, DCK* y *TYMS*.

Funcionalmente, el silenciamiento de E2F1 y E2F2 condujo a la acumulación de las células en la fase S y a una disminución significativa del porcentaje de células pH3+ marcadoras de mitosis. Este perfil anómalo del ciclo celular de las células PC3 tras la eliminación de E2F1/E2F2 dio lugar a un aumento de las células positivas para el marcador de daño en el ADN $\gamma$-H2AX, y una reducción de la viabilidad celular. Curiosamente, la adición de nucleósidos o simplemente los productos de las actividades enzimáticas de TK1 y DCK mejoró la viabilidad celular, lo que respalda la idea de que el mecanismo E2F/TK1-DCK es crucial para preservar la integridad del ADN en las células mPCa. Cabe destacar que el silenciamiento combinado de TK1 y DCK también resultó en daño en el ADN, aunque el porcentaje de células que mostraban daño en el ADN fue menor que en las células con silenciamiento de E2F.

Hemos encontrado asimismo que la depleción de E2F1/E2F2 conlleva una activación aberrante de la quinasa mitótica CDK1, una situación que puede dar lugar a daño en el ADN (Szmyd et al., 2019). La inhibición de la activación de CDK1 durante la fase S se logra mediante su fosforilación en Tyr15, la cual es inhibitoria. Esta fosforilación está regulada por la quinasa WEE1 y la fosfatasa CDC25A, ambas dianas transcripcionales de E2F (Akopyan et al., 2014; Deng et al., 2019; Lemmens et al., 2018; Elbæk et al., 2020). En este trabajo hemos mostrado que el silenciamiento de E2F1, y en mayor medida el silenciamiento combinado de E2F1 y E2F2 disminuyó significativamente los niveles de pCDK1. Esto sugiere que E2F1 y E2F2 promueven la fosforilación inhibidora de CDK1 con objeto de asegurar la estabilidad genómica, probablemente a través de la regulación transcripcional de WEE1 y CDC25A. Curiosamente, el silenciamiento combinado de TK1 y DCK no alteró el estado de fosforilación de CDK1, lo que implica que E2F preserva la integridad del ADN al controlar tanto la producción de nucleótidos como la actividad de CDK1.

**E2F1/E2F2 como posibles dianas terapéuticas en cáncer de próstata**

Las estrategias terapéuticas novedosas son un requisito apremiante para combatir la resistencia a los medicamentos y mejorar las tasas de respuesta a los medicamentos. Estas estrategias están actualmente centradas en el uso combinado de tratamientos que atacan las células tumorales mediante la inhibición simultánea de diferentes vías metabólicas.

Hemos demostrado que la actividad de E2F es esencial para la correcta expresión de genes implicados en la biosíntesis de nucleótidos en células mPCa, para su progresión en el ciclo celular y para su viabilidad. Esto convierte a E2F en un objetivo atractivo a considerar para el tratamiento de este tipo de cáncer. El metabolismo de nucleótidos es una diana muy empleada en el tratamiento del cáncer. De hecho, los análogos de nucleótidos, como el 5-fluorouracilo (5-FU), se utilizan hoy en día para tratar varios tipos de cáncer, incluido el cáncer de próstata (Longley et al., 2003). 5-FU induce citotoxicidad principalmente al interferir con la *vía de novo* de síntesis de nucleósidos, a través de su interacción con la enzima TS (que codifica el gen *TYMS*) (Longley et al., 2003). Sin embargo, las células de PCa desarrollan con frecuencia resistencia a 5-FU (Longley et al., 2003). El análisis de la viabilidad celular después de la titulación de 5-FU (dosis-respuesta) en líneas celulares LNCaP, DU145 y PC3 demostró que la línea celular con el mayor potencial metastásico, PC3, presentaba la mayor resistencia a la apoptosis inducida por 5-FU. Este resultado implica que la malignidad en las líneas celulares de PCa se correlaciona con la resistencia al 5-FU.

Dado que el 5-FU bloquea la vía *de novo* de síntesis de nucleótidos, planteamos la hipótesis de que las células de cáncer de próstata podrían hacer uso de la *vía de rescate* de síntesis de nucleótidos como mecanismo de resistencia. Quizá las células mPCa podrían sobreponerse a la reducción de las reservas de nucleótidos impuesta por 5-FU activando la expresión de genes diana de E2F que codifican enzimas de la vía de rescate de la síntesis de nucleósidos. En efecto, el silenciamiento de E2F revirtió la resistencia de las células mPCa al 5-FU. La depleción de E2F1/E2F2 en presencia de 5-FU condujo a una reducción de los niveles de TK1, DCK y TYMS inducidos por 5-FU y sensibilizó a las células mPCa hacia la muerte. También se ha observado la reversión de la resistencia al 5-FU tras la eliminación de la expresión de la proteína Bcl-XL por parte del ARN de interferencia pequeño específico de Bcl-XL en el cáncer de colon resistente al 5-FU, aunque el efecto fue solo moderado (Zhu et al., 2005), y más recientemente, en varias líneas de células cancerosas, incluidas las prostáticas, tras el uso de una molécula pequeña inhibitoria de E2F1, en línea con nuestros hallazgos (Rather et al., 2021).

Nuestros resultados en mPCa están de acuerdo con los publicados recientemente por el grupo de Lunt en cáncer de mama, donde muestran que los distintos subtipos histológicos exhiben diferentes vulnerabilidades metabólicas en términos de sus vías de biosíntesis de nucleótidos preferidas, y que la inhibición de la vía preferida también tiene un gran impacto en el metabolismo (Ogrodzinski et al., 2021). Fundamentalmente, también muestran que inhibir la vía no preferida no solo es menos eficaz para controlar el crecimiento tumoral, sino que puede tener el efecto contrario de aumentar el crecimiento tumoral. De manera similar, nuestros resultados subrayan la necesidad crítica de dilucidar las distintas preferencias metabólicas de diferentes tipos de cáncer para diseñar terapias dirigidas efectivas para cada uno de ellos.

Según nuestros datos sobre células de cáncer de próstata metastásico, la inhibición de E2F1/E2F2 podría ser una estrategia prometedora para prevenir por completo la biosíntesis de nucleótidos y sensibilizar a las células tumorales a la muerte celular después del tratamiento con 5-FU. Las proteínas E2F, al igual que la mayoría de los factores de transcripción, no son buenas dianas farmacológicas, y todavía no hay inhibidores de E2F en uso clínico. Consideramos que una posibilidad alternativa para inhibir la actividad de E2F sería utilizar inhibidores de CDK4/6, que han entrado en el ámbito clínico para pacientes con cáncer de mama metastásico (palbociclib), y se están probando actualmente en múltiples tipos de tumores, incluidas las células de cáncer de próstata (Comstock et al., Oncogene, 2013), en la mayoría de los casos en combinación con fármacos disponibles dirigidos a otras vías celulares (Asghar et al., 2015; Salvador-Barbero et al. al., 2020). Este tipo de fármacos inhiben la actividad de E2F al prevenir la fosforilación de RB y la posterior liberación de E2F (Roberts et al., 2020).

Curiosamente, el ensayo de formación de colonias realizado con células PC3 demostró un efecto aditivo tras la combinación de palbociclib y 5-FU en la capacidad de formación de colonias. De hecho, el tratamiento individual con 5-FU o una dosis baja de palbociclib tuvo un efecto menor en la formación de colonias, mientras que la combinación de ambos inhibidores redujo de forma potente la viabilidad de las células PC3. En línea con nuestros resultados, varios estudios preclínicos sugieren que la combinación de quimioterapia e inhibición de CDK4/6 puede tener efectos antitumorales cooperativos; observaciones similares están comenzando a surgir de estudios clínicos (Cao et al., 2019; Franco et al., 2014; Salvador-Barbero et al., 2020). Nuestros resultados subrayan el interés de realizar estudios clínicos a corto plazo con una terapia combinada de inhibidores de CDK4/6 y 5-FU en pacientes con cáncer de próstata avanzado con objeto de retrasar la resistencia o proporcionar efectos antiproliferativos sinérgicos.

# Contents

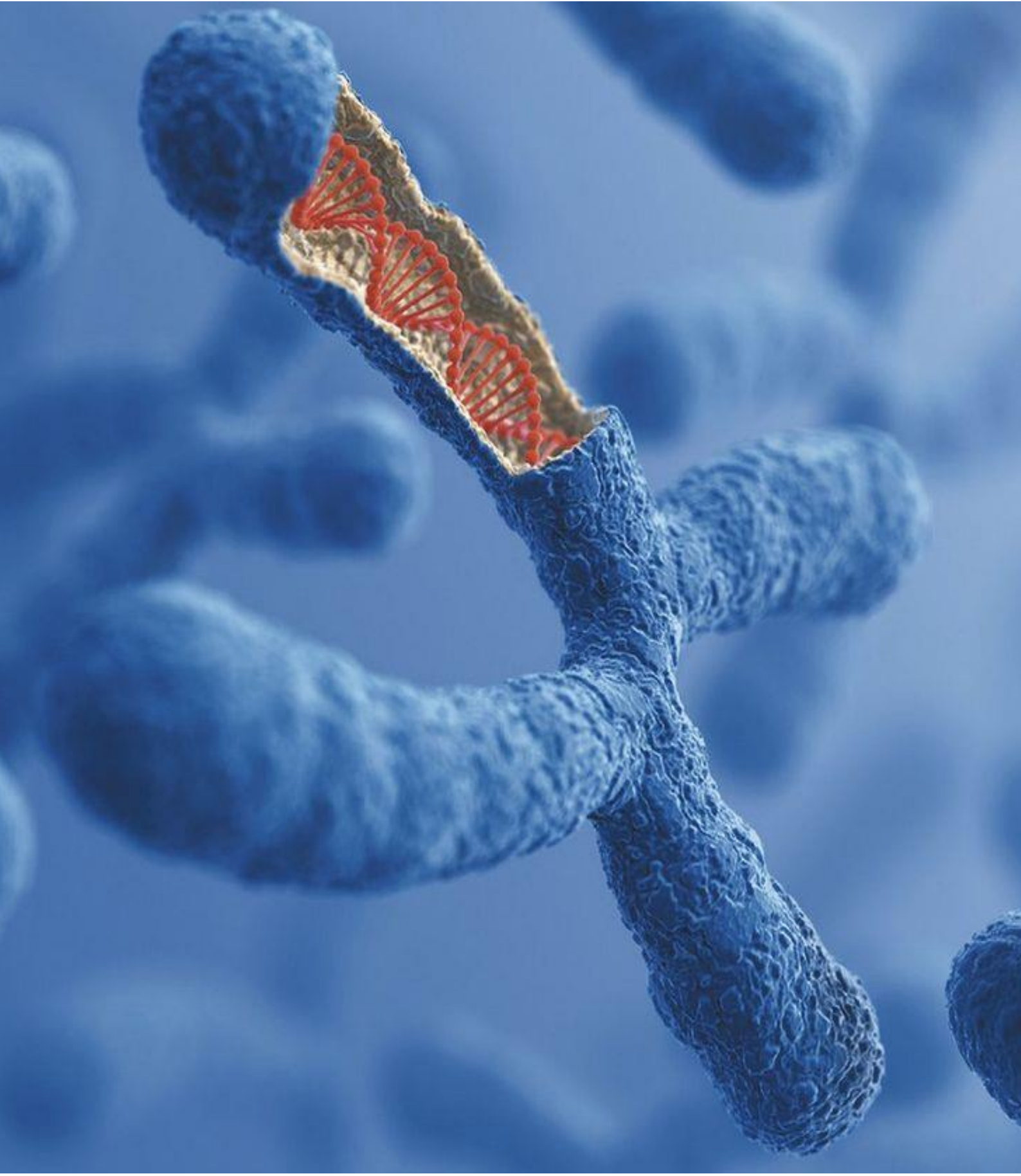

# Abbreviations

| | |
|---|---|
| ADT | Androgen deprivation therapy |
| ATM | Ataxia-Telangiectasia Mutated |
| ATR | Ataxia-Telangiectasia Related |
| BrdU | 5-bromodeoxyuridine |
| BSA | Bovine Serum Albumin |
| CDK | Cyclin Dependent Kinase |
| cDNA | Complementary DNA |
| ChIP | Chromatin immunoprecipitation |
| CHK1 | Checkpoint Kinase 1 |
| CHK2 | Checkpoint Kinase 2 |
| DBD | DNA Binding Domain |
| DCK | Deoxycytidine Kinase |
| DDR | DNA Damage Response |
| DKO mice | Double knockout (*E2f1*$^{-/-}$; *E2f2*$^{-/-}$) mice |
| DMEM | Dulbecco's Modified Eagle Medium |
| DNA | Deoxyribonucleic acid |
| dNTP | Deoxynucleotide |
| DSB | Double-Stranded Break |
| EDTA | Ethylenediaminetetraacetic acid |
| 5- FU | 5- Fluorouracil |
| FBS | Fetal Bovine Serum |
| GFP | Green Fluorescent Protein |
| HU | Hydroxyurea |
| IF | Immunofluorescence |
| mRNA | Messenger RNA |
| M phase | Mitosis phase |
| NSP | Nucleotide salvage pathway |
| NDP | Nucleotide *de novo* pathway |
| Noco | Nocodazole |
| NT | Non-target |
| PCa | Prostate cancer |
| PBS | Phosphate Buffered Saline |
| PCR | Polymerase Chain Reaction |
| PMSF | Phenylmethanesulfonyl Fluoride |
| RB | Retinoblastoma |
| ROS | Reactive Oxygen Species |

| | |
|---|---|
| RS | Replication stress |
| RT-qPCR | Reverse transcription- Quantitative PCR |
| RNA | Ribonucleic acid |
| RNR | Ribonucleotide reductase |
| S phase | Synthesis phase |
| SDS-PAGE | Sodium Dodecyl Sulfate-PolyAcrylamide Gel Electrophoresis |
| siCtrl | Small interfering RNA Control |
| siRNA | Small Interfering RNA |
| ssDNA | Single-stranded DNA |
| TAE | Tris/Acetic acid/EDTA |
| TBS-T | Tris Buffered Saline-Tween 20 |
| TCGA | The Cancer Genome Atlas |
| TK1 | Thymidine kinase 1 |
| TS | Thymidylate synthase (protein) |
| TYMS | Thymidylate synthase (gene) |
| UT | Untreated |
| UV | Ultraviolet |
| VC | Vehicle |
| WT | Wild Type |

# Summary

E2F-dependent transcriptional network ensures the timely entry of cells into S-phase through the regulation of a vast array of genes involved in DNA replication and cell cycle progression. In this Thesis, we aimed to decipher the role of E2F1 and E2F2 in the metabolism of nucleotides and the implications that E2F activity might have in tumor progression and resistance against chemotherapy.

We show that in non-tumoral cells, targeted depletion of E2f1 and E2f2 in mice leads to a downregulation of genes encoding Tk1 and Dck (rate-limiting enzymes of the salvage pathway for nucleotide production), as well as to the induction of DNA damage. Importantly, this phenotype could be rescued with an exogenous supply of nucleotides.

In tumor cells, enhanced E2F activity is thought to provide the nucleotides required for their exacerbated DNA replication. We found that E2F1/E2F2, whose expression correlates with malignancy in human prostate cancer, are necessary to maintain steady-state levels of TK1, DCK and TYMS and to prevent genomic instability during S phase. Silencing of E2F1/E2F2 in metastatic prostate cancer (mPCa) cells leads to DNA damage and compromises cellular viability, whereas addition of nucleosides, or the products of TK1 and DCK enzymatic activities improves cellular viability of E2F1/E2F2 knockdown cells, suggesting that the E2F/TK1-DCK-TYMS axis is crucial to preserve DNA integrity in mPCa cells. Furthermore, we show that mPCa cells are resistant to the apoptosis induced by the nucleoside analog 5-fluorouracil (5-FU) through the induction of TK1, DCK and TYMS expression. Remarkably, combined depletion of E2F1/E2F2 prevents 5-FU-induced upregulation of TK1, DCK and TYMS and reverses resistance of mPCa cells to 5-FU, whereas adding nucleosides or the products of TK1 and DCK activities increases the viability of E2F1/E2F2 knockdown cells treated with 5-FU. Interestingly, treatment of mPCa cells with the E2F pathway inhibitor Palbociclib in combination with 5-FU dramatically reduced their viability.

Collectively, our findings emphasize the relevance of the E2F pathway for providing nucleotide intermediates necessary to preserve DNA integrity in normal and cancer cells, and for driving resistance to 5-FU of mPCa cells. Inhibition of E2F activity could be a promising strategy to fully prevent nucleotide biosynthesis and sensitize tumor cells to cell death after treatment with 5-FU.

# Introduction

# 1. Cancer and cell cycle

Cancer comprises a group of diseases in which cells proliferate continuously and excessively. Cell proliferation is tightly regulated by multiple cell cycle control mechanisms that ensure the production of two genetically identical daughter cells. The major control in the cell cycle is primarily focused on the correct and timely replication of genomic DNA and in its subsequent segregation between daughter cells. This process is tightly regulated by several checkpoints that are established along the cell cycle. Typically, cancer cells have disrupted some checkpoints to bolster their proliferation (for example, the DNA damage checkpoint), but not all are impaired. Indeed, many cell cycle control functions are also essential for cancer cell viability. Consequently, these functions enable cancer cells to endure high levels of stress that are associated with their aberrant proliferation (Matthews et al., 2022). At the same time, this dependency on specific checkpoints raises new therapeutic opportunities for cancer treatment.

# 2. Cell cycle control

Cell division is controlled by a complex network of regulatory mechanisms that ensure a correct progression of the cell through the cell cycle. These mechanisms aim to get the timely and accurate duplication and segregation of the genetic material. DNA replication occurs in interphase during S phase (Synthesis phase), and the duplicated DNA is accurately segregated during M phase (Mitosis phase). The periods of interphase that separate S phase from M phase have historically been named ‘gap phases’, or G1 before S phase and G2 after S phase. These phases are key periods for cell cycle regulation and include the crucial decision to enter into the cell cycle (during G1), and to initiate the process that leads to chromosome segregation (during G2).

Cyclin-dependent kinase (CDK) and E2F activities are key regulators of cell cycle processes (Figure 1). Specific cyclins accumulate during different stages of the cell cycle, driven by cell cycle-regulated transcription, mostly guided by E2F, and/or by the inhibition of protein degradation (Malumbres, 2014). In turn, E2F-regulated transcription depends on CDK activity for activation, thereby ensuring a sequential and unidirectional cell cycle progression (Fisher, 2012; Kovacs et al., 2008). CDK activity during G1 phase is required for initiation of DNA replication, through the regulation of E2F activity, leading to cell cycle entry commitment. Subsequently, during G2 phase, CDK activity plays a key role in preparing for chromosome segregation, upon disintegration of the nuclear envelope and alignment of the replicated chromosomal DNA.Inactivation of CDK activity via ubiquitination-dependent destruction of cyclins, coincides with chromosome segregation and return to interphase (Fisher, 2012; Kovacs et al., 2008).

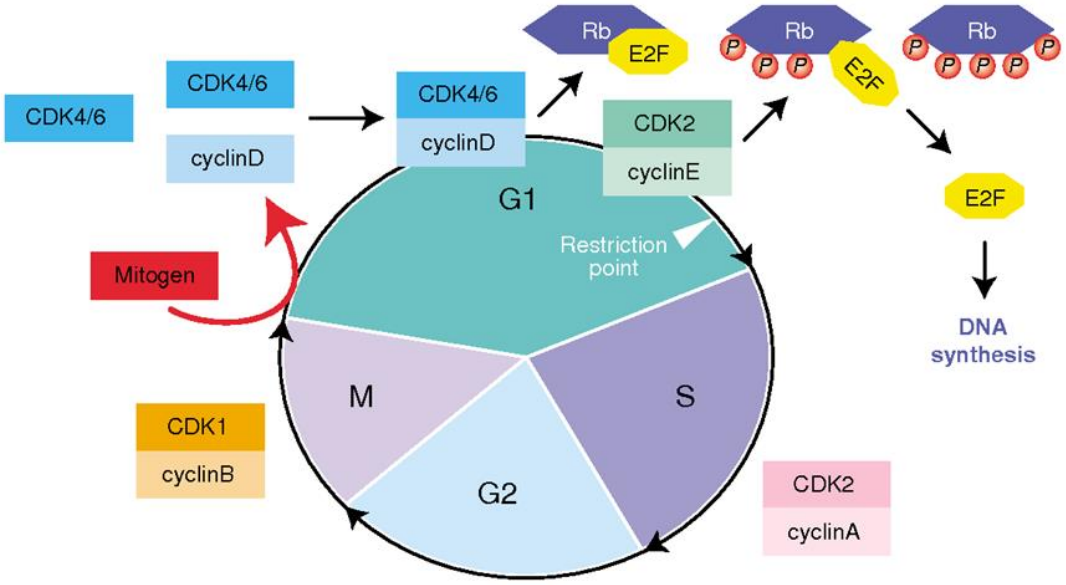


Figure 1. **Cell cycle progression by Cyclin/Cyclin-dependent kinase (CDK) complexes and RB/E2F complexes**. In the G1 phase of the cell cycle, synthesis of cyclin D is increased. This cyclin partners with CDK4/6 to promote cell cycle entry. CDK2/CyclinE complex phosphorylates RB, which liberates E2F factors to induce the expression of genes involved in DNA synthesis and G1/S transition. During S phase, CDK2 in complex with cyclin A controls the phosphorylation of targets involved in DNA replication and mitotic entry. Cyclin A is found highly expressed in this phase and until the last stages of G2. In the G2 phase, the primary regulator of the cell cycle is CDK1 (Kolch et al., 2002).

Activation of E2F-dependent transcriptional network is closely linked to DNA replication initiation and S phase entry, whereby E2F factors control the transcriptional regulation of a myriad of genes encoding key proteins involved in DNA replication and repair as well as cell cycle progression (Dyson, 1998). E2F activity during S phase also ensures that cells do not enter prematurely into mitosis by restraining the activation of the mitotic CDK. Importantly, aberrant E2F activity is considered a hallmark of a large number of tumors, owing to mutations that commonly occur in the pathway that controls E2F function (loss-of-function of *RB1* or *CDKN2A*, gain-of-function of *CCND1*, among others) (Dimova & Dyson, 2005).

## 2.1. E2F family of transcription factors in the cell cycle

It was discovered more than three decades ago that infection by DNA tumor viruses caused excessive host cell proliferation, which was associated with the binding of specific cellular factors (later named E2Fs) to viral gene promoters (Kovesdi et al., 1986). The key finding that overexpression of E2Fs could trigger quiescent cells to enter G1-phase and to transition into S-phase, independent of growth factor stimulation, linked this transcriptional module to cell cycle control (Johnson et al., 1993) and bolstered the initial identification of E2F target genes.

Subsequent studies established that E2F target gene expression is regulated by the temporal association of E2F proteins with members of the Retinoblastoma family of tumor suppressors (RB), known for their key role in the 'decision' to enter into a new cell cycle (Rubin et al., 2020; Weinberg, 1995). According to the classical model of cell cycle regulation, during early G1-phase, RB is bound to E2F and keeps E2F-dependent transcription inactive (Figure 1). CDK4/CK6-CyclinD-dependent phosphorylation of RB in G1 leads to its partial inactivation and subsequent induction of some E2F-dependent transcription (Trimarchi & Lees, 2002). This results in the expression of E-type cyclins, which further increases the overall activity of CDKs, particularly CDK2 (Pennycook & Barr, 2020). The increased CDK2 activity induces further phosphorylation (and inactivation) of RB, which now fully activates E2F-dependent gene transcription. This positive feedback loop drives the accumulation of CDK2/CyclinE and CDK2/CyclinA activities, and creates a commitment point required to initiate DNA replication and cell cycle entry. This classical model has been challenged recently, based on the findings by several groups suggesting that CDK4/6-CyclinD activity is not involved in the initial inactivation of RB. Instead, monophosphorylation of RB by CDK4/6 mainly serves to poise cells at the cell cycle entry point without affecting E2F activity, whereas subsequent phosphorylation by CDK2/CyclinE is the key event to activate E2F-dependent transcription, driving cells to the S-phase commitment point (Caillot et al., 2020; Narasimha et al., 2014).

Since the identification of the founding E2F family member, E2F1 (Helin et al., 1992), two distinct genes in *Drosophila melanogaster* and seven additional genes in mammals have been found. They share a considerable degree of homology at their DNA binding domain, which gives these transcription factors their DNA binding specificity (Attwooll et al., 2004; Dimova & Dyson, 2005; Trimarchi & Lees, 2002). In addition, several E2F isoforms have been discovered that arise from alternative splicing or multiple transcription start sites, increasing the complexity of this family (Adams et al., 2000; Carr et al., 2015). Mammalian E2Fs (E2F1-8) have been classified into several subsets; owing to their distinct expression and activity patterns during the cell cycle (Figure 2). So-called "activator E2F" (E2F1, E2F2 and E2F3a) protein levels peak at the G1–S phase

transition, and “atypical repressor E2F” (E2F7 and E2F8) protein levels peak later in late S phase, whereas “canonical repressor E2F” (E2F3b, E2F4, E2F5 and E2F6) proteins remain constitutively expressed throughout all phases of the cell cycle (Chen et al., 2009). Their transcriptional activity is tightly regulated throughout the cell cycle via transcriptional and translational regulation, post- translational modifications, protein degradation, binding to cofactors and subcellular localization (Kent & Leone, 2019). Given that my doctoral thesis work has been focused on E2F1 and E2F2, the content of the Introduction chapter will be circumscribed mainly to these activator E2Fs.

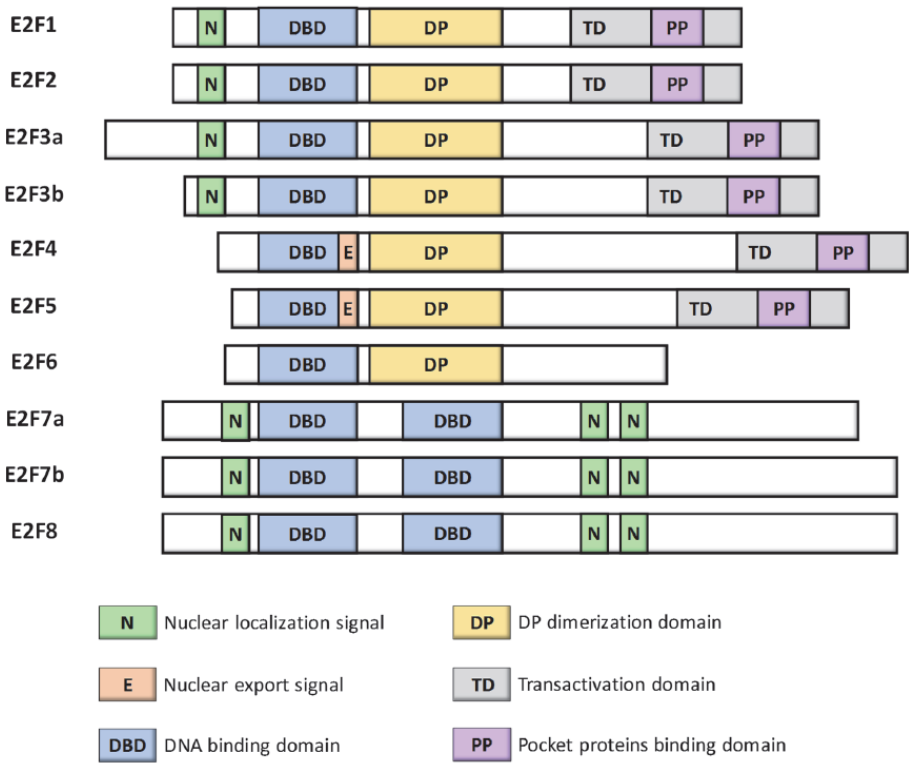


Figure 2. **Schematic representation of the mammalian E2F family of transcription factors.** The most representative domains identified in E2F proteins are shown (Lv et al., 2017).

Initially, E2F target genes were identified by searching for E2F-binding sites in the promoters of genes already known to be induced at the G1/S transition. In this way, E2F was found to regulate several genes with functions in cell cycle control (e.g. *CCNE1* and *CDC25A*) DNA replication (e.g. *MCM2-7* and *CDC6*) or nucleotide biosynthesis (e.g. *RRM2* , *DHFR)* (Chabes et al., 2004; DeGregori et al., 1995; Müller & Helin, 2000; Nevins, 2000). With the development of high throughput genomic technologies, large-scale systematic approaches were used to identify many hundreds of E2F target genes. Such approaches included identifying global gene expression changes in E2F-overexpressing or E2F-deficient cells by using DNA oligonucleotide

microarrays or by RNA-sequencing (Infante et al., 2008; Mitxelena et al., 2016; Polager et al., 2002; Young et al., 2003), as well as chromatin immunoprecipitation (ChIP) assays using E2F-specific antibodies (Laresgoiti et al., 2013; Weinmann et al., 2001, 2002). These approaches have been advantageous in that they are unbiased and can be done on a large scale. Predictably, they have shown that many additional DNA replication and cell cycle control genes are regulated by E2F (Figure 3).

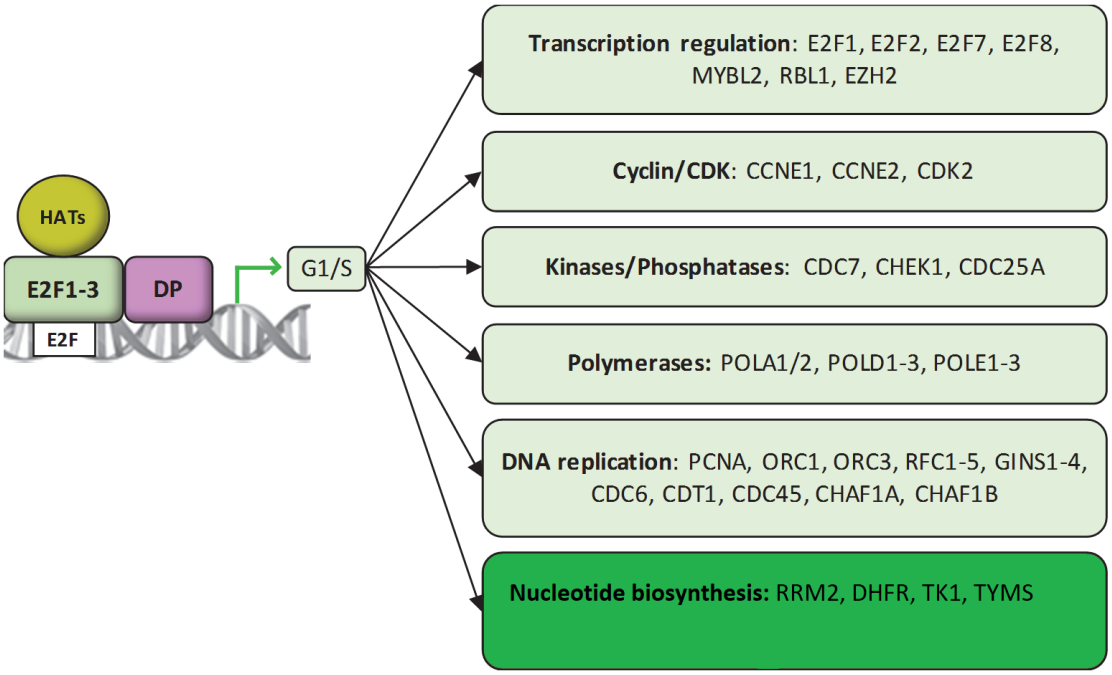


Figure 3. **G1/S phase genes regulated by E2Fs.** A selection of genes activated by E2F1-3 in the G1-S transition are represented by their different molecular functions. Nucleotide biosynthesis, the focus of this thesis, is depicted in dark green.

## 2. 2. *In vivo* relevance of E2F activity

Analysis of mouse strains carrying targeted mutations for individual E2F genes has been critical to understand the *in vivo* role of E2F factors. The characterization of these mouse models by our group and others has shown that loss of individual E2Fs can have distinct developmental and physiological consequences, implying the existence of specific target genes for each E2F. *E2f1*$^{-/-}$ mice display defective thymocyte apoptosis and impaired thymic negative selection, increased tumor susceptibility, exocrine gland dysplasia, and testicular atrophy (Field et al., 1996; García et al., 2000; Yamasaki et al., 1996). *E2f2*$^{-/-}$ mice exhibit increased proliferation of hematopoietic cells and

frequently develop autoimmunity and tumors, depending on the genetic background of the mouse (Murga et al., 2001; Zhu et al., 2001) (Table 1).

Table 1. Phenotypes of E2f1/E2f2 deficient mice

| Mouse Genotypes | Phenotypes |
|---|---|
| *E2f1*$^{-/-}$ | Defective thymocyte apoptosis<br>Exocrine gland dysplasia, and testicular atrophy<br>Tumors |
| *E2f2*$^{-/-}$ | Hyper proliferation of hematopoietic cells<br>Development of autoimmunity<br>Tumors. |
| *E2f1*$^{-/-}$ / *E2f2*$^{-/-}$ | Diabetes and pancreas atrophy<br>Involution of hematopoietic system, salivary glands and testicles |

Studies of mice carrying two or more mutant E2F loci simultaneously have also revealed an important degree of redundancy among specific E2F members, such as in the case of E2F1 and E2F2. The studies by our group and others have demonstrated the critical role of E2F1 and E2F2 transcription factors in tissue homeostasis, a process involving tight regulation of cellular proliferation and apoptosis. Combined inactivation of E2f1 and E2f2 transcription factors leads to exocrine and endocrine pancreatic dysfunction, causing diabetes and the collapse of the entire pancreas (Iglesias et al., 2004; Li et al., 2003).

This phenotype is absent from the individual *E2f1*$^{-/-}$ and *E2f2*$^{-/-}$ mice, implying a functional redundancy among these E2F members. After a period of strong cell division cycles, which take place during embryonic development and finalize by the second week after birth, pancreatic tissue in wild-type mice is virtually post-mitotic (Heller et al., 2001). By contrast, pancreatic cells lacking E2f1 and E2f2 continue cycling aberrantly well beyond this age and undergo massive apoptosis (Iglesias et al., 2004). Other organs in E2F1/E2F2 DKO mice also show a singular involution, particularly the hematopoietic system, salivary glands and testicles (Iglesias et al., 2004). Importantly, depletion of p53 rescues apoptosis and tissue atrophy in DKO mice (Iglesias-Ara et al., 2015).

## 2.3. Role of E2F in cancer

Given that the functions of a large set of "activator E2F" target genes are tied to inducing cell cycle progression, such as DNA replication and G1/S phase transition, these E2Fs have been considered to be tumor promoters, with its deregulation contributing to unrestrained cell cycle progression (Poppy Roworth et al., 2015). However, studies with animal models of gain-of-function and loss-of-function have shown conflicting data regarding the roles of E2Fs as oncogenic or oncosuppressive. The initial studies by Jacks and colleagues exploring the role of activator E2Fs in driving tumor initiation showed that ablation of E2f1 in $Rb1^{+/-}$ mice significantly reduced the incidence of both pituitary and thyroid tumors, prolonging the tumor-free lifespan of $Rb1^{+/-}$ mice (Yamasaki et al., 1996). This was the first genetic evidence to support an oncogenic role for an E2F family member in the context of Rb1 inactivation. The interpretation that E2F1 has a uniform oncogenic role, however, is inconclusive, given the observation that $E2f1^{-/-}$ mice develop lymphoma or occasionally tumors of mesenchymal origin, implying a tumor suppressor role for E2F1 (Field et al 1996; Yamasaki et al, 1996). Similarly, to E2F1, both oncogenic and tumor suppressor roles have been assigned to E2F2 (Opavsky et al, 2007; Pusapati et al., 2010; Scheijen et al., 2004; Zeng et al., 2020) suggesting that the cellular and tissue contexts play a key role in determining the oncogenic or oncosuppressive function of these E2F factors.

In humans, it is generally believed that genetic alterations resulting in the loss of RB function (a common feature of many tumors) cause oncogenesis by unleashing E2F activity and deregulating cell proliferation in the RB–E2F paradigm. In fact, E2F expression and/or elevated E2F target expression have been linked with poor prognosis, including recent studies examining liver and pancreatic cancers (Kent et al., 2016, 2017; Lan et al., 2018). However, whether E2Fs are the drivers of tumorigenesis or whether the high expression of E2F reflects merely the highly proliferative nature of aggressive tumors remains to be resolved.

Several mechanisms have been postulated for E2F-mediated tumor development (reviewed in Kent & Leone, 2019). One such mechanism is that E2Fs regulate cell cycle progression by gradually increasing the expression of its targets during G1, which must reach to a critical level in order for cells to pass the restriction point and progress to S phase. Once a threshold of E2F activity is met, the cell cycle progresses with or without additional mitogen stimulation (Kwon et al., 2017; Yao et al., 2008). If cells exhibit an increased E2F activity, the threshold would be easier to overcome, which would push cells more easily into the next cell cycle. Key upstream regulatory components of this pathway include negative regulators of E2F ($p21^{CIP1}$, RB, p130) or positive E2F regulators (MYC or CCND1), whose overexpression can alter the threshold necessary to activate E2Fs and push cells into the cell cycle (Figure 4). This indicates that cells

would otherwise remain quiescent can be pushed to proliferate via oncogenic activation of the E2F transcriptional program. Thus, increased E2F activity can provide a strong growth advantage (Kent & Leone, 2019).

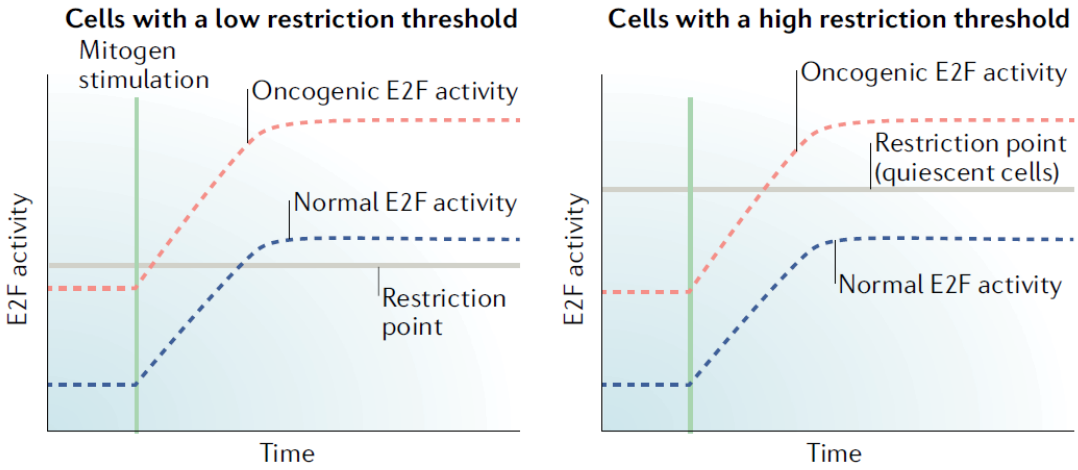


Figure 4. **E2F functions during the cell cycle**. High E2F activity influences commitment to the cell cycle and induces aberrant cell proliferation. In cycling cells with a lower restriction threshold, oncogenic E2F activity can commit cells to the cell cycle much more quickly after mitogenic stimulation than in cells with normal E2F activity. Similarly, in cells with a higher restriction threshold that would normally have stayed quiescent, oncogenic E2F activity can commit cells to the cell cycle (Kent & Leone, 2019).

A second mechanism by which activator E2Fs could promote cancer is by generating chromosomal instability (CIN). Many E2F targets have well-established roles during mitosis, and misregulated expression of these genes can cause chromosome instability, characterized by lagging chromosomes, chromosome breaks and deletions leading to aneuploidy (Ishida et al., 2001; Manning & Dyson, 2012). In a large-scale loss-of-function screen carried out by Vassilev and colleagues to identify genes that are needed to restrict genome duplication to once per cell division, a number of genes were identified that are essential to prevent aberrant DNA replication, a key step to CIN (Vassilev et al., 2016). Many of the genes identified are well-known E2F target genes involved in the licensing of DNA replication origins or in mitosis, such as MAD2 (Sotillo et al., 2010; Schvartzman et al., 2011) and APC/C inhibitor FBXO5, whose overexpression leads to high aneuploid tumors in mice and humans (Vaidyanathan et al., 2016; Vassilev et al., 2016). This indicates that cells may be very sensitive to the expression levels of proteins involved in aberrant DNA replication and CIN, with either too much or too little being detrimental to genomic stability (Kent & Leone, 2019).

A third mechanism that has been suggested is that E2Fs are involved in controlling DNA replication stress responses. This subject will be expanded in the following sections.

# 3. DNA replication stress

Every time a mammalian cell divides, billions of nucleotides must be accurately copied in coordination with the cell cycle. During DNA replication, cells are particularly vulnerable to genomic instability, as replication forks are prone to stall and collapse when encountering replication blocks or damaged DNA (Gaillard et al., 2015). Faulty DNA replication can lead to mutations or replication blockage, which can result in chromosomal breakage and rearrangement as well as their missegregation. A number of conditions, including those leading to high levels of DNA damage, may interfere with DNA replication and hamper its progression. This phenomenon (termed replication stress, RS) is characterized by a slowdown in DNA synthesis and/or by replication fork stalling, and is the primary cause of genomic instability (Gaillard et al., 2015).

Importantly, cells are endowed with a DNA replication stress checkpoint, which prevents the accumulation of DNA damage as a result of replication stress by stabilizing stalled replication forks, preventing late origins from firing and enabling replication to resume once the stress has been resolved (Lin & Pasero, 2021).

## 3.1 Sources of replication stress

Several DNA replication stress sources have been described in the literature (some are depicted in Figure 5):

a) During S phase, a number of intermediate structures intrinsic to the replication itself, such as nicks, gaps and single-stranded DNA (ssDNA) are typically formed in the DNA molecule.
b) Furthermore, unrepaired DNA lesions caused by products of cellular metabolism, UV light, and chemical mutagens are physical barriers to replication fork progression (MacDougall et al., 2007).
c) Additionally, there are a number of DNA sequences that are intrinsically challenging for the replication machinery. For example, trinucleotide repeats can form secondary DNA structures (hairpins, triplexes, etc) and G-quadruplexes. Secondary structures, which form in GC-rich DNA, have also been presented as a significant source of DNA damage (McMurray, 2010; Paeschke et al., 2013).
d) As replication and transcription both operate on DNA, the two processes will frequently interfere with each other and collisions between replication and transcription complexes are a common problem for the replication machinery (Helmrich et al., 2013).

e) Natural processes that affect DNA accessibility, such as chromatin compaction, may also be problematic for the replication machinery (Lambert & Carr, 2013).

f) Replication requires a number of components which, when limiting, can slow replication fork speed and induce replication stress. These factors include nucleotides and replication machinery components (Sørensen & Syljuåsen, 2012), as well as histones and histone chaperones, which package the replicated DNA (Aguilera & García-Muse, 2013).

g) Overexpression or constitutive activation of oncogenes, such as HRAS and MYC, as well as the E2F target genes CCNE, CDC6 and CDT1 have emerged as a source of RS (Liontos et al., 2007; Teixeira et al., 2015; Zeman & Cimprich, 2014), although the mechanism remains unclear. These factors promote increased replication initiation or origin firing, a condition that can lead to depletion of nucleotide pools and/or increased collisions with transcription complexes (Srinivasan et al., 2013). In fact, supplementing cancer cells with exogenous nucleotides helps to decrease genomic instability, arguing for a depletion of nucleotide pools as a possible source of RS upon oncogenic activation, at least in some contexts (Bester et al., 2011; Burrell et al., 2013; Mannava et al., 2012, 2013)

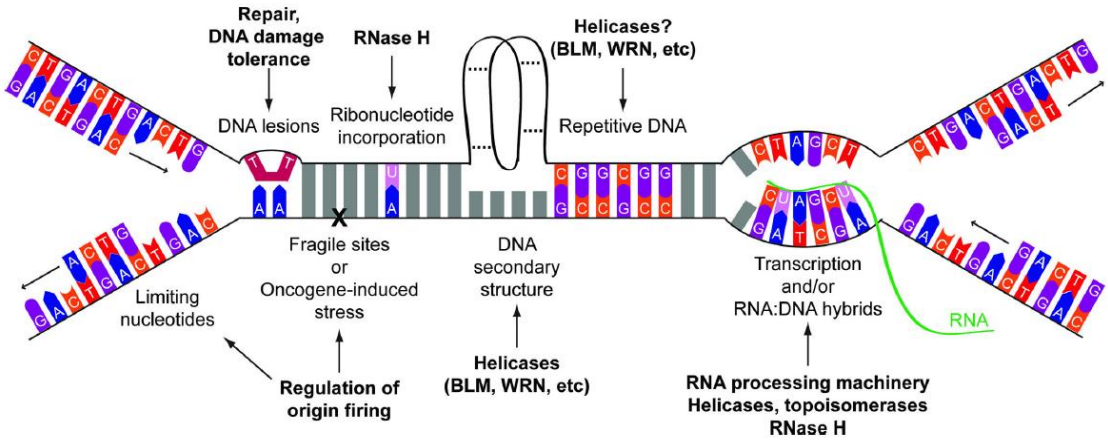


Figure 5. **Sources of replication stress**. There are a number of conditions or obstacles which can slow or stall DNA replication, including limiting nucleotides, DNA lesions, ribonucleotide incorporation, repetitive DNA elements, transcription complexes and/or DNA hybrids, DNA secondary structure, fragile sites, and oncogene-induced stress. Some of the key resolution pathways, which are known for each source of stress are indicated in bold (Zeman & Cimprich, 2014).

## 3.2. Replication stress response

When trying to replicate damaged DNA, polymerases at replication forks temporarily stop DNA synthesis, a phenomenon known as 'fork stalling'. These stalled forks sometimes manage to repair the DNA and continue replication by inducing a replication stress response (Figure. 6). Briefly, when replication forks are halted, the replicative minichromosome maintenance (MCM) helicase is thought to continue unwinding DNA for a few hundred base pairs directly downstream of the fork, thereby exposing ssDNA. Replication protein A (RPA) coats the ssDNA, which leads to activation of the serine/threonine protein kinase ATR by ATR-interacting protein (ATRIP). The subsequent ATR signaling cascade includes the phosphorylation of checkpoint kinase 1 (CHK1), the cell cycle checkpoint protein RAD17 and histone H2AX. These phosphorylation events are thought to facilitate the continuation of DNA replication and the attenuation of replication stress (Matsuoka et al., 2007; Sabatinos, 2010).

Mutations in the ATR signaling cascade have been shown to increase DNA replication stress and genomic instability, and thereby promote premature aging and cancer susceptibility (Fang et al., 2004; Murga et al., 2009). Interestingly, the group of Fernández-Capetillo demonstrated that ATR mutant mice reduce their replication stress levels when an extra allele of the ribonucleotide reductase (RNR) regulatory subunit Rrm2 is introduced in the animals, suggesting that an increased nucleotide biosynthetic activity can help attenuate RS in the context of a defective ATR signaling pathway (Lopez-Contreras et al., 2015).

Stalled replication forks that are not resolved may undergo 'fork collapse' and lose the association between the DNA molecule and the replication apparatus. Collapsed forks often undergo endonuclease-mediated DNA cleavage, which produces double-stranded DNA breaks (DSBs) (Sabatinos, 2010; Zeman & Cimprich, 2014). Damaged DNA also triggers specific signaling cascades (termed DNA damage response), although the signals induced by replication fork stalling and/or collapse differ somewhat from those that originate from primary DSBs that occur outside S phase (Dobbelstein & Sørensen, 2015).

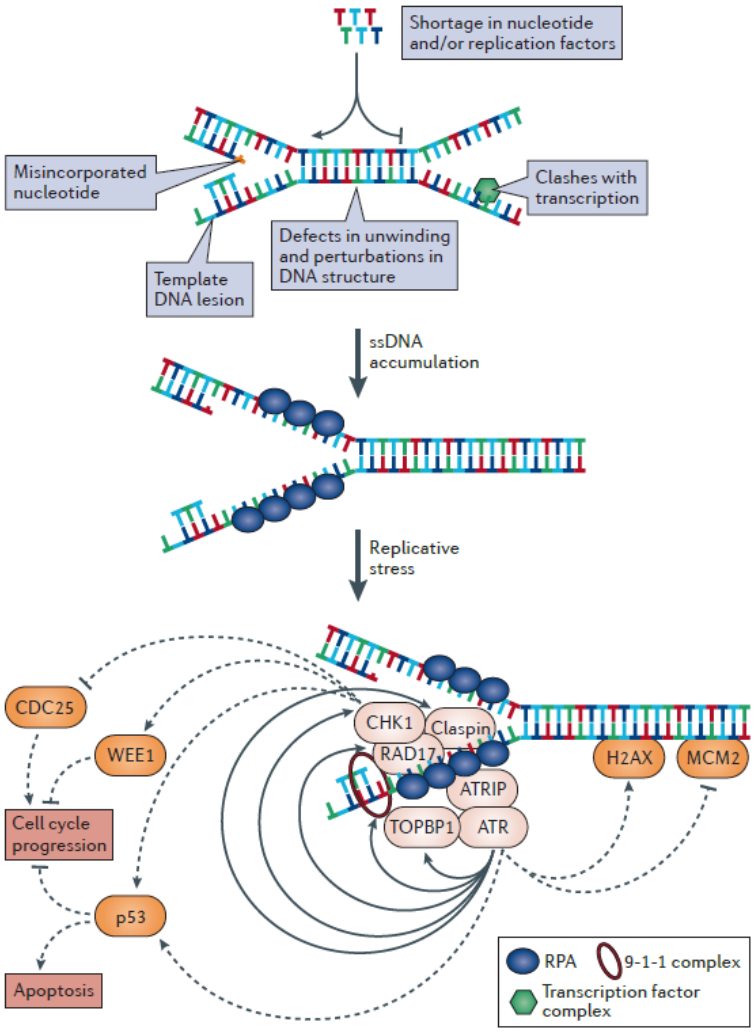


Figure 6. **Generation of replication stress and the resulting signaling cascades.** When the replication machinery encounters a stalled replication fork, DNA helicases move ahead of DNA polymerases, and single-stranded DNA (ssDNA) accumulates. This ssDNA recruits replication protein A (RPA), which is the primary trigger for the signaling response to replication stress. The recruitment of response factors results in activation of the kinase ATR, which in turn phosphorylates not only the regulatory factors in the initial complex but also additional factors that regulate the firing of replication origins, cell cycle progression or apoptosis. The solid arrows indicate phosphorylation events that occur at the stalled fork, and the dashed arrows indicate phosphorylation of proteins that act elsewhere, ATR-interacting protein; CDC25, cell division cycle 25; CHK1, checkpoint kinase 1; MCM2, minichromosome maintenance protein 2; TOPBP1, DNA topoisomerase 2-binding protein 1 (Zeman & Cimprich, 2014).

## 3.3. A role for E2F1 and E2F2 in replication stress responses

E2F factors are distinctly linked to DNA replication stress in several ways. In cells with normal E2F activity, a situation of replication stress prolongs the expression of E2F target genes (Figure 7), such as those encoding ribonucleotide reductase regulatory subunit M2 (RRM2) and checkpoint kinase 1 (CHK1), which then stabilize the replication fork, resulting in the resolution of replication stress and decreased DNA damage (Bester et al., 2011; Herlihy & de Bruin, 2017). In this context, E2Fs appear to be involved in recovery and tolerance of replication stress.

Interestingly, both under situations of too much or too little E2F activity, cells experience replication stress. In transformed cells, which typically exhibit an increased E2F activity, the aberrant expression of E2F targets is expected to induce replication stress and genomic instability (Figure 7). Indeed, this is the case for cells overexpressing the known E2F targets CCNE, CDC6 and CDT1 (Liontos et al, 2007; Teixeira et al, 2015).

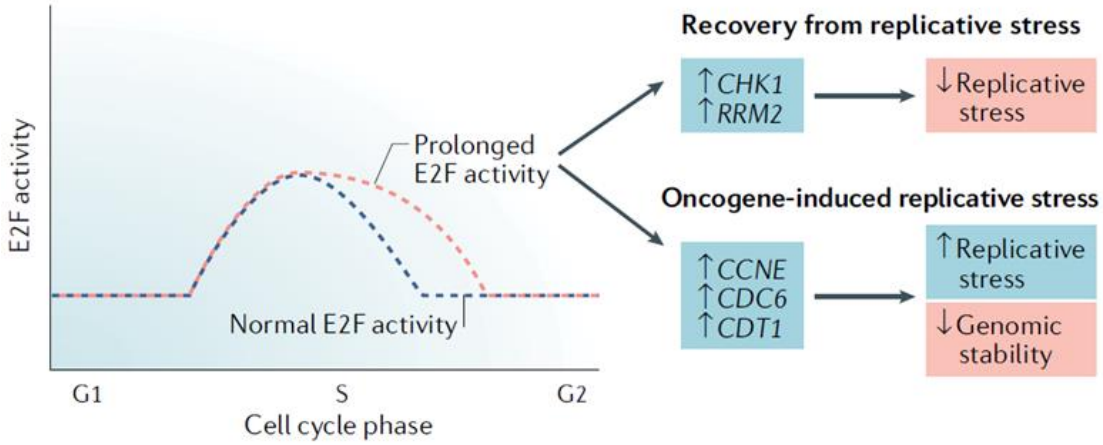


Figure 7. **E2F levels and replication stress.** Prolonged E2F activity in S phase allows normal cells to recover from replication stress. Under oncogenic situations, such as E2F overexpression, this can induce additional replication stress, resulting in decreased genomic stability (Kent & Leone, 2019).

Loss of E2F factors similarly results in increased replication stress in normal cells *in vivo*. Our group has shown that cells derived from $E2f1^{-/-};E2f2^{-/-}$ double-knockout (DKO) mice exhibit an aberrant cell cycle regulation, characterized by overexpression of E2f target genes involved in DNA replication or cell cycle progression and repression of cell cycle inhibitors. Furthermore, the activities of both G1 and mitotic cyclin/CDKs appear to be aberrantly elevated in DKO cells, along with augmented DNA replication rates, evidencing a situation of replication stress (Iglesias-Ara et al., 2015). Furthermore, a strong DNA damage response (DDR) is detected in a variety of tissues derived from DKO

mice, including bone-marrow-derived macrophages and pancreatic cells (Iglesias et al., 2004; Iglesias-Ara et al., 2015).

The mechanism underlying increased DNA damage upon E2F1 and E2F2 loss remains to be resolved, and several scenarios are possible. For example, the increased expression of genes involved in the establishment of the DNA replication complex detected in E2f1/E2f2 DKO cells could lead to illegitimate replication origin firing and fork stalling, as shown after overexpression of CDT1 (Davidson et al., 2006). Another possibility is that excessive CDK activity observed upon E2f1/2 loss could negatively impact genome integrity during S phase.

A third possibility is that consumption of nucleosides due to the excessive DNA replication in DKO cells could account for the activation of DNA damage response, similarly to what has been demonstrated for oncogene-induced replication stress (Bester et al., 2011; Mannava et al., 2012, 2013). In this situation, given that the transcription of key enzymes in the biosynthesis and recycling of nucleosides is under the control of E2F factors, loss of E2F1/2 would reduce nucleotide pools and thereby aggravate replication stress. However, it is presently unknown whether cells lacking E2F1 and E2F2 undergo nucleotide pool depletion and accumulation of aberrant G1 and mitotic CDK activities that may affect the efficiency of DNA replication processes. Moreover, dependency on E2F-driven nucleotide production would be expected preferentially in cells with high turnover, such a cancer cells.

# 4. Nucleotide metabolism in normal and cancer cells

A correct nucleotide balance is necessary for the prevention of multiple pathologies, and probably plays a role in cancer. Nucleotides consist of a heterocyclic nucleobase B, which is either a purine (adenine or guanine) or pyrimidine (cytosine, uracil, and thymine) attached to the (deoxy)ribofuranose sugar/sugar−phosphate (Figure 8). Nucleotides have various functions essential for cell viability, acting as an energy source (ATP, GTP and CTP), as part of coenzymes (AMP in NAD or Coenzyme A), as structural components of phospholipids or, and most prominently, as building blocks of DNA and RNA (dNTPs in the DNA molecule; NTPs in the RNA molecule) (Yadav et al., 2020).

Both proliferating and non-proliferating cells need to fine-tune nucleotide and dNTP synthesis to allow for both nuclear and mitochondrial DNA replication and repair to maintain a healthy cell (Buj & Aird, 2018). Thus, disruptions in dNTP balance are associated with enhanced mutagenesis, leading to genomic instability and cancer development (Mathews, 2006). An unbalanced dNTP supply may also have a role in metabolic disease (Shimizu et al., 2014). To produce dNTPs, cells have developed two

biosynthetic pathways (depicted in figure 9): the *de novo* pathway (DNP) and the nucleotide salvage pathway (NSP) (Blakley & Vitols, 1968).

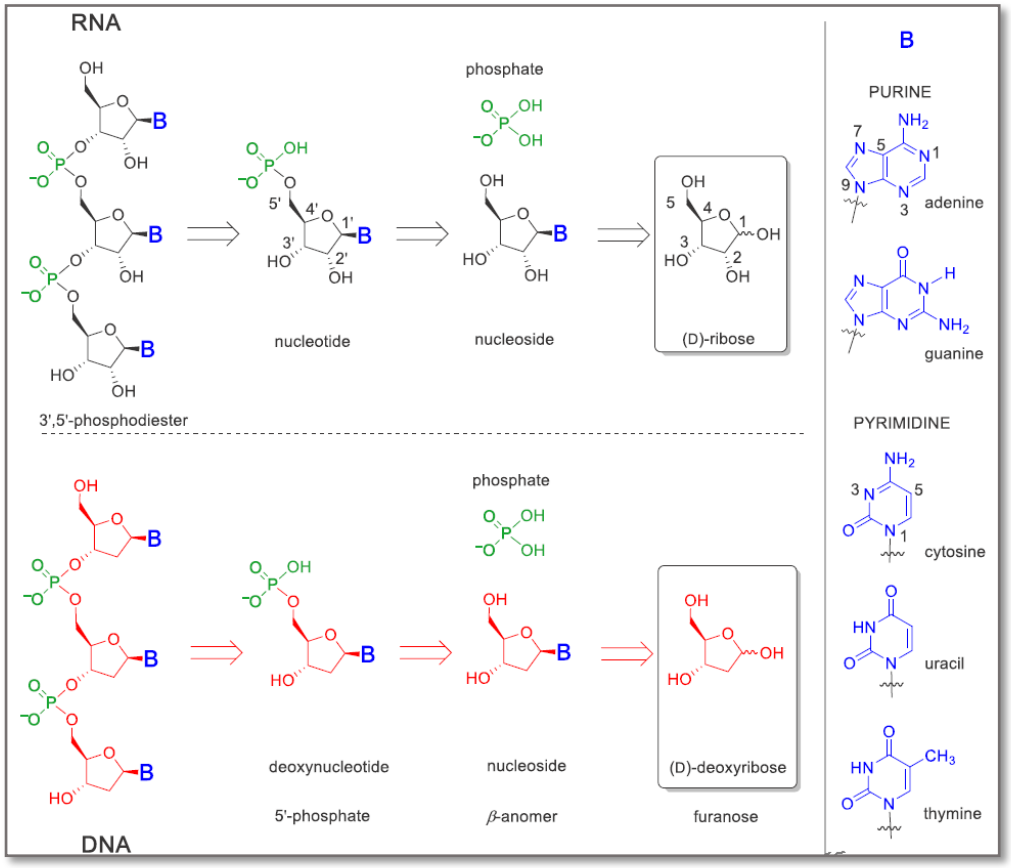


Figure 8. **Structural depiction of RNA, DNA, and its canonical building blocks**. Shown are the nucleotides, nucleosides, phosphate, sugars, and heterocyclic nucleobases B, the purines and the pyrimidines (Yadav et al., 2020).

The *de novo* biosynthesis of both purines and pyrimidines requires the generation of 5-phosphoribose-1-pyrophosphate (PRPP), the activated form of ribose derived from ribose 5-phosphate, which is produced through the oxidative and nonoxidative arms of the pentose phosphate pathway (PPP) parallel to glycolysis. The pyrimidine ring is first assembled from glutamine, bicarbonate, and aspartate and is then attached to PRPP through six reactions. Purine synthesis differs from pyrimidine synthesis in that all reactions occur in the cytosol, and the purine ring is directly built onto the activated ribose, PRPP. The purine ring is synthesized from various substrates, including glutamine, glycine, bicarbonate, and N10-formyl-tetrahydrofolate (THF) (Figure 9) (Villa et al., 2019). The *de novo* nucleotide synthesis pathway is highly energy-intensive. By contrast, the nucleotide salvage pathway is a more energy-efficient route to synthesize nucleotides (Moffatt & Ashihara, 2002).

The NSP is considered a recycling plant, whereby nucleoside transporters and deoxyribonucleoside kinases enable recycling of extracellular deoxyribonucleosides originating from DNA degradation in apoptotic cells (E. S. J. Arnér & Eriksson, 1995), liver biosynthetic processes (Fustin et al., 2012), and food intake (Austin et al., 2012).

The metabolic flux through the NSP is regulated by rate-limiting kinases, particularly deoxycytidine kinase (DCK) and thymidine kinase 1 (TK1). DCK phosphorylates deoxycytidine to produce deoxycytidine monophosphate (dCMP), a precursor of both dCTP and dTTP pools (Sabini et al., 2008). Deoxyadenosine and deoxyguanosine can also be phosphorylated by DCK, albeit with significantly lower efficacy than deoxycytidine (Sabini et al., 2008). TK1 phosphorylates thymidine to generate dTMP, a precursor of thymidine triphosphate (dTTP) pools (Arnér & Eriksson, 1995). Addition of the nucleobase to ribose is achieved either via the PRPP step for purines, or catalyzed by specific pyrimidine phosphorylase to add the base to ribose-1-phosphate (Figure 9). The relative importance of salvage versus *de novo* synthesis likely depends on the growth conditions and on the specific tissue (Austin et al., 2012).

Ribonucleotides obtained by either pathway can be reduced to their deoxyribonucleotide counterpart in a reaction catalyzed by ribonucleotide reductase (RNR)(Fairman et al., 2011)**,** the rate-limiting step in dNTP synthesis (Figure 9). In particular, RNR catalyzes the first step specifically dedicated to DNA synthesis by reducing all four types of nucleoside diphosphates (NDP) to deoxynucleoside diphosphates (dNDP) in a tightly controlled process. In fact, and although dNTP production is a multistep process including many different enzymes, the balance of the dNTP pool is primarily determined by the regulatory mechanisms of the RNR (Mathews, 2006).

The mammalian RNR complex is a heterotetramer formed by two identical RRM1 subunits and two RRM2 subunits. Mammals contain an additional R2 gene, p53R2, which encodes a protein called RRM2B. RRM2B can form a functional complex with RRM1 and provides dNTPs for mitochondrial replication and DNA repair outside of S-phase (Lozano and Elledge, 2000; Nakano et al., 2000; Tanaka et al., 2000).

Multiple levels of RNR regulation exist, which are conserved from yeast to human. They function in concert to strictly limit RNR activity to those stages of the cell cycle when the requirement for dNTPs is highest, namely S/G2- phase and during DNA damage repair (Zhou & Elledge, 2000). RRM1 has a very long half-life (>20 hours), which results in almost constant levels that are thought to be in excess throughout the cell cycle (Engstrom et al., 1985). In contrast, RRM2 has a short half-life (3 hours) and is only stable during S-phase. Therefore, it is thought that the cell cycle-dependent activity of RNR is regulated by RRM2 levels (Mathews, 2006). Furthermore, altered regulation of

its activity is highly mutagenic (Chabes et al., 2003; Mathews, 2006) and its upregulation has been described in certain types of human cancer including gastric, ovarian, bladder and colorectal cancer (Liu et al., 2011; Morikawa et al., 2010; Wang et al., 2012).

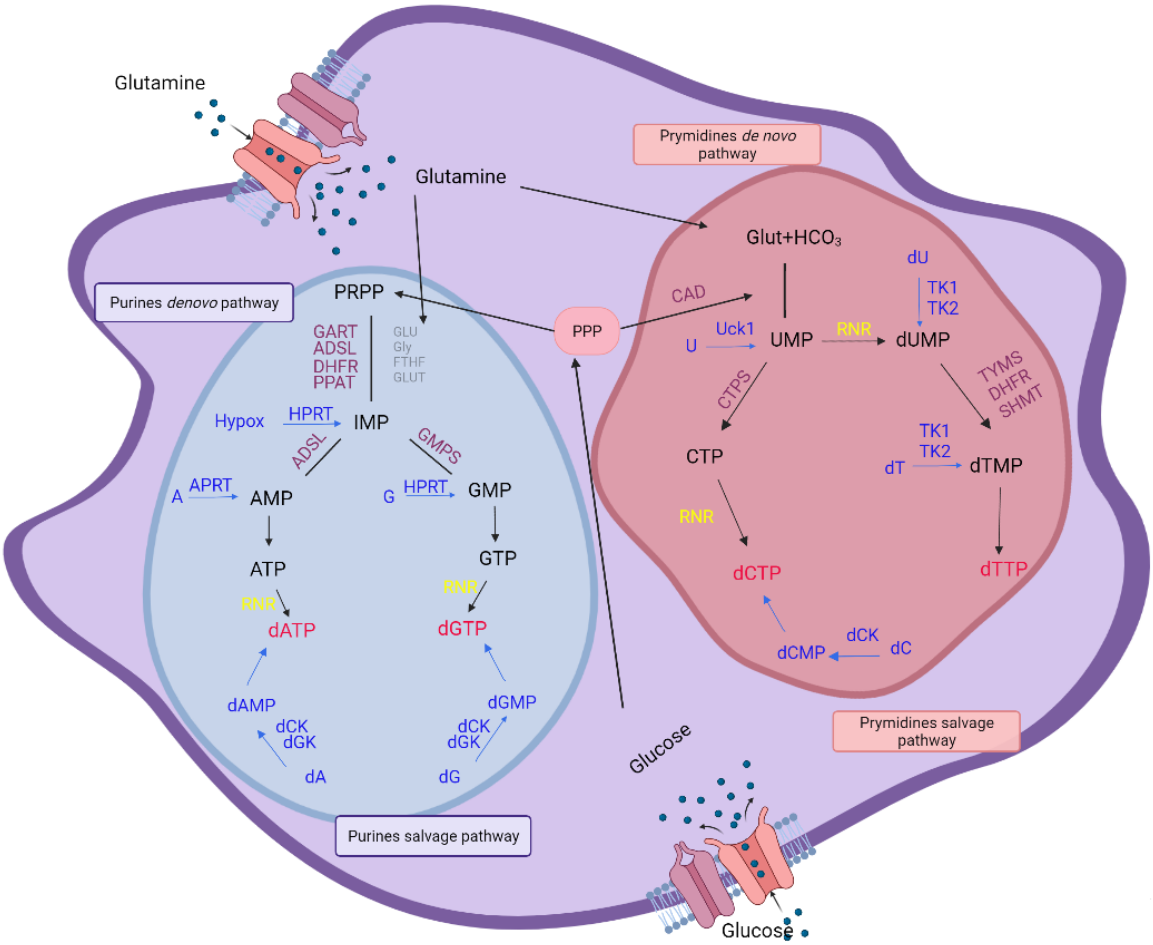


Figure 9. **Pathways of deoxyribonucleotide metabolism in mammalian cells**. Schematic representation of salvage pathways (blue) and its crosstalk with de novo pathway. With key metabolic enzymes (brown), their principal reactive substrates (black), and the four deoxyribonucleotide triphosphate (dNTP) end-products (red), Purine (light blue) and pyrimidine (dark orange) metabolism and their crosstalk with the pentose phosphate pathway [(PPP), pink are shown. Glucose feeds into both purine and pyrimidine metabolism to donate carbons and nitrogens to all dNTPs. Abbreviations: PPP, Pentose Phosphate Pathway, PRPP: Phosphoribosyl-pyrophosphate, GART, glycinamide ribonucleotide transformylase; ADSL, adenylosuccinate lyase; DHFR: dihydrofolate reductase; PPAT, Phosphoribosyl Pyrophosphate Amidotransferase; IMP: Inosine monophosphate; ADSL, adenylosuccinate lyase; GMPS, guanosine monophosphate synthetase; AMP, adenosine monophosphate; GMP, guanosine monophosphate; ATP, adenosine triphosphate; GTP guanosine triphosphate; RNR, ribonucleotide reductase; CAD, Carbamoyl-Phosphate Synthetase 2, Aspartate Transcarbamylase, And Dihydroorotase; UMP, uridine monophosphate; UDP, uridine

diphosphate; CPTS, cytidine triphosphate synthetase; CTP, cytidine triphosphate; dUDP, deoxyuridine diphosphate; dUMP, deoxyuridine monophosphate; TYMS, thymidylate synthase; SHMT, serine hydroxymethyltransferase; dTMP, deoxythymidine monophosphate. Hypox., hypoxanthine; HPRT, hypoxanthine phosphoribosyltransferase; A, adenine; APRT, adenine phosphoribosyltransferase; G, guanine ; HGPRT, hipoxantina guanina fosforibosiltransferasa; U, uridine; UCK, uridine-cytidine kinase; dAMP, deoxyadenosine monophosphate; dCK, deoxycytidine kinase; dA, deoxyadenosine; dGMP, deoxyguanosine monophosphate; dG, deoxyguanosine; dCMP, deoxycytidine monophosphate; dC, deoxycytidine; dU, deoxyuridine; TK, thymidine kinase; dT, deoxythymidine.

## 4.1. Role of E2F in nucleotide metabolism

E2F transcription factors regulate the expression of genes encoding nucleotide synthesis enzymes (Dyson, 1998). These genes include TK1, TYMS, DCK, DHFR, RRM1, RRM2, GMPS or UMPS (Hirschey et al., 2015; Ishida et al., 2001; Lane & Fan, 2015; Polager et al., 2002; Ren et al., 2002; Vernell et al., 2003). Thus, E2F regulates both arms of dNTP production, namely the *de novo* and salvage pathways. Transcription of RRM1 and RRM2 is controlled by E2F activity at late G1 phase (Bjorklund & Harnishfeger, 1990). As a consequence, RNR activity starts to rise at the G1/S border, leading to a ten-fold increase in dNTP levels, which decrease before cells enter into mitosis (Mathews, 2006). In the case of RRM2, it has been described that during G1, E2F4 binds to the conserved E2F binding site present in the promoter of RRM2, leading to repression of transcription. Upon entry into S-phase, E2F4 dissociates and relieves RRM2 repression leading to transcriptional activation mediated by E2F1 (Chabes et al., 2004). Evidence for a similar E2F-dependent mechanism has been provided for TK1 expression (Dou et al., 1994; Ogris et al., 1993). The promoter of TK1 harbors an E2F binding site that is required for its S phase-dependent transcription, and mutations of this site abolish transactivation of TK1 expression by polyoma large T antigen (which inactivates Retinoblastoma protein) or upon serum stimulation (Ogris et al., 1993). The initiation region DCK promoter also contains an E2F binding site, and E2F transactivates DCK through this site. However, E2F binds weakly to this motif *in vitro* and does not appear to mediate cell cycle-specific expression of DCK *in vivo* (Chen et al., 1995). The mechanism of E2F-mediated transcription initiation in constitutively expressed genes, such as DCK, is not known. It is possible that an E2F-like factor is constitutively expressed and functions as an initiator, similar to the constitutively expressed TATA binding proteins (Johansson & Norda, 2000).

Interestingly, nucleotide biosynthesis genes have also been described to be under the control of ATR/ATM-CHK1-E2F signaling in response to DNA replication stress and DNA damage, whereby exposure to a variety of genotoxic agents activates the ATR/ATM-CHK1 signaling cascade and maintains an E2F-dependent transcriptional program at high levels (Bertoli et al., 2013; Eaton et al., 2007; Gong et al., 2016; Zhang et al., 2009).

The mechanisms involved in this response appear to be diverse. Hydroxyurea-induced replication stress results in CHK1-dependent phosphorylation of E2F6, leading to its dissociation from promoters. This promotes E2F-dependent transcription, including nucleotide biosynthesis genes *RRM2*, *DHFR* and *DCK*, which facilitates cell survival by preventing DNA damage and cell death (Bertoli et al, 2016). By contrast, exposure to N-methyl-N'-nitro-N-nitrosoguanidine (MNNG) results in phosphorylation and stabilization of E2F3, which together with NFY co-transactivates *RRM2* expression for DNA repair (Gong et al., 2016). Still, another mechanism to induce RRM2 expression under replication stress involves E2F1 upregulation following treatment with the topoisomerase I inhibitor camptothecin (Zhang et al., 2009).

## 4.2. Nucleotide metabolism and DNA replication stress in cancer cells: therapeutic opportunities

Most tumor cells show enhanced levels or activities of proteins that stimulate the G1–S transition, such as RAS or MYC. This is thought to lead to an induction of E2F-dependent transcription and excessive rate of S phase entry. Consequently, these cells may contain insufficient amounts of key molecules (i.e. DNA replication enzymes and/or nucleotides) that are necessary for accurate and efficient DNA replication (Bester et al., 2011; Burrell et al., 2013; Mannava et al., 2012, 2013). Importantly, reduced activity of some tumor suppressors, such as RB, p53, the CDK inhibitor $p16^{INK4A}$ and the p53-activating MDM2 ligand $p14^{ARF}$ can also elicit replication stress by promoting the G1–S transition (Tort et al., 2006). These tumor cells would be largely dependent on pathways that ensure the production of metabolites for DNA synthesis. Indeed, increased dNTP levels have been shown to reduce oncogene-induced replication stress (Bester et al., 2011; Burrell et al., 2013; Mannava et al., 2012, 2013).

Thus, cancer cells experiencing high levels of replication stress might become dependent on increased dNTP levels, thereby opening the window for novel therapeutic strategies. Targetable aspects of replication stress vulnerability could include proteins and processes involved in preventing replication stress. RNR and other dNTP metabolic enzymes are already major targets in several types of cancer treatments (Bonate et al., 2006; Aye et al., 2015; Zhang et al., 2009). However, to date,

limited understanding of the proteins and processes involved in the specific aspects of replication stress vulnerability has been achieved.

In contrast to the common assumption that anti-cancer therapy should aim to attenuate the proliferation of cancer cells, the idea of pushing tumor cells through the cell cycle by further lowering their checkpoint barriers, and promoting cancer cell death, has emerged as an attractive alternative approach. This could be achieved, for example, by further increasing replication stress in a catastrophic manner. Cancer cells typically rely on the DNA replication stress response to lower their genomic instability and remain viable. In fact, cancer cells rarely accumulate mutations in this signaling checkpoint to ensure continuing cellular proliferation (Dobbelstein & Sørensen, 2015).

But how could replication stress be enhanced in a targeted manner? According to Dobbelstein and Sørensen, several key biological transitions and responses could be subject to manipulation: the entry into S phase; the stalling of replication forks; the collapse of such replication forks; the repair of damaged DNA during S phase; and the premature entry into mitosis. Each of these processes is governed by signaling pathways, and each of these pathways can be manipulated by drug candidates (Dobbelstein & Sørensen, 2015).

This raises the possibility of eliminating cancer cells by exaggerating the same checkpoint losses that initially caused their uncontrolled proliferation. In this regard, targeting E2F1/E2F2 could be exploited therapeutically for cancer treatment, given the high levels of DNA damage that are induced upon their depletion (Iglesias-Ara et al, 2010; 2015).

Targeted inhibitors can also be combined with each other to achieve synergistic effects on tumor cells. For example, the combination of CHK1 inhibitors and WEE1 inhibitors (Chaudhuri et al., 2014) enhances replication stress and promotes mitotic catastrophe. Inhibition of CHK1 also suppresses homologous recombination repair, thereby further sensitizing cells to WEE1 inhibitors (Sørensen et al., 2005), and PARP inhibitors can be synergistically combined with CHK2 inhibitors (Antoni et al., 2007). These combinations enhance replication stress, although the exact mechanisms have not been fully elucidated.

Once origins of replication fire and DNA replication commences, cells need to balance accuracy, speed, and the consumption and distribution of relevant resources such as nucleotides and replication factors to complete replication in an efficient manner (Zeman & Cimprich, 2014). The control of dNTP pools is mainly achieved via allosteric and transcriptional regulation of enzymes involved in dNTP metabolism. Malfunctioning of those control mechanisms leads to altered dNTP pools resulting in enhanced mutagenesis, DNA recombination, chromosomal aberrations and cell death

(Kunz et al., 1994). An excess of dNTPs primarily causes replication errors by driving misinsertions and promoting translesion DNA synthesis (Mathews, 2006), while dNTP scarcity slows down replication fork progression and increases the frequency of fork stalling (Koç et al., 2004). dNTP levels also influence replication by affecting origin choice, inter-origin distance and dormant origin usage (Anglana, 2003; Courbet, 2008).

The nucleotide salvage pathway (NSP) was long considered irrelevant for the regulation of dNTP pools (Xu et al., 1995) but, more recently, studies indicate that it might affect DNA replication and repair under certain conditions. Depletion of dCTP pools in $DCK^{-/-}$ mice leads to replication stress, S-phase arrest and DNA damage in hematopoietic progenitor cells, which can be rescued by concomitant depletion of TK1 (Austin et al., 2012; Toy et al., 2010).

Although the bulk of NSP-derived free dNTPs does not contribute to DNA synthesis under unchallenged conditions (Nathanson et al., 2014), dNTP synthesis via the NSP becomes critical for the maintenance of nucleotide levels when de novo dNTPs synthesis is inhibited (Austin et al., 2012). Moreover, DCK is a target of ATM and ATR kinases (Matsuoka et al., 2007), supporting the notion that induction of the NSP pathway might be important to produce sufficient dNTPs in response to DNA damage and replication stress. The induction of an alternative dNTP production mechanism might also explain resistance towards the cytotoxic effects of drugs targeting dNTP *de novo* synthesis such as thymidine, which inhibits RNR-dependent pyrimidine synthesis (Reichard, 1988).

Terminally differentiated cells, such as neurons, do not replicate their DNA. Thus, in order to maintain nucleotide levels in balance there is greater reliance on salvage pathways compared to *de novo* synthesis (Fu et al., 2013). Furthermore, the group of Radivoyevitch found that *de novo* dNTP supply system compensates for p53R2 losses with increases in RNR subunit RRM1, RRM2, or both. Also, compensatory increases were detected in cytosolic DCK and TK1 and in mitochondrial deoxyguanosine kinase (DGK), all of the salvage dNTP supply system (Radivoyevitch et al., 2012). Interestingly, the combination of thymidine and DCK inhibitors was found to be efficient in the treatment of hematological malignancies in mice (Nathanson et al., 2014). Therefore, concomitant targeting of DNP and NSP could provide an effective alternative to target cancer cells and reduce the development of resistances to treatment.

### 4.2.1. Drugs that target nucleotide metabolism

A large collection of drugs has been developed by the pharmaceutical industry to target nucleotide metabolism in cancer cells and thereby induce replication stress (Table1). Nucleoside and base analogues, also called antimetabolite drugs, induce replication stress by several mechanisms. For example, gemcitabine and cytarabine inhibit ribonucleotide reductase, whereas 5-fluorouracil (5-FU) inhibits thymidylate synthase (TS), the enzyme involved in the biosynthesis of thymidylate. These drugs reduce the size of the available dNTP pools that are needed for DNA synthesis and enhance replication stress by blocking replication fork activity (Plentz et al., 2010).

Many nucleoside analogues, including 5-FU and fludarabine can also be incorporated into RNA, and this substantially contributes to their cytotoxicity (Huang & Plunkett, 1991; Longley et al., 2003). Perturbing rRNA synthesis in this manner releases ribosomal proteins from the nucleolus, thus inhibiting the ubiquitin ligase activity of MDM2 and activating p53 (Donati et al., 2013). This could arrest p53 proficient cells in the G1 phase or G2 phase, thus decreasing the proportion of cells that replicate their DNA and counteracting the induction of replication stress. In general, p53 may protect cells from drug-induced replication stress, which would enhance drug selectivity for p53-mutant tumor cells.

Various drugs can be used in combination with nucleoside analogs such as gemcitabine or 5-FU to further boost replication stress, and synergistic effects have been observed in several cases. The specific targeting of checkpoint signaling combined with nucleoside analogues has been extensively studied. Gemcitabine efficacy is cooperatively increased when combined with inhibitors of CHK1, ATR or WEE1 (Ewald et al., 2007; Rajeshkumar et al., 2011). A Phase I clinical trial was completed with the CHK1 inhibitor AZD7762, with or without gemcitabine, but revealed unexpected cardiotoxicity (Sausville et al., 2014). Therefore, alternative compounds for this target should be tested.

Table 2. Selected agents targeting nucleotide metabolism that are approved, or are in trials, for the treatment of cancer (Luengo et al., 2017).

| Drug | Target Enzyme |
|---|---|
| Methotrexate | dihydrofolate reductase (DHFR) |
| Pemetrexed | DHFR<br>thymidylate synthase (TS)<br>glycinamide ribonucleotide formyltransferase (GARFT) |
| 6-Mercaptopurine<br>6-Thioguanine | PRPP amidotransferase |
| Capecitabine<br>5-Fluorouracil | thymidylate synthase (TS) |
| Gemcitabine<br>Cytarabine | DNA polymerase/ribonucleotide reductase (RnR) |
| Leflunomide | dihydroorotate dehydrogenase (DHODH) |
| CB-839 | glutaminase (GLS) |
| PEG-BCT-100 (ADI-PEG20)<br>AEB-1102 | depletion of circulating arginine |
| L-Asparaginase | depletion of circulating asparagine |
| TVB-2640 | fatty acid synthase (FASN) |
| AG-120 (ivosidenib)<br>IDH305<br>BAY1436032<br>FT-2102<br>AG-221 (enasidenib)<br>AG-881 | mutant IDH1<br><br><br><br>mutant IDH2<br>mutant IDH1/2 |
| AZD3965 | monocarboxylate transporter 1 (MCT1) |
| CPI-613 | pyruvate dehydrogenase (PDH)/ α-ketoglutarate dehydrogenase |
| Metformin | mitochondrial complex I |

#### 4.2.1.1. Mechanism of action of 5-Fluorouracil

5-fluorouracil (5-FU) is an antimetabolite drug that has been widely used since 1957 to treat different types of cancer, and is actually one of the most commonly used drugs in oncology (Longley et al., 2003). 5-FU enters into cells by facilitated transport using the same mechanism as that of uracil. In the anabolic route, following intravenous administration, 5-FU is transformed to numerous active metabolites which disrupt thymidylate synthase (TS) activity and DNA/RNA synthesis, thereby leading to DNA/RNA damage and cell death (Sethy & Kundu, 2021) (Longley et al., 2003). Briefly, after entering into the cells, 5-FU is converted into 5-fluorouridine monophosphate (FUMP) either by direct route using orotate phosphorylase (OPRT) using phosphoribosyl transferase (PRPP) as a cofactor, or indirectly through uridine phosphorylase (UP) and uridine kinase (UK) via fluorouridine (FUR) (Fig. 10). FUMP is then phosphorylated to fluorouridine diphosphate (FUDP) which is either converted to the active metabolite fluorodeoxyuridine triphosphate (FUTP) or fluorodeoxyuridine diphosphate (FdUDP) by ribonucleotide reductase (RNR) (Longley et al., 2003). Finally, these active metabolites are misincorporated into RNA and DNA in place of uridine -5'-triphosphate/ 2′ - deoxythymidine -5'- triphosphate (UTP/ dTTP). On the other hand, 5-FU is converted to fluorodeoxyuridine monophosphate (FdUMP) either by an indirect mechanism involving a sequential action of thymidine phosphorylase (TP) and thymidine kinase (TK) or via reduction of FUDP by RNR (a predominant process).

Binding of FdUMP to TS forms a stable ternary complex that blocks the access of dUMP by inhibiting the synthesis of dTMP (Sethy & Kundu, 2021). A decrease in the level of dTMP subsequently leads to the reduction of deoxythymidine triphosphate (dTTP) levels, which perturbs the level of other deoxynucleotides resulting in severe disruption of DNA synthesis and repair (Hagenkort et al., 2017).

Despite its several advantages, the clinical application of 5-FU has been limited, due to the development of drug resistance after chemotherapy (Sethy & Kundu, 2021). Most studies of 5-FU resistance have focused on *TYMS*, the gene coding for its target enzyme TS. Overexpression of *TYMS*, an E2F target gene, is linked to resistance to 5-FU, both *in vitro* and *in vivo* (Johnston et al., 1995; Leichman et al., 1997). In addition to *TYMS* expression, increased expression in tumor cells of other enzymes from the 5-FU metabolic pathway such as DPYD or thymidine phosphorylase have been correlated with resistance to 5-FU (Oguri et al., 2005; Soong et al., 2008).

Studies investigating the role of tumor suppressor p53 in modulating the response to 5-FU are quite contradictory. While *in vitro* studies demonstrated that loss of p53 confers cell resistance to 5-FU (Bunz et al., 1999), another study demonstrated that increased p53 expression in tumor tissue correlated with 5-FU resistance (Liang et al.,

2002), yet another study suggested that p53 had no predictive value in the outcome of 5-FU-based therapy (Jakob et al., 2005). Sulzyc et al. proposed that 5-FU-based adjuvant chemotherapy could provide improved prognostic significance in patients assessed for TS expression in conjunction with $p21^{CIP1}$/p53 expression (Sulzyc-Bielicka et al., 2014). Later this group demonstrated that the combined immuno-phenotype of transcription factor E2F1 and TS could be an important predictor of 5-FU sensitivity in colon cancer (Sulzyc-Bielicka et al., 2016) . In addition, Varghese et al. showed that FOXM1, which is regulated by E2F1 plays a pivotal role in 5-FU resistance, at least partially through the regulation of *TYMS* in colorectal cancer (V. Varghese et al., 2019).

An improvement in response to cancer treatment has been reported when 5-FU has been administered in combination with other drugs. For example, sequential treatment of 5FU and the CDK4/CDK6 inhibitor palbociclib inhibited cell proliferation and induced cell death in triple negative breast cancer (Cretella et al., 2019) and in pancreatic adenocarcinoma (Salvador-Barbero et al., 2020) more efficaciously than single agent treatments.

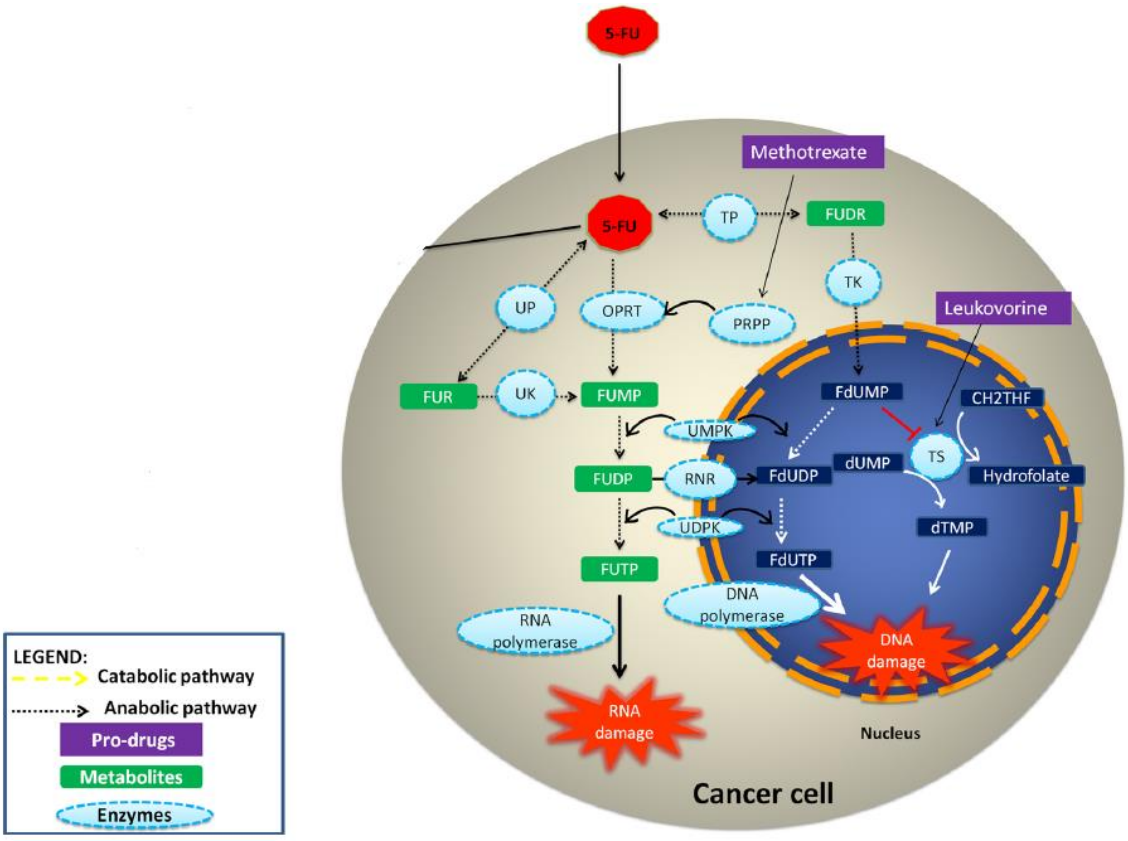

Figure 9. **Metabolic action of 5-FU, its prodrugs, and other typical agents in the cancer cell**. Structures of 5-FU and fluoropyrimidine (5'dUMP, 5'FdUTP, and 5'FUTP). methotrexate, Leucovorin, and major pro-drugs depicting of catabolic pathway of metabolism in cancer cells. **Abbreviations**: FdUMP, fluorodeoxy uridinemonophosphate; FdUTP, fluorodeoxyuridinetriphosphate; FdUDP, Fluorodeoxyuridinediphosphate; dTMP, deoxythymidinemonophosphate; MTHFR, methylene tetrahydrofolate; OPRT, orotate phosphribosyl transferase; RNR, ribonucleotide reductase; PRPP, phosphoribosyl pyrophosphate; TK, Thymidine kinase; TP, Thymidine phosphorylase; TS, thymidylate synthase; UK, uridine kinase; UP, uridine phosphorylase; dUMP, deoxyuridinemonophosphate CH2THF, 5,10-methylenetetrahydrofolate. (Sethy & Kundu, 2021).

## 5. Prostate cancer. Role of E2F

According to the last IARC report in 2020, prostate cancer (PCa) is the second most common cancer in men and the sixth cause of death from cancer in men worldwide (https://gco.iarc.fr/). In 2020, approximately 1.4 million men worldwide were diagnosed with PCa. In Spain, PCa is the first most common cancer in men, with a number of 34,613 new cases in 2020 (https://gco.iarc.fr/). PCa arises from the accumulation of genetic alterations in the epithelium of the prostate gland, whereby the prostate epithelium invades the basal membrane and arrives to the surrounding stroma, establishing a localized invasive adenocarcinoma. This adenocarcinoma can stay confined in the prostate, or can become more aggressive and invade other organs, causing metastasis that ultimately may result in lethality. Lymph nodes, bone, lung and liver are the most frequent sites of distant PCa metastases. Remarkably, metastasis to the bone with skeletal involvements accounts for approximately 90% of patients with advanced PCa (Bubendorf et al., 2000).

The process requires the vascular spread of tumor cells to the bone marrow through the lymph or blood circulatory system. Then, cancer cells adhere to the bone microvasculature and matrix components, invading and surviving into the bone marrow. Finally, a new tumor is stablished in the bone microenvironment and there is a recruitment of reactive stroma from cells in the marrow. Tumor dissemination to the bone can cause bone marrow replacement, spinal cord compression, severe bone pain, cachexia and death (Morrissey & Vessella, 2007).

A common early aberration in prostate cancer is the allelic loss or reduced expression of RB, which occurs in 25% to 50% of prostate tumors (Melamed et al., 1997), including in early lesions (Phillips et al., 1994). Furthermore, targeted inactivation of the RB family of proteins in mice induces epithelial proliferation and apoptosis and is sufficient to produce prostatic intraepithelial neoplasia lesions (Hill et al., 2005). Moreover, inactivation of $p16^{INK4A}$, the upstream activator of RB, has been observed in up to 80% of prostate cancers (Jarrard et al., 2002).

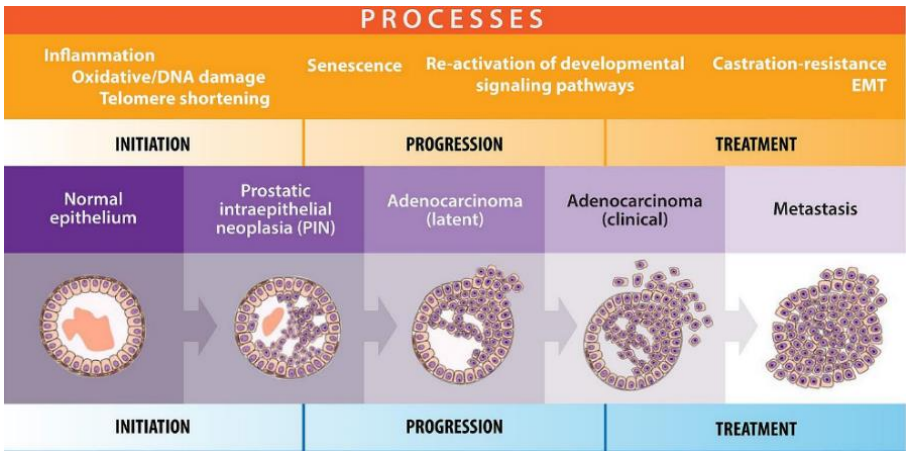


Figure 10. Preclinical model of prostate cancer development. (https://blog.crownbio.com/prostate-cancer-preclinical-models).

Increased expression of E2F1 has been reported to be associated with tumor growth and cell survival of prostate cancer. However, its impact on PCa has not been fully elucidated. Elevated E2F1 expression in prostate cancer represses androgen receptor transcription, which might contribute to the progression of hormone independent PCa (Davis et al., 2006). Furthermore, an E2F1-mediated cancer cell survival pathway involving NF-κB-dependent induction of EGR1 transcription has also been described in prostate cancer (Zheng et al., 2009), and Libertini and collaborators have described E2F1-dependent modifications of androgen dependence, differentiation, and sensitivity to apoptotic stimuli in PCa cell lines (Libertini et al., 2006). More recently, an elevated E2F1 expression was observed in advanced PCa and found that E2F1 knockdown could inhibit prostate tumor growth by sensitizing tumor cells to ICAM-1 mediated anti-tumor immunity (Ren et al., 2014). However, little is known on the role of E2F in promoting resistance of PCa cells to chemotherapy and which E2F targets are key resistance mediators in this type of cancer.

## 5.1. Treatments for prostate cancer

Locally defined disease is often successfully treated with surgery and/or radiotherapy; however, disease recurs in an estimated 15% to 30% of patients (S. G. Roberts et al., 2001). Androgen ablation therapy is highly successful for the treatment of hormone-sensitive prostate cancer, but hormone resistance significantly limits its benefits. Hormonal ablation therapy will control metastatic disease for 18 to 24 months (Denis & Murphy, 1993) but once metastatic prostate cancer ceases to respond to hormonal therapy, median survival decreases significantly (Eisenberger et al., 1998). Although radical prostatectomy (RP) and radiation therapy are the most appropriate treatment for patients with localized PCa, the risk of disease recurrence in RP patients is ~25% (Lapointe et al., 2004).

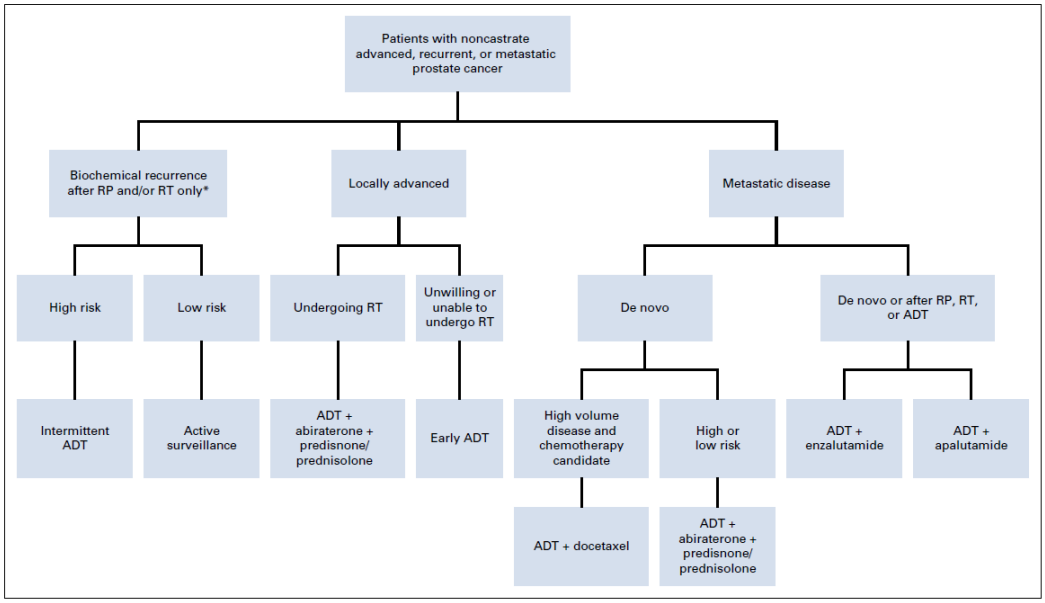


Figure 11. **Initial management of noncastrate advanced, recurrent, or metastatic prostate cancer algorithm**. ADT, androgen deprivation therapy; RP, radical prostatectomy; RT, radiotherapy (Virgo et al., 2021).

There are currently eight FDA-approved therapies indicated for metastatic castrateresistant prostate cancer (mCRPC) that include: docetaxel, abiraterone, enzalutamide, cabazitaxel, sipuleucel-T, radium-223, rucaparib, and olaparib. Unfortunately, the overall survival benefit from these therapies ranges from 2.4 to 4.8 months.

Other therapies, such as 5-FU treatment, either individually or in combination with other agents, have also been examined. Early clinical trials on the role of single-agent 5-FU in advanced prostate cancer reported a low response rate (Yagoda & Petrylak, 1993). Efforts at combining 5-FU or its derivatives with other known anticancer agents have shown limited success owing to the surge of resistances (Blesa et al., 2011, Hellerstedt et al., 2003; Manogue et al., 2018; Woodman et al., 1980). Therefore, it is essential to better understand the biology of prostate cancer in order to identify novel therapeutic strategies to combat drug resistance and improve drug response.



# Hypothesis and objectives

Cell division is controlled by a complex network of regulatory mechanisms that ensure a correct progression of the cell through the cell cycle. An E2F-dependent transcriptional network ensures the timely entry into S-phase through the regulation of genes involved in nucleotide biosynthesis and DNA replication. Remarkably, either a diminished or an elevated E2F activity negatively impact cellular homeostasis, leading to tissue atrophy or oncogenesis, respectively.

Targeted loss of *E2f1* and *E2f2* factors in mice leads to the activation of DNA damage response and subsequent pancreatic atrophy and diabetes (Iglesias-Ara et al., 2015). However, the source of DNA damage in E2f1/E2f2-null pancreas awaits to be resolved. We hypothesize that in the absence of E2f1/E2f2, genes involved in the biosynthesis of nucleotides are downregulated, which would trigger replication stress and subsequent activation of DNA damage response. The restoration of nucleotide levels could attenuate this genomic instability.

Increased E2F expression is commonly associated with tumor growth (Kent et al., 2016, 2017; Lan et al., 2018; Poppy Roworth et al., 2015). Enhanced E2F activity in tumor cells is thought to supply the nucleotides required for their exacerbated DNA replication and cellular proliferation (Villa et al., 2019). Given that nucleotide biosynthesis is central to the capacity of a cell to proliferate, cancer cells are sensitive to nucleotide pool levels for their growth. For this reason, antimetabolite drugs blocking nucleotide production, such as 5-FU, have been widely used to treat different types of cancer, including prostate cancer (Longley et al., 2003).

5-FU irreversibly binds to and blocks the activity of thymidylate synthase (Sethy & Kundu, 2021), an E2F target involved in the *de novo* synthesis of thymidine (Danenberg, 1977; Ishida et al., 2001), resulting in apoptosis of prostate cancer cells (Zhao et al., 2009). However, highly metastatic prostate cancer cells show resistance to 5-FU (Blesa et al., 2011). We hypothesize that other E2F target genes involved in the *de novo* or salvage nucleotide biosynthesis pathways could account for the resistance to 5-FU. Thus, targeting E2F could be an approach to sensitize cells to 5-FU treatment.

To address these hypotheses, the following objectives have been established:

**1. Assessment of the relevance of E2F-regulated nucleotide metabolism *in vivo*.** We will analyze the expression of nucleotide synthesis regulator genes of *de novo* and salvage pathways in *E2f1/E2f2* DKO mice showing pancreatic genome instability and atrophy. Subsequently, we will analyze E2F-mediated transcriptional regulation of those genes deregulated in DKO mice, using *in vitro* approaches. We will use rescue experiments in order to test whether nucleotide scarcity is responsible for the phenotype of DKO mice.

**2. Study the relevance of E2F1/E2F2-regulated nucleotide metabolism in prostate cancer.** We will analyze the role of E2F1 and E2F2 in malignancy, cell cycle progression and genome stability of prostate cancer cells.

**3. Assessment of the use of E2F1/E2F2 as targets for the treatment of prostate cancer.** We aim to elucidate whether silencing E2F1/E2F2 or their target genes involved in nucleotide biosynthesis reverses resistance of metastatic prostate cells to 5-FU, and whether nucleotide scarcity enables a reversion of resistance.

**4. Test a clinical approach to reverse resistance to 5-FU using inhibitors of E2F activity.** We aim to check the possible benefit of combining drugs that inhibit E2F activity, such as palbociclib, with 5-FU to reduce the viability of cancer cells.

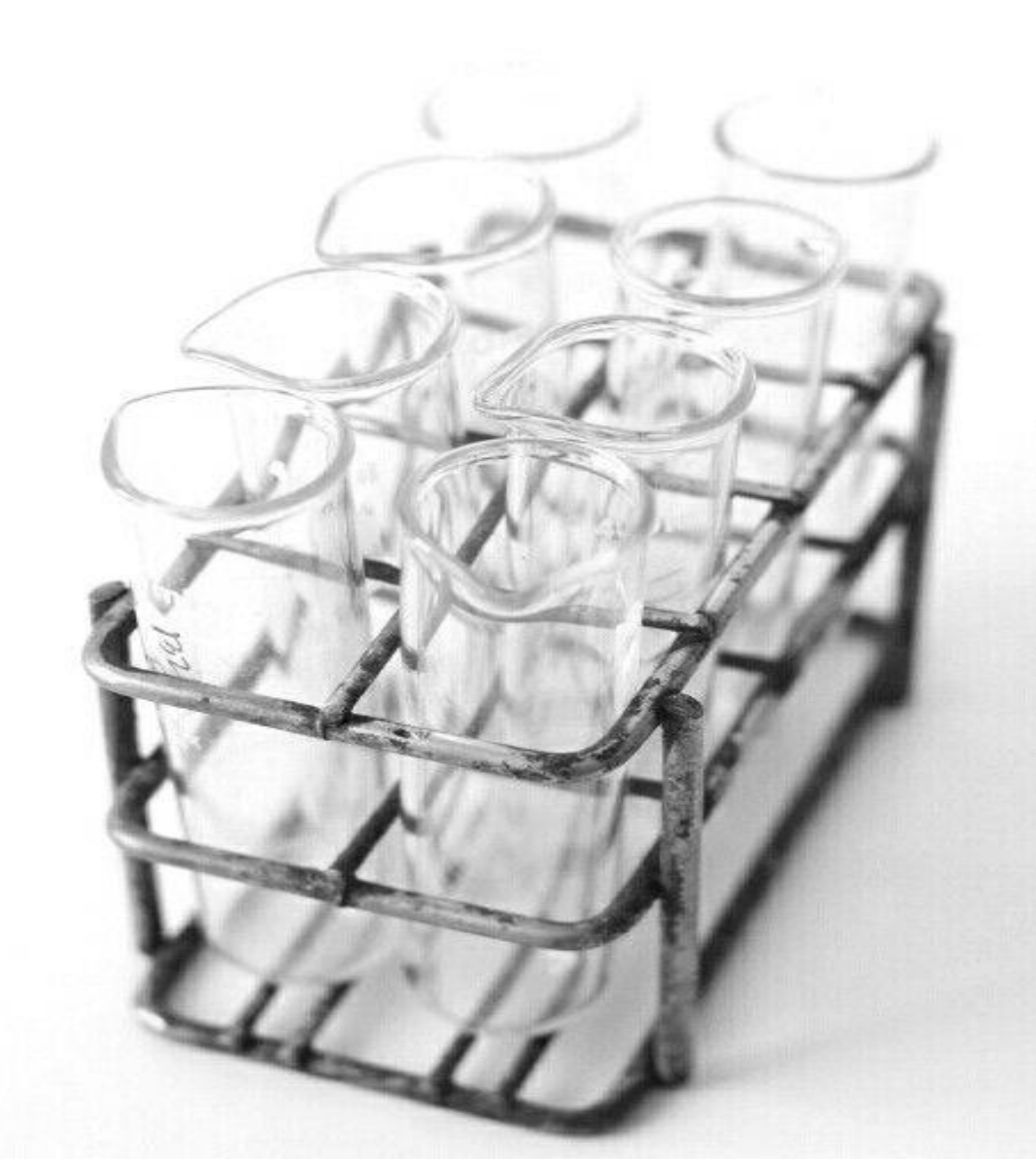

Created by cassie railly

# Material and methods

# 1-MOUSE MODEL

## 1.1 Mouse strains

The E2*f1*$^{-/-}$ and E2*f2*$^{-/-}$ mice belong to the mixed strain 129/Sv x C57BL/6. They were generated by homologous recombination in the laboratory of Dr. Michael E. Greenberg (Children's Hospital, Harvard Medical School, Boston, United States) and have been previously characterized by members of our research group (Field et al., 1996; Murga et al., 2001).

Double knockout mice for E2*f*1 and E2*f*2 (DKO) were generated in our laboratory, by crossing knockout mice for the E2*f*2 gene (E2*f*2 -/-) and heterozygous for the E2*f*1 gene (E2*f*1 +/-). This crossing is carried out in each generation since DKO mice are sterile. The initial characterization of DKO mice has been previously carried out by members of our research group (Iglesias et al., 2004).

In this thesis *E2f1/E2f2* DKO mice were crossed with *Rrm2*$^{TG}$ (kindly provided by Dr. Fdez-Capetillo) mice to generate *E2f1/E2f2* DKO; *Rrm2*$^{TG}$. All procedures were approved by the University of the Basque Country Animal Care and Use Committee.

## 1.2 Mouse genotyping

### 1.2.1 DNA extraction

Animal genotyping was performed using DNA extracted from small tail pieces that were digested for 1 hour at 95°C in 200µM lysis buffer (50 mM NaOH). Cellular lysates were treated with 40 µM Tris-HCT (0.5M, pH8) and extracted DNA was prepared in the supernatant after being centrifuged for 5 min at 1400rpm.

### 1.2.2 PCR (Polymerase chain reaction) assay

The genotyping of the mutant mice for E2f1 was carried out by multiplex PCR, with three different primers that make it possible to simultaneously detect the wild-type and mutated alleles of E2f1. The sequences 5'-GAG GGT TAG GGC TGA TGG AT-3 'and 5'-GAG TCC TCC GAA AGC AGT TG-3' of exon 3 of the E2f1 gene were used as primers, and also the sequence that hybridizes with the inserted region by homologous recombination into exon 3 of the E2f1 gene, corresponding to the Neomycin resistance gene (5'-CCA GAG GCC ACT TGT GTA GC-3'). The amplified fragment size for the wild-type allele was 207 bp and for the mutated allele 180 bp (Figure 12A).

In the same way, the wild and mutated alleles of E2f2 were detected. The sequences 5'-GAT GGA GTC CTG GAC CTG AA-3 'and 5'-CCT AAC ACA TGC ACC CAT TG-3' of exon 3 of the E2f2 gene were used as primers, and also the sequence that hybridizes with the inserted region by homologous recombination in exon 3 of the E2F2 gene, corresponding to the Neomycin resistance gene (5'-CCA GAG GCC ACT TGT GTA GC-3'). The amplified fragment for the wild-type E2f2 allele was 182 bp and for the mutated allele 200 bp. (Figure 12B).

Genotyping of *Rrm2* $^{TG}$ has been performed by the primer sequence of 5'- AAG GAG GGA GGG AGG CTA TT-3' and 5'- TGC CCT GGA GAG CCA GTC TT-3' of the *Rrm2* gene. Transgenic mice can be detected by the sequence of 5'- ACT GGC CGT CGT TTT TAC AAC-3'. The amplified fragment for the *Rrm2* wild type 266bp and additional insertion allele 434bp. (Figure 12C).

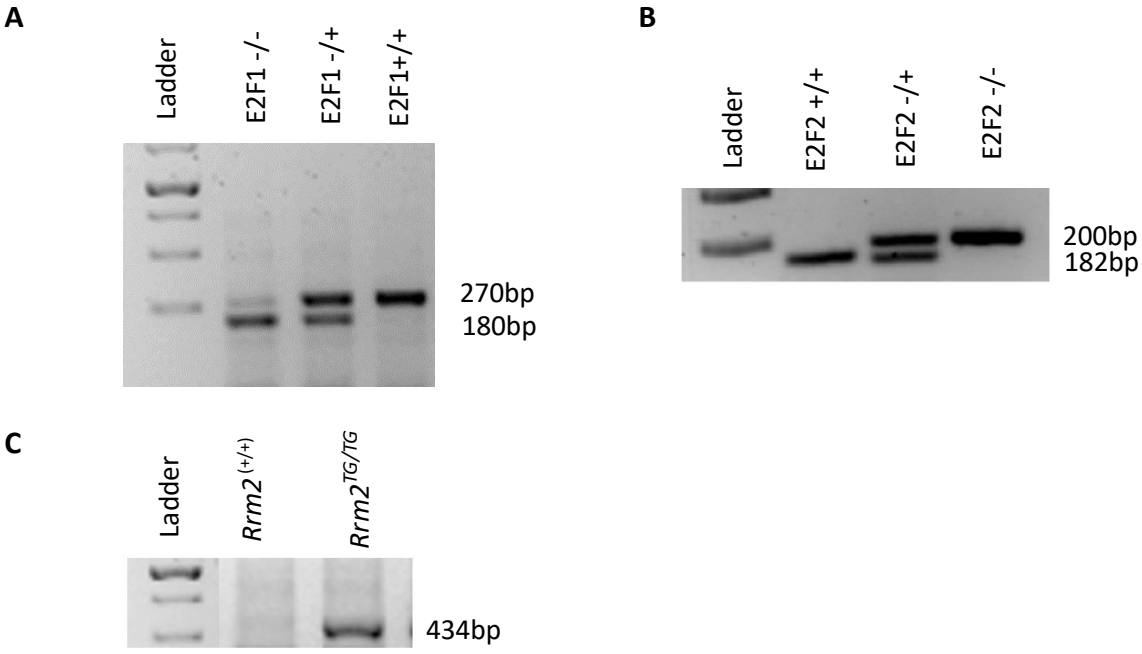


Figure 12. **The figure representing genotyping the E2*F1*, E2*F2*, *Rrm2*$^{TG}$ genes by PCR in mice.**

Genotyping PCRs of DKO were performed in a reaction mix composed of 4mM dNTPs, 17 µM MgCl2, 2µl reaction buffer 10X, 1 µl Taq polymerase 5 µM of each oligonucleotide and 1 µl of genomic DNA. In the case of *Rrm2*$^{TG}$ transgenic mice a reaction mix was composed of 4mM dNTPs, 31 µM MgCl2, 1µl reaction buffer 10X, 0.5 µl Taq polymerase 20 µM of each oligonucleotide and 2.5 µl of genomic DNA. The

amplified PCRs were subjected to electrophoresis in agarose gels at 2% (weight/vol) and 0.01% ethidium bromide in electrophoresis buffer.

This dye is sandwiched between the DNA double helix and fluoresces after being excited with UV light, allowing visualization of nucleic acids.

### 1. 3 Glucose analysis

Blood glucose levels were determined from blood taken from mouse tails, using an automatic glucose monitor (Glucocard). It is an electrochemical measurement biosensor, based on the detection of the product that is formed after the catalysis of glucose by the enzyme Glucose Oxidase. The system has a measurement range from 20 to 600 mg/dl of glucose. Briefly, a test strip is inserted into the glucose meter and is brought into contact with whole blood, so that the blood migrates along the test strip by capillarity. After 30 seconds, the automatic meter shows the blood glucose concentration on its screen. Measurements were made at the same time of day to avoid detecting alterations in glucose concentration due to food intake.

## 2. Cellular biology methods

### 2.1 Cell lines and culture conditions

Prostate cancer cell lines (PC3, DU145, LNCap, 22RV1) and epithelial human prostate cell line BPH-1 were used (Table 3). All these cell lines were kindly provided by Dr. Carracedo. HCT-116 cells were purchased from ATCC.

If nothing else was stated, cell lines were maintained in DMEM medium supplemented with 10% (vol/vol) fetal bovine serum (FBS) at 37°C in a humidified atmosphere containing 5% CO2. Culture media for BPH-1 cell line, as specified by the cell line provider, was the following: RPMI medium +10% FBS +20 ng/ml testosterone (Ref A83380 Merck) +5 μ/ml insulin (Ref 9278 Merck) +5 μ/ml transferrin (Ref 90190 Merck) +5ng/ml sodium selenit (Ref 163 Sigma).

For culturing LNCaP cells, first culture dishes were coated with (5ml) 10% polylysine. After 5 minutes, the solution was removed by aspiration and thoroughly rinsed the surface with sterile tissue culture grade water or PBS. Plates were allowed drying at least hours before introducing cells and medium.

Cells in culture were detached by incubation with trypsin-EDTA solution for about 3 minutes at 37°C and resuspended in a culture medium containing FBS to inhibit further trypsin activity. The cell density of the suspension was evaluated using a Neubauer cell-counting chamber. To count only viable cells, an aliquot of the cell suspension was diluted in the vital dye trypan blue (Ref T8154 Sigma). This dye allows discriminating between live and dead cells since the latter have their plasma membrane damaged,

and thus are blue-stained when treated with trypan blue. For each type of experiment, cells were seeded at a specific concentration, as detailed in Table 4.

Table 3. Detailed list of the different cell lines used during this work. Mutation data was taken from COSMIC database (www.sanger.ac.UK/genetics/CGP/cosmic/).

| Cell line | Cell type | Derivation | Feature | Mutation |
|---|---|---|---|---|
| PC3 | Prostate Adenocarcinoma | Derived from metastatic site: Bone metastasis. 62 year old White man. | Androgen-independent | TP53-STAT3-ATR |
| DU145 | Prostate Adenocarcinoma | Derived from metastatic site: Brain. 69-year-old white man | Androgen-independent | TP53-BRCA2 |
| LNCaP | Prostate Adenocarcinoma | Derived from metastatic site: lymph node. 50-year-old Caucasian man | Androgen-dependent | AR, STAG2, |
| 22RV1 | Prostate carcinoma epithelial cell line | Derived from: Mice Xenograph CWR22R | Androgen insensitive | AR |
| BPH-1 | Human prostate cell lines | Derived from: benign prostate epithelial cells hyperplasia 68-year man | | - |
| HCT | Human colon carcinoma cell line | Derived from: metastatic site Human colon. Man | | ABC36, AATYK |

Table 4. Cell seeding conditions in each experimental setting.

| Procedure | Cell line | Type of plate | Cell density |
|---|---|---|---|
| Western blot | PC3 | 6-well | $0.15\times10^6$/well |
| RT-qPCR | PC3 | 6-well | $0.15\times10^6$/well |
| | DU145 | 6-well | $0.15\times10^6$/well |
| | LNCaP | 6-well | $0.25\times10^6$/well |
| | 22RV1 | 6-well | $0.15\times10^6$/well |
| | BPH-1 | 6-well | $0.15\times10^6$/well |
| | HCT | 6-well | $0.2\times10^6$/well |
| PI staining | PC3 | 6-well | $0.15\times10^6$/well |
| | DU145 | 6-well | $0.15\times10^6$/well |
| pH3/PI staining | PC3 | 6-well | $0.15\times10^6$/well |
| gh2ax/PI staining | DU145 | 6-well | $0.15\times10^6$/well |
| Colony formation assay | PC3 | 6-well | $10\times10^3$/well |
| Cell survival assay (Trypan Blue) | PC3 | 6-well | $0.15\times10^6$/well |
| Cell survival assay (Crystal violet) | PC3 | 96-well | $5\times10^3$ /well |
| | DU145 | 96-well | $5\times10^3$ /well |
| | LNCap | 96-well | $7\times10^3$/ well |

## 2.2 Drugs

All the compounds used in this thesis were subjected to a dose-response analysis to find the best concentration for their maximum activity without any cytotoxic effect.

Table 3. Experimental specifications for the different drugs used during the thesis work

| Drug | Supplier | Function | Procedure | Dose |
|---|---|---|---|---|
| 5-fluorouracil (5-FU)F6627 | Sigma | Inhibitor of cell proliferation | Colony formation assay | 5µM |
| | | | Cell survival assay (Crystal violet) | 0.1, 0.5, 1, 5, 10 µM |
| Palbociclib (PD-0332991) HCl | Selleckchem | Inhibitor of CDK4/6 | Colony formation assay | 0.25, 0.5, 1 µM |
| Nocodazole | Sigma | Inhibit the mitosis | Synchronization | 50ng/ml |

## 2.3 Cell synchronization

### 2.3.1 Synchronization in mitosis

To synchronize cell cultures in M phase, after seeding the HCT cells and incubating for 24 hours to collect cells in mitosis and to prevent their progression to the next cell division cycle, the antimitotic drug nocodazole (50ng/ml) was added to the cultures for another 12 hours. To induce cell cycle entry from the mitotic arrest, nocodazole-treated cells were harvested by mechanical agitation ("mitotic shake off"), washed 2 times with PBS, and reseeded in complete medium in the absence of the drug.

### 2.3.2 Harvest, purification and activation of T lymphocytes

Complete medium (RPMI 1640 supplemented with 10% FCS, 2 mM l-glutamine, 50 U/ml penicillin and 50 ug/ml streptomycin) was used for cell preparation and culture. Lymph nodes were harvested from 4-to-6 week-old wild-type, *E2f1-/-, E2f2-/-* and DKO mice as previously described (Field et al., 1996c), with minor modifications. Lymph node T cells were purified by negative enrichment, consisting of B lymphocyte depletion with magnetic beads coated with biotinylated anti-B220 antibodies, followed by separation with a magnetic particle concentrator (IMagnet, Becton-Dickinson). More than 95% of the remaining cells were T lymphocytes.

For analysis of TCR-mediated responses, purified T lymphocytes (106/ml) were stimulated for the indicated times with immobilized antibodies against CD3 (145.2C11, 0.1–1.5 µg/well; BD).

## 2.4 Transfection

### 2.4.1 DNA Transfection

Plasmid transfection was performed using XtremeGENE HD (Roche) transfection reagent following the manufacturer´s recommendations. For 35 mm culture dishes, the following transfection mixture was prepared: 1µg of DNA, 300 µl Optimem culture medium (GIBCO), and 3 µl of XtremeGene HD. The mixture was incubated for 15 minutes at room temperature and added dropwise to cell cultures.

### 2.4.2 RNA Transfection (Reverse transfection)

Transfection of small interfering RNAs (siRNAs) was performed using Lipofectamine RNAiMAX transfection reagent (Life Technologies) following the manufacturer´s recommendations. Briefly, the transfection reagent was mixed with Optimem (3 µl transfection reagent + 150 µl Optimem per 35mm dish) and incubated for 2 min at room temperature. The transfection reagent/Optimem mix was added dropwise into a tube containing 0.6 µl siRNA (50 µM) diluted in 150 µl of Optimem. The mixture was

incubated for 20 minutes at room temperature and added to the freshly passaged cells suspension, afterward cells were seeded in 6 wells plate.

To knock down the endogenous expression of *E2Fs*, *TK1*, and *DCK*, we used commercial siRNAs from Ambion (Life technologies). As a control, an oligonucleotide with no sequence specificity for any human RNA (siCtrl) was used (Life technologies) table 5.

Table 5. List of small interfering RNAs (siRNAs) used in this work

| siRNA | Reference |
|---|---|
| siE2F1 #1 | s4406 |
| siE2F1 #2 | s4407 |
| siE2F2 #1 | s4408 |
| siE2F2 #2 | s4410 |
| siTK1 #1 | s14160 |
| siTK1 #2 | s14159 |
| siDCK #1 | s103564 |
| siDCK #2 | s187 |
| siCtrl | 4390843 |

## 2.5 Cell cycle analysis

### 2.5.1 DNA content analysis by Propidium iodide (PI) staining

To analyze cell cycle distribution, cells were stained with PI as a measure of DNA content. Cell cultures were fixed with cooled 70% ethanol (vol/vol) at an approximate concentration of $10^6$ cells per ml of ethanol. Fixed cultures were centrifuged for 5 min at 1400 rpm, and the cell pellet was washed with PBS. After washing, cells were resuspended in a 300 µl staining solution composed of 140µM PI, 38mM NaCitrate, and 0.01% Triton X-100 (vol/vol). One µl of RNase A was added and samples were incubated for 30 min in darkness at 37°C. Samples were analyzed on Attune NxT flow cytometer (Thermo Fisher). Data generated by the flow cytometer were processed with the Attune NxT software.

### 2.5.2. Mitotic index analysis by Phospho-Histone H3 staining

To analyze the percentage of cells in mitosis cells were stained with an antibody against the phosphorylated form of Histone H3 on serine 10 (pH3), a specific marker for chromosome condensation occurring in mitosis (Crosio et al., 2002).

Cell cultures were ethanol-fixed as described in section 3.5.1., centrifuged for 5 min at 1400 rpm, and permeabilized with 0.05% Tween-20 in PBS. Subsequently, cells were incubated for 2 hours at room temperature with a specific antibody against pH3 (06-570, Millipore) diluted at 1:500 in 0.05% Tween-20/3% BSA solution. Samples were washed twice with permeabilization solution (0.05% Tween-20), followed by

incubation with the secondary antibody against rabbit immunoglobulin labeled with a green fluorophore (*Alexa Fluor 488*) (A-11008, Invitrogen), for 1 hour at room temperature. After incubation with the secondary antibody three washes were performed with permeabilization solution to finally stain the DNA with PI, as detailed in section 2.5.1.

Samples were analyzed on Attune NxT flow cytometer (Thermo Fisher). Data generated by the flow cytometer were processed with the Attune NxT software.

### 2.5.3 Cytometric Assessment of Histone H2AX Phosphorylation

DNA damage that leads to the formation of DNA double-strand breaks (DSBs) induces phosphorylation of histone H2AX on Ser-139 at sites flanking the breakage. Immunocytochemical detection of phosphorylated H2AX (denoted as γH2AX) thus provides a marker of DSBs (Huang & Darzynkiewicz, 2006.). In order to analyze the percentage of cells undergoing DNA damage repair, cells were stained with an antibody against γ-H2AX protein as a key protein localized on damage sites (Stope, 2021).

Cell cultures were ethanol-fixed as described in section 2.5.1., centrifuged for 5 min at 1400 rpm, and permeabilized with 0.05% Tween-20 in PBS. Subsequently, cells were incubated for 2 hours at room temperature with a specific antibody against γH2AX (05-636, Millipore) diluted 1:500 in 0.05% Tween-20/3% BSA solution. Samples were washed twice with permeabilization solution (0.05% Tween-20), followed by incubation with the secondary antibody against mouse immunoglobulin labeled with a green fluorophore (*Alexa Fluor 488)* (A11001, Invitrogen), for 1 hour at room temperature. After incubation with the secondary antibody three washes were performed with permeabilization solution to finally stain the DNA with PI, as detailed in section 3.5.1., Samples were analyzed on Attune NxT flow cytometer (Thermo Fisher). Data generated by the flow cytometer were processed with the Attune NxT software.

## 2.6. Proliferation assays

### 2.6.1 Trypan Blue Exclusion Test of Cell Viability

In order to analysis the cell viability by Trypan Blue staining, Adherent cells were washed with 1% PBS (phosphate-buffered saline) two times they were incubated with trypsin-EDTA solution at 0.05% for 5 minutes at 37ºC, and re-suspended in the corresponding fresh complete media. To do the cell counting, cells were diluted 1:1 in Trypan Blue Dye 0.4% (Sigma) and 10 µL were loaded in a Neubauer chamber to count viable cells by optical microscopy.

### 2.6.2 Crystal violet staining

To measure cell proliferation by the crystal violet staining method, cells were seeded in 6-well Plates under indicated experimental conditions and then fixed with 3.7% of paraformaldehyde. Then, cells were stained with 0.1% crystal violet (in 70% ethanol/PBS) for 30 minutes and washed twice with PBS. Finally, the stained cells were dissolved in 20% acetic acid in water and the signal was measured at 590 nm.

### 2.6.3 Colony formation assay

The effect of genotoxic compounds on cell survival was assessed by the colony formation assay. First, cells were seeded in low-density conditions (10.000 cells/well on a 6-well plate). Subsequently, cells were transfected and treated as indicated in each case. After 14 days in culture, surviving cell colonies were fixed with 3.7% of paraformaldehyde, stained with 0.1% crystal violet (in 70% ethanol/PBS) for 30 minutes, and washed twice with PBS. Finally, pictures of each well were taken.

## 2.7 Rescue Experiments

### 2.7.1 *In vivo* supply with nucleosides in *E2f1/E2f2* DKO mice

The mice used in this experiment were aged 15 days. WT and DKO mice were injected with 4–40 µg/g nucleoside mixture (EmbryoMax® Nucleosides, Sigma) once every day during 6 days. Controls received an equivalent volume of vehicle PBS. After 4h of the last injection, mice were sacrificed and pancreases were harvested. Freshly collected tissues were placed immediately in liquid nitrogen to perform protein extraction (Figure 13).

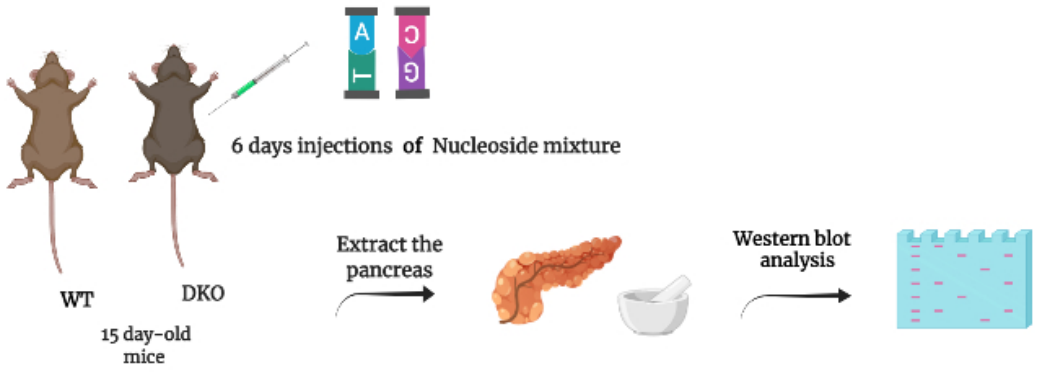


Figure 13. **Figure representation of the experimental design.**

### 2.7.2 *In vitro* supply with nucleosides in PC3 cells

PC3 cells where transfected with non-target control siRNAs (siCTRL) or for E2F1 and E2F2 (siE2F1/2) in 6-well plates. After 4 hours, nucleoside (EmbryoMax® Nucleosides) mixture with increasing concentrations (0, 8, 16, 40 ug/ml), or deoxynucleoside monophosphate (dNMP) mixture (dTMP, dCMP, dGMP, dAMP) (Merck) were added. 24 hours later, the cells were treated with vehicle or 5FU (5µM) during 48h. Cell viability was assessed 48 hours later by trypan blue staining in the rescue experiments with nucleosides and by PI-staining and FACS analysis in the rescue experiments with dNMPs (Figure 14). Samples were analyzed on Attune NxT flow cytometer (Thermo Fisher). Data generated by the flow cytometer were processed with the Attune NxT software.

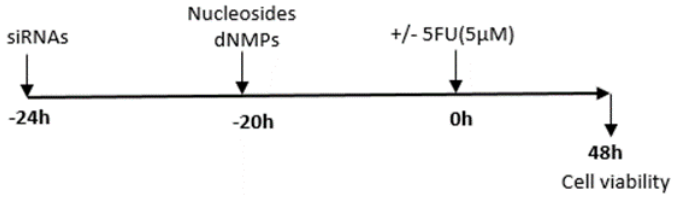


Figure 14. **Schematic representation of the experimental design.**

## 3. Molecular biology techniques

### 3.1 Analysis of gene expression

#### 3.1.1 RNA extraction from cells in culture

RNA was extracted with a total RNA Isolation kit (Nzytech) which is designed for the easy purification of total RNA. This method uses a denaturing lysis buffer containing guanidine thiocyanate, which inactivates cellular RNases, to ensure the recovery of intact RNA molecules. Ethanol is added to provide selective binding of total RNA into the silica membrane column and impurities are efficiently washed away. To prevent contamination with DNA, a DNase I solution is directly added onto the silica membrane of the binding column. High-quality RNA is then eluted in RNase-free water.

Adherent cells were washed with 1% PBS (phosphate-buffered saline) two times, they were prepared for extraction of the RNA by NZY Total RNA Isolation kit. The concentration of purified RNA was determined with a NanoDrop spectrophotometer (Thermo Fisher), by measuring absorbance at 260 nm. RNA samples were stored at –80°C until use.

### 3.1.2 RNA extraction from murine pancreases and T lymphocytes

Total RNA was isolated from pancreatic tissue and T lymphocytes with Trizol reagent (Invitrogen), according to the manufacturer's instructions, purified using the RNeasy kit (Qiagen), and electrophoresed on a denaturing agarose gel to examine for RNA integrity.

### 3-1-3 Real-time PCR

RNA was reverse-transcribed into cDNA using the High-Capacity cDNA Reverse Transcription kit (Life technologies). One µg of previously extracted and purified RNA was reverse-transcribed following the manufacturer's instructions.

To determine the abundance of specific mRNAs, quantitative PCRs (qPCR) were conducted using SYBR Green chemistry. This chemistry uses SYBR Green I dye, which binds to double-stranded nucleic acids emitting fluorescence at 580 nm. During the PCR reaction, SybrGreen dye binds to each new copy of double-stranded DNA, increasing fluorescence as PCR products accumulate during PCR cycles.

Due to the nonspecific nature of SYBR Green I dye´s detection, primer optimization needs to be performed with caution. The amplicon should span one or more introns to avoid amplification of the target gene in genomic DNA. In our case, primers were designed using the PrimerQuest tool from the Integrated DNA Technologies website (https://eu.idtdna.com/site). To identify the optimal primer concentrations that provide optimal assay performance, several optimization reactions were performed by independently varying forward and reverse primer concentrations and using as a template cDNA obtained from control samples.

cDNA samples were mixed with specific primers for each gene in the optimized concentrations (Table 5,6) together with the Power SYBR Green PCR Master Mix product containing SYBR Green dye, AmpliTaq Gold DNA polymerase, dNTPs with a mixture of dUTP/dTTP, ROX dye as a passive reference and buffer components. Quantitative PCR reactions were performed in an ABI Prism 7000 thermocycler (Applied Biosystems) as described previously (Infante et al., 2008). The following PCR program was used: the first cycle at 95 ° C for 10 minutes, required for activation of the polymerase and, the second step of 40 repetitions consisting of 15 s at 95°C for DNA denaturation to take place and 1 min at 60°C to allow annealing between primers and target sequence. After completing these cycles samples were subjected to a dissociation protocol to look for the presence of multiple products and nonspecific amplification, to this end the temperature was gradually increased from 60 to 90°C.

The qPCR method allows reactions to be quantitated by the point in time during cycling when amplification of a PCR product achieves a fixed level of fluorescence, rather than the amount of PCR product accumulated after a fixed number of cycles, as in semi-quantitative PCR reactions. This fixed fluorescence level, known as the threshold, is set within the exponential phase of the amplification curve, which is when the amount of amplified product is proportional to the amount of initial cDNA. The amount of cDNA of a particular sequence is estimated from the number of necessary cycles (CT) for fluorescence to reach the established threshold (T). ABI Prism 7000 SDS Software automatically calculates the optimal threshold.

Relative target gene quantity was determined from a standard curve prepared using serial dilutions of a control cDNA sample. In addition, the quantity of an endogenous control (L19 and EIF2C2) was determined to normalize the amount of cDNA present in each sample. Tables 6 and 7 show the nucleotide sequence of the primers used for qPCR, and the concentration used for each particular primer.

Table 6. List of murine primers used and working dilution in this work

| | **Forward(F)** | | **Reverse(R)** | |
|---|---|---|---|---|
| Target gene | Sequence(5´-3´) | [nM] | Sequence (5´-3´) | [nM] |
| *Tk1* | CAACGAGGGCAAGACAGTAA | 300 | GTGAGCTTCACCACACTCTC | 300 |
| *Ppat* | GGGCAATACTATCTCACCCATC | 300 | TCCCATGAAGCACGGATATTT | 300 |
| *Gart* | CATCCTTGCTCCCTTCCTTTA | 300 | TTGTCCGGCATCTACATCTTC | 300 |
| *Adsl* | TCATGGCCACAGAGAACATC | 300 | CTGCTGGGAAAGCACTCTAA | 300 |
| *Gmps* | GTGCTCTTAACCTCTGAGTCATC | 300 | GTGGGCAGGAGAAATGGTATAA | 300 |
| *Cad* | GTATCCTCTCATCGGCAACTAC | 300 | GACAGCATTCTCCCACTACAA | 300 |
| *Shmt* | CTTCCGTAGAGTCGTCGATTT | 300 | GTCTTTGAGCAGGAAGGATTTG | 300 |
| *Tyms* | CCAACCCTGATGACAGAAGAA | 300 | CACCACATAGAACTGACAGAGG | 300 |
| *Dhfr* | CAACCGGAATTGGCAAGTAAAG | 300 | CCTTGTCACAAAGAGTCTGAGG | 300 |
| *Rrm2* | AGAACTTGGTGGAGCGATTTAG | 300 | CATGGCAATTTGGAAGCCATAG | 300 |
| *Rrm2* | CAGAACCTGGGAACCATCAA | 300 | GCCAGAGAAGCCAAGTTACA | 300 |
| *Dck* | GCAGAGCACTCAAGAGGAAT | 300 | CCACCGTTCAGGTTTCTCATA | 300 |
| *Tk2* | GGTCAATTTACAGCGCAAGATAC | 300 | GTTCCTGACGATCCAGTCAAA | 300 |
| *Uck1* | CCTTTGTGAAACCAGCCTTTG | 300 | CAGGTTGATGGCCACCATATTA | 300 |
| *Aprt* | TGTGTGCTCATCCGGAAAC | 300 | GGGTTCCAAGGCATCTTTCT | 300 |
| *Hprt* | CGAGATGTCATGAAGGAGATGG | 300 | AGCAGGTCAGCAAAGAACTTA | 300 |
| *Gapdh* | CAACGACCCCTTCATTGACC | 300 | CTTGACTGTGCCGTTGAATTTG | 300 |

Table 7. List of human primer used and working dilution in this work

| | **Forward(F)** | | **Reverse(R)** | |
|---|---|---|---|---|
| **Target gene** | Sequence(5´-3´) | [nM] | Sequence(5´-3´) | [nM] |
| *TK1* | AGAAGGAGGTCGAGGTGATT | 300 | CACTGGGCAGTTCTCTTTGT | 300 |
| *Dck* | CCAGATGGTGCAATGTTCAAAG | 300 | CCATCGTTCAGGTTTCTCATACA | 300 |
| *Tyms* | GATTCTCCACCAGAGAAGAAGG | 300 | GTCAACTCCCTGTCCTGAATAA | 300 |
| *E2F1* | TGACATCACCAACGTCCTTGA | 300 | CTGTGCGAGGTCCTGGGTC | 300 |
| *E2F2* | ACGTGCTGGAAGGCATCC | 300 | GCTCCGTGTTCATCAGCTCC | 300 |
| *Aprt* | GCTGAGCTGGAGATTCAGAAA | 300 | CTCACAGGCAGCGTTCAT | 300 |
| *Uck1* | GAGGTGCCGACCTATGATTT | 300 | CTGGCTGTAGAACACCAAGAT | 300 |
| *Hprt* | AGGATTTGGAAAGGGTGTTTATTC | 300 | CCCATCTCCTTCATCACATCTC | 300 |
| *Gmps* | CCTTGGAAACACCAGCATTTG | 300 | GATCAAACCAGGGAGCATCTT | 300 |
| *Umps* | GTTGGAAGCAGGAGGAGATAAT | 300 | GAGATTATGCCACGACCTACAA | 300 |
| *Rrm2* | TATCCCATGTTCTGGCTTTCTT | 300 | ACAGCGGGCTTCTGTAATC | 300 |
| *L19* | CTTCAGGTACAGGCTGTGATAC | 900 | CTTCAGGTACAGGCTGTGATAC | 300 |

## 3.2 Analysis of protein expression

### 3.2.1 Protein extraction from cell in culture

For *in vitro* protein expression analysis, cells were seeded for gene expression analysis in 6 wells plate. All the steps were performed on ice. Cells were lysed using 70 µl Laemmli buffer 5X and boiled for 10 min at 95$^{o}$C Protein concentration was determined using the colorimetric kit DC Protein Assay (Bio-Rad), which is based on the Lowry method. Standards of bovine serum albumin (BSA) prepared at known concentrations were used to determine the concentration of the protein extracts. Protein samples were diluted with 6X protein loading buffer and boiled for 5 min immediately before electrophoresis.

### 3.2.2 Protein extraction from murine pancreases

Total pancreatic homogenates were prepared in liquid nitrogen in a mortar cooled in a bath of methanol with dry ice. The powder was transferred to a tube and proteins were solubilized in lysis buffer (1% SDS, 25 mM Tris pH 7.5, 1 mM EGTA pH 8, 1 mM EDTA pH 8, 2 mM pefabloc, 10 µg/ml leupeptin, 10 µg/ml pepstatin, 10 µg/ml benzamidine, 10 µg/ml aprotinin and 10 mM sodium orthovanadate). 10 µg/ml benzamidine, 10 µg/ml aprotinin and 10 mM sodium orthovanadate). After vortexing, extracts were boiled for 15 min, centrifuged at 13 000 r.p.m. for 5 min at 4 °C, and the pellet was discarded.

Protein concentration was determined using the colorimetric kit DC Protein Assay (Bio-Rad), which is based on the Lowry method. Standards of bovine serum albumin (BSA) prepared at known concentrations were used to determine the concentration of the protein extracts.

### 3.2.3 Western blotting

Proteins were separated according to their molecular weight by SDS-PAGE. Protein samples (20-40 µg per lane) were migrated in a MiniPROTEAN Tetra Cell Vertical Electrophoresis system (Bio-Rad) at constant amperage (25 mA per gel) in 1x Running buffer. BenchMark Pre-Stained Protein Ladder (Life technologies) was loaded as a protein standard to determine the size of the proteins under analysis. Following electrophoresis, proteins were transferred from the gel to a nitrocellulose membrane (Bio-Rad). The transfer was performed using the Mini Trans-Blot Cell transfer system (Bio-Rad) in 1x transfer buffer for 2 hours at 100 V. The membrane was then stained with Ponceau S (Sigma), to confirm the successful transfer of the proteins. Membranes were blocked with 5% (w/v) non-fat dry milk powder in TBS-T (TBS + 0.05 % Tween-20) for 1 hour at room temperature with gentle shaking.

Membranes were incubated with a specific primary antibody diluted in blocking solution overnight at 4°C with gentle shaking (Table 8,9), washed three times for 5 minutes with TBS-T, and subsequently incubated with the corresponding horseradish peroxidase (HRP)-labeled secondary antibody in blocking solution for 1 hour at room temperature. Membranes were again washed as described above. The detection of the antibodies bound to their target proteins was carried out using Pierce ECL Western Blotting Substrate (Thermo Fisher) in a ChemiDoc Imaging System (Bio-Rad). Quantifications were performed by densitometry analysis using the Quantity One software (Bio-Rad).

Table 8. List of murine antibodies used in this work. Antibody, provider, reference, host and working dilution

| Antibody | Provider | Reference | Host | Dilution |
|---|---|---|---|---|
| MCM2 | Santa Cruz | sc-9839 | Goat | 1/3000 |
| γ-H2AX | Millipore | ser 139 | Rabbit | 1/1000 |
| P53 | Santa Cruz | sc-126 | Mouse | 1/200 |
| P21 | Santa Cruz | sc-6246 | Mouse | 1/400 |
| BAX | Santa Cruz | sc-526 | Rabbit | 1/400 |
| B-actin | Sigma | A 5441 | Mouse | 1/3000 |

Table 9. List of Human antibodies used in this work. Antibody, provider, reference, host and working dilution.

| Antibody | Provider | Reference | Host | Dilution | Method |
|---|---|---|---|---|---|
| E2F1 | Santa Cruz | Sc-256 | Mouse | 1/400 | Western blotting |
| E2F2 | Santa Cruz | Sc-633 | Rabbit | 1/400 | Western blotting |
| DCK | Santa Cruz | Sc-393099 | Mouse | 1/1000 | Western blotting |
| TK1 | Invitrogen | A5-29686 | Rabbit | 1/1000 | Western blotting |
| TYMS | Santa Cruz | Sc-3930945 | Mouse | 1/1000 | Western blotting |
| Hsp90 | Santa Cruz | Sc-13119 | Mouse | 1/2000 | Western blotting |
| pH3 (Ser 10) | Millipore | 06-570 | Rabbit | 1/500 | Immuno-staining |
| γH2AX | Millipore | 05-636 | Mouse | 1/500 | Immuno-staining |
| Rabbit AF488 | Invitrogen | A-11008 | Goat | 1/500 | Immuno-staining |
| Mouse AF488 | Invitrogen | A11001 | Goat | 1/500 | Immuno-staining |
| Anti-mouse-HRP | Santa Cruz | sc-3697 | Goat | 1/3000 | Immuno-staining |
| Anti-rabbit-HRP | Santa Cruz | sc-2030 | Goat | 1/3000 | Immuno-staining |
| Cdc2 | Abcam | Ab18 | Mouse | 1/400 | Western blotting |
| Phospho-cdc2 | Cell signaling | 9111 | Rabbit | 1/1000 | Western blotting |

## 3.3 Cloning

### 3.3.1 Plasmid description

Mammalian expression plasmid pRc-CMV-HA-E2F1 has been previously described (Krek et al., 1993).

To construct the wild-type pGL2-TK1Promoter-luc (pTK1-WT-luc) reporter plasmid, 840 bp (-600 to +240) of the human TK1 promoter region was amplified by PCR using human genomic DNA as a template while template primers carried a MluI restriction sequence in their forward 5'-ATTACAGAGGTACATCACCACGCCCGGCTAATTTTTG-3' and XHOI Restriction sequence forward 5'-TGCGCCTCCGGGAAGTTCACGAACCCGAGTACTC-3'. Following PCR program was used: the first cycle at 95 ° C for 3 minutes. The second step of 45 repetitions consisting of 1min at 95°C, 1 min at 55°C and 3 min at 77°C and

a third step 3 min at 77°C. The orientation and integrity of all constructions were confirmed by DNA sequencing. PCR product was digested with MluI and XHOI and cloned into the pGL2-basic luciferase reporter vector (Promega).

### 3.3.2 Luciferase activity assays

For luciferase activity assays HCT-116 cells seeded in six-well plates were transfected with Ectopic E2F1 expression induces TK1 promoter activity. Asynchronously growing HCT116 cells were transfected as described in 2-4-1 with pTK1-luc (250 ng) along with increasing amounts (50, 80, 150, 250, 500 ng) of a plasmid overexpressing E2F1 (pCMV-E2F1-HA) or empty pCMV vector (pRc-CMV) and 50 ng of the Renilla luciferase reporter vector (pRL-TK). The luciferase activity was measured 48 h after transfection of HCT116 cells. Data were normalized to the transfection efficiency estimated by the activity of *Renilla* luciferase control in each sample.

Using the Dual-Luciferase Reporter Assay System (Promega), the reporter firefly luciferase activity was measured 48 h after transfection, following the manufacturer´s recommendations. Data were normalized to the transfection efficiency estimated by the activity of Renilla luciferase in each sample, thus obtaining Relative Luciferase Units (RLU). The luciferase activity measured in cells transfected only with reporter vector was used as a reference to calculate fold induction.

## 4. Bioinformatics analysis

*cBioportal* (Cerami et al., 2012; Gao et al., 2013)and *KM plotter* (Nagy et al., 2021) online tools, open-access resources for performing correlations between gene expressions in many cancer patients, using samples obtained from TCGA database. To investigate *in silico* the possible correlation between the expression of *E2F1* and *E2F2* genes and disease-free survival (DFS).

*CANCERTOOL* (Cortazar et al., 2018) is an open-access resource for the analysis of gene expression and functional enrichments in different types of cancer, including prostate cancer Here, it was used to explore the relationship between *E2Fs, TK1, dCK, TYMS* expression in PCa. A Student T-test was performed to compare the mean gene expression between two groups. We also analyzed the relationship between *E2Fs, TK1, TYMS*, and *dCK* expression levels in PC and disease-free survival (DFS). A Mantel-Cox test was performed to compare the differences between curves, while a Cox proportional hazards regression model was performed in survival analysis to calculate de Hazard Ratio (HR) between the groups analyzed and Gleason score analysis which present mRNA expression levels of samples grouped by their Gleason grade.

*ConSite* is a user-friendly, web-based tool for finding *cis*-regulatory elements in genomic sequences. Predictions are based on the integration of binding site prediction

generated with high-quality transcription factor models and cross-species comparison filtering (phylogenetic footprinting) (Sandelin et al., 2004). We examined the sequence of the *TK1*and *DCK* gene promoter to identify transcription factor motifs.

## 5. Statistical analysis

GraphPad Prism 8.0 (GraphPad Software) was used for statistical analysis and data representation. Data are given as mean ± SD. Statistical analysis was performed using ANOVA and Fisher's test. Significance was defined by $p < 0.05$

## 6. Solutions

**Protein lysis buffer**

10 mM $NaH_2PO_4$ (pH7.2)

1 mM EDTA

1 mM EGTA

150 mM NaCl

1% NP-40 (v/v)

10 mM β-glycerophosphate

10 mM PMSF

10 mM $Na_3VO_4$

10 µg/ml Leupeptin

10 µg/ml Aprotinin

10 µg/ml Pepstatin

**1X PBS (pH 7.6)**

137 mM NaCl

2.7 mM KCl

1.8 mM $KH_2PO_4$

8.1 mM $Na_2HPO_4$

**6X Protein Loading Buffer**

350 mM Tris-HCl pH 6.8

34.4% Glycerol (v/v)

10% SDS (w/v)

10% β-mercaptoethanol (v/v)

0.06% Bromophenol blue (w/v)

**SDS-PAGE Running buffer**

0.25 mM Tris base

1.92 mM Glycine

1% SDS

**Transfer buffer**

120 mM Tris base

40 mM Glycine

20% Methanol

**Tris Buffered Saline (TBS) (pH 7.6)**

20 mM Tris base

137 mM NaCl

**Stacking gel for SDS-PAGE**

63 mM Tris HCl pH6.8

0.1% SDS (v/v)

5% Acrylamide

0.1% TEMED

0.1% APS

**Resolving gel for SDS-PAGE**

376 mM Tris HCl pH8.8

0.1% SDS (v/v)

Acrylamide (variable %)

0.04% TEMED

0.1% APS

**TE**

10mM Tris HCl pH8

# Results

# Objective 1. Assessment of the relevance of E2f-regulated nucleotide metabolism *in vivo*

## 1.1. Depletion of E2f1 and E2f2 in mice results in DNA damage and pancreatic tissue atrophy

Our group has previously shown that simultaneous depletion of *E2f1* and *E2f2* (DKO) leads to the activation of p53-dependent apoptosis, and subsequent pancreatic atrophy (Iglesias-Ara et al., 2015). To begin to assess the mechanism by which compound loss of E2f1/E2f2 induces this phenotype in mice, we first confirmed DNA damage induction by examining the expression of γ-H2AX, a typical molecular marker of DNA damage, in pancreatic tissue collected from DKO and WT mice (n=3 per genotype). Consistent with the results previously published by our group, DKO samples showed increased levels of γ-H2AX, compared to the WT controls (Figure 15A). Associated with the induction of a DNA damage response, pancreas from DKO mice underwent significant atrophy in 3-4 month-old animals (Figure 15B).

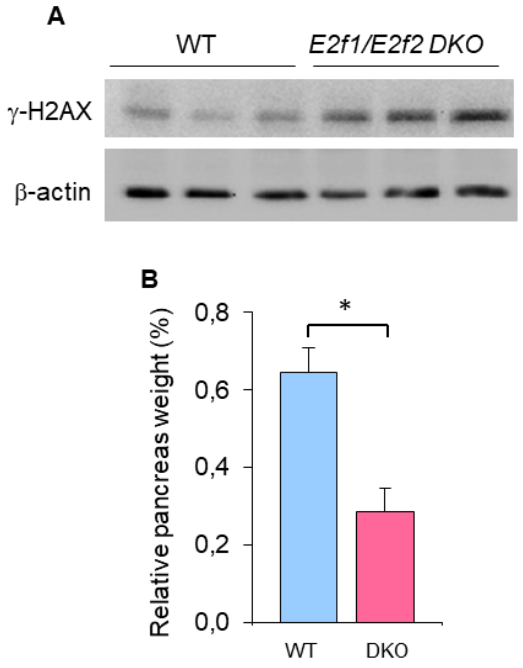


Figure 15. **Pancreas of *E2f1/E2f2* DKO mice exhibits evidence of activation of a DNA damage response.** A) Western blot analysis of γ-H2AX in extracts prepared from pancreas of 1-month-old WT and DKO mice. The results obtained from 3 mice per genotype are shown. Expression of β-actin was used as the loading control. B) Pancreas weight expressed as the fraction of total body weight of 3 to 4 month-old animals. Shown are means ± SD for 5 mice per genotype. *p<0.0001.

## 1.2. Role of E2f factors in the regulation of nucleotide biosynthetic genes

### 1.2.1 Gene expression analysis of nucleotide synthesis regulators of the *de novo* pathway in E2f1/E2f2 DKO pancreas

The sources of DNA damage in E2f1/E2f2-null pancreas could be several, including reactive oxygen species, lipid peroxidation or DNA replication stress, among others (Iglesias et al., 2004). Given that E2f factors' main role is to promote the expression of genes necessary for the duplication of DNA molecules, we wondered whether the observed DNA damage response in DKO samples could be the result of some nucleotide deficiency that would lead to replication stress. To explore this possibility, we set out to analyze the expression of genes coding for enzymes involved in nucleotide metabolism.

To examine the expression level of genes that regulate DNA metabolism, we isolated RNA from pancreatic tissue of DKO and WT mice (n=3 per genotype) and we carried out reverse transcription Q-PCR (RT-QPCR) analyses of genes involved in the *de novo* nucleotide synthesis pathway. RT-QPCR analyses showed that none of the examined genes has a significantly different expression level in DKO and WT pancreatic extracts (Figure 16).

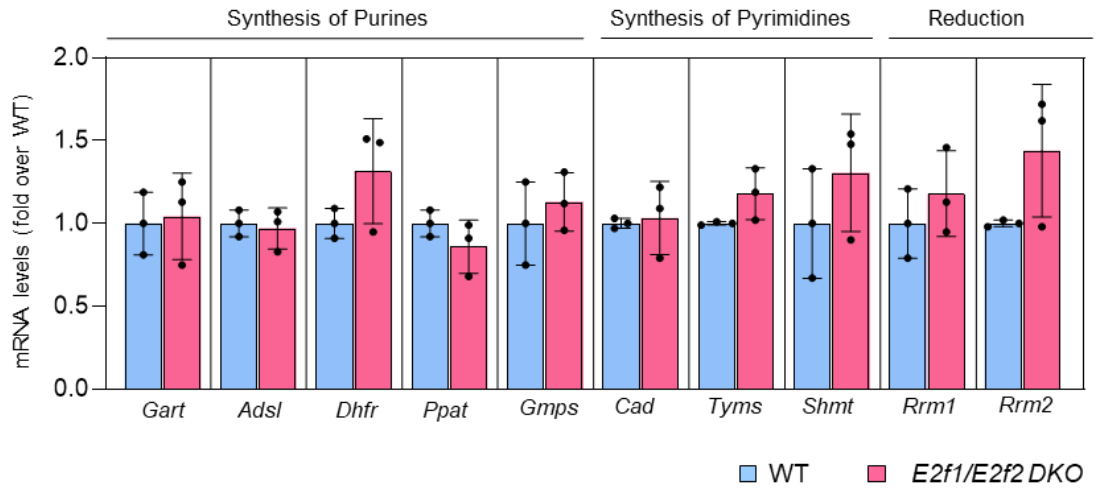


Figure 16. **Gene expression analysis of regulators of *de novo* pathway for the synthesis of nucleotides in WT and DKO pancreas**. RT-QPCR expression analysis of the indicated genes in pancreas isolated from 1 month-old WT and DKO mice. The genes are grouped based on their role in the synthesis of purinic or pyrimidinic ribonucleosides, or in their subsequent reduction to desoxynucleosides. *Gapdh* was used as a normalization control. Results are expressed as fold over WT (mean±S.D.) from three mice per genotype.

These results suggested that genes involved in *de novo* nucleotide synthetic pathway may not be involved in the DNA replication stress of DKO cells.

### 1.2.2. Gene expression analysis of nucleotide synthesis regulators of the nucleotide salvage pathway in E2f1/E2f2 DKO pancreas

The alternative pathway of nucleotide synthesis, known as the *nucleotide salvage pathway*, is used preferentially to the *de novo* pathway to synthesize nucleotides by certain cell types, such as brain cells and polymorphonuclear leukocytes (Fasullo & Endres, 2015). Pancreatic cancer cells have also been reported to depend on the salvage pathway to facilitate survival and growth (Lyssiotis & Cantley, 2013). We wondered whether the levels of enzymes involved in the salvage pathway of nucleotide biosynthesis were deregulated in DKO mice.

To check the expression of genes involved in the salvage pathway, we performed RT-QPCR analysis in the pancreatic extracts of WT and DKO mice (n=3 per genotype). Interestingly, the expression levels of genes encoding for key proteins of the salvage pathway, namely *Tk1*, *Tk2*, and *Dck*, were found significantly downregulated in cells lacking E2f1/E2f2 compared to WT cells (Figure 17).

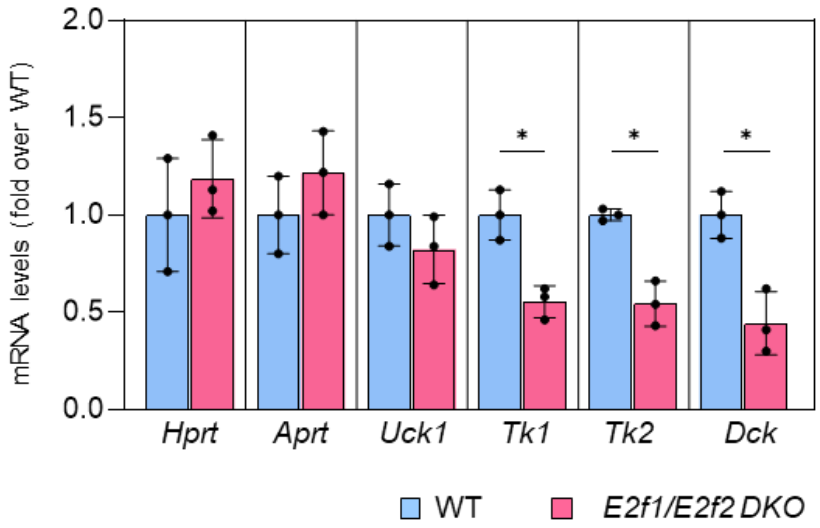


Figure 17. **Gene expression analysis of regulators of the salvage pathway for the synthesis of nucleotides in WT and DKO pancreas**. RT-QPCR expression analysis of the indicated genes in pancreas isolated from 1 month-old WT and DKO mice. *Gapdh* was used as a normalization control. Results are expressed as fold over WT (mean±S.D.) from three mice per genotype.

These results suggest that E2f1/E2f2 could be controlling cellular nucleotide pools through the salvage pathway, by regulating the expression of *Tk1*, *Tk2* and *Dck*.

### 1.2.3. Assessment of Tk1, Tk2, and Dck expression during cell cycle progression

It is well established that expression of *E2f1/2* and of their target genes is cell cycle-regulated, with an increase in gene transcription at the G1/S transition (Ishida et al., 2001). To examine in more detail the regulation of *Tk1*, *Tk2* and *Dck*, we analyzed their expression during cell cycle progression. Pancreatic tissue is not a suitable organ in which to study cell-cycle regulated gene expression. For this reason, we made use of two *in vitro* systems that are commonly used for this purpose: primary mouse T lymphocytes purified from lymph nodes and HCT116 human colorectal cancer cells (Infante et al., 2008; Lim et al., 2006).

Primary mouse T lymphocytes purified from lymph nodes are arrested in G0 and undergo a synchronized cell cycle entry and subsequent cell division in response to the activation of the T cell receptor complex (TCR) with anti-CD3, providing a good model to study cell cycle progression. According to the results previously reported by our group, G1/S transition occurs around 36-48 hour after TCR activation (Infante et al., 2008), followed by several rapid cell cycles over the subsequent ~96 hours (Lea et al., 2003). Keeping this in mind, we extracted RNA from murine WT T lymphocytes after 0, 24, 48, 72 and 96h of TCR activation with anti-CD3 (n=4). RT-QPCR analyses of *E2f1*, *Tk1*, *Tk2* and *Dck* were performed. Despite gene expression variability from mouse to mouse, RT-QPCR data show (Figure 18A) that at least in 3 different experiments *E2f1* expression increased at 24 hours and was maintained at 48 hours, as in our previous study (Infante et al., 2008). *Tk1* was expressed slightly later than *E2f1*, consistent with its role as an E2f target. By contrast, *Tk2* expression did not change during the cell cycle, suggesting that *Tk2* is not transcriptionally regulated by E2f. Regarding *Dck*, the results were less consistent, although in 2 experiments its expression was moderately increased in the time-points where *E2f1* expression was upregulated.

HCT116 cells can be synchronized in mitosis (M) after treatment with the microtubule inhibitor nocodazole (Noco) (Fox, 2004). This method provides the best synchrony for the G1 and G1/S transition, which can be monitored by flow cytometry analysis of DNA content. As shown in the schematic diagram (Figure 18B), HCT116 cells were treated with Noco for 24 h to synchronize the cells in mitosis. Subsequently, cells were released from mitosis and collected at the indicated time-points for cell cycle profiling and RNA analysis. The cells that were treated with Noco were blocked in M, and upon removal of the drug, cells were released into the cell cycle and progressed through G0/G1, S and G2/M phases in a synchronized manner, as evaluated by propidium iodide staining and flow cytometry analysis (Figure 18C). RNA was extracted at the same time points after the release, and RT-QPCR analyses of the indicated genes were performed during the cell cycle progression (Figure 18D).

**A**

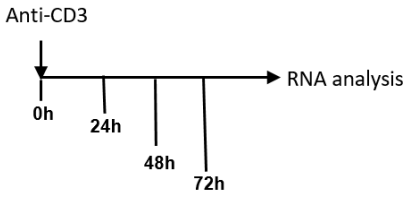


**B**

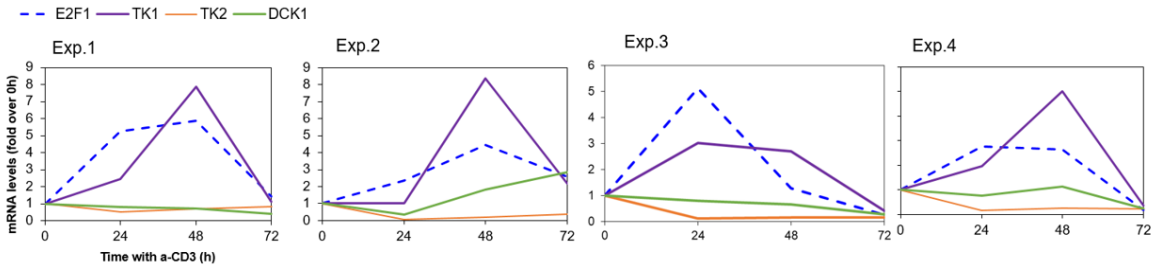


**C**

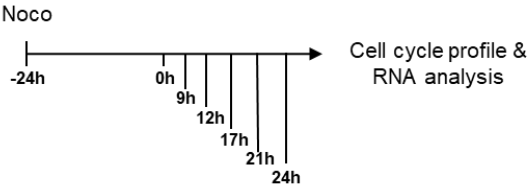


**D**

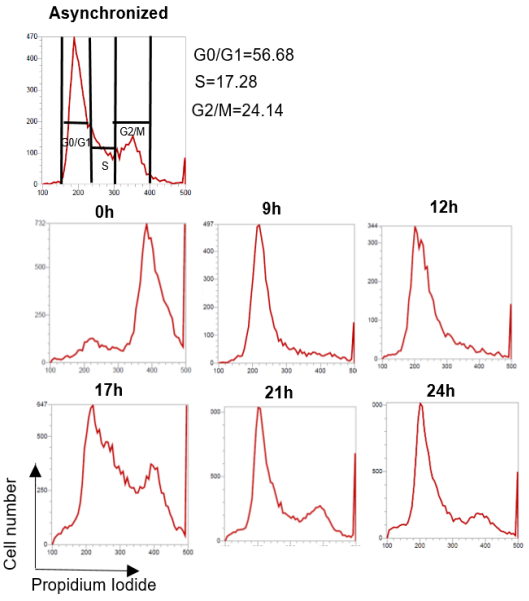


**E**

| | 0h | 9h | 12h | 17h | 21h | 24h |
|---|---|---|---|---|---|---|
| G0/G1(%) | 11.8 | 46.4 | 40.6 | 30.9 | 42.4 | 47.8 |
| S(%) | 7.8 | 24 | 24.5 | 27.6 | 21.7 | 20.6 |
| G2/M(%) | 62 | 11.1 | 13.5 | 28.5 | 21.8 | 17.3 |

**F**

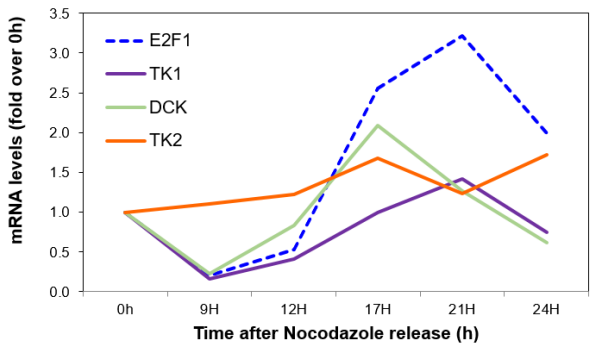

Figure 18.***TK1* and *DCK* gene expression correlates with *E2F1* expression during cell cycle progression in murine primary T lymphocytes after activation of the TCR and in mitosis-synchronized HC116 cell line after nocodazole release.** A) Experimental setup for cell cycle and gene expression analysis in murine primary T lymphocyte after activation of TCR. B) RT-QPCR analyses of *E2f1*, *Tk1*, *Tk2* and *Dck* performed using RNA extracted from murine T lymphocytes at several time-points after their activation with anti-CD3. Expression values were normalized to the expression of *Eif2c2*, used as standard control. Data from 4 independent experiments are shown (n=1 per experiment). Data are represented as fold-change (mean±SD) relative to the sample at 0 h. C) Experimental setup for cell cycle and gene expression analysis in mitosis-synchronized HCT116 cells. HCT116 cells were treated with noco (50ng/ml) for 24 h to synchronize the cells in mitosis. Mitotic cells were harvested by mitotic shake-off and stimulated to enter cell cycle by plating in noco-free medium. Cells were harvested at the indicated time points after exit from mitotic arrest. D) Flow cytometry analysis of the DNA content of PI-stained HCT116 Asynchronous cells. E) DNA content analysis of cell cycle distribution are shown. F) RT-QPCR analyses of *E2F1*, *TK1*, *TK2* and *DCK* are shown. The expression values were normalized to *EIF2C2* expression, used as a standard control.

RNA expression data indicated that *E2F1* levels, which were low at 9h after mitotic release, accumulated during the following hours with a peak at 17-21 h. The expression pattern of *TK1* and *DCK* correlated with that of *E2F1* during the cell cycle. By contrast, the levels of *TK2* did not change substantially throughout the experiment. These results suggest that that *TK1* and *DCK* are transcriptionally regulated by E2F1, whereas *TK2* is not. The downregulated expression of Tk2 in E2f1/2-deficient pancreatic tissue is probably an indirect effect of E2f absence.

### 1.2.4. Analysis of the role of E2F1 in the transcriptional regulation of TK1 gene

To functionally demonstrate that E2F1 regulates the expression of *TK1* and DCK at the transcriptional level, we examined their promoters to search for E2F binding motifs. Human *TK1* promoter sequence analysis using *ConSite* tool identified 5 possible E2F binding sites (Figure 19B), suggesting that regulation of *TK1* promoter requires binding of E2F to its target elements to induce transcription. In the case of DCK, *ConSite* tool only identified 1 possible E2F binding site (Figure 19A). Thereby, we selected TK1 for further studies.

To analyze the transcriptional regulation of TK1 by E2F1, we cloned the promoter region of *TK1* (-600 to +240) (Figure 5B) into the pGL2-Basic reporter vector that carries the firefly luciferase gene, to generate pTK1-luc reporter plasmid. Subsequently, we transfected HCT116 cells with the pTK1-luc construct along with increasing amounts of a plasmid overexpressing E2F1 (pCMV-E2F1-HA) or empty pCMV vector. The luciferase activity was measured 48 h after transfection of HCT116 cells. Data were normalized to the transfection efficiency estimated by the activity of *Renilla* luciferase control in each sample. Luciferase analyses showed that ectopic E2F1 expression induced a

significant *TK1* promoter activity in a dose-dependent manner, from 1.5- to over 2.5-fold (Figure 19C).

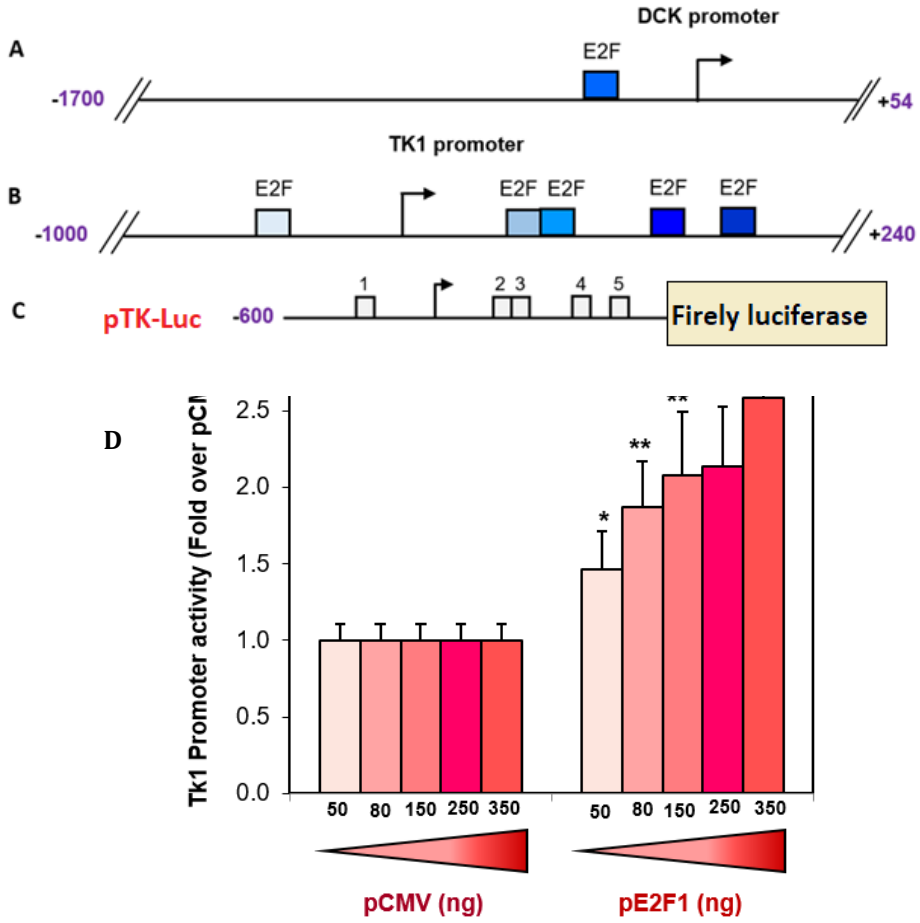


Figure 19. ***TK1* gene is regulated by E2F1 at the transcriptional level.** A) Schematic representation of E2F transcription factor binding sites in human *DCK* regulatory region (-1700 to 54). E2F motifs are indicated as boxes and transcriptional start site is depicted with an arrow. B) Schematic representation of E2F transcription factor binding sites in human *TK1* regulatory region (-600 to +240). E2F motifs are indicated as boxes and transcriptional start site is depicted with an arrow. C) Promoter-luciferase construct of *TK1*. The nucleotide positions of the promoter construct are numbered relative to the transcription start site. C) Asynchronously growing HCT116 cells were transfected with pTK1-luc and increasing amounts of E2F1 (50 ng, 80, 150, 250, 350 ng) per well in a 12-well plate. Values are represented as luciferase activities relative to pTK1-luc activity of cells transfected with empty pCMV control. Shown are the results (mean±SD) of four independent experiments. *p<0.05, **p<0.005, ***p<0.0001 *vs.* pCMV.

The results obtained from the luciferase reporter assay indicate that *TK1* is directly regulated by E2F1.

## 1.3. Experimental approaches to rescue the aberrant phenotype of E2f1/E2f2-null mice

### 1.3.1. Phenotypic impact of an extra allele of *Rrm2* gene in DKO mice

Our gene expression analyses showed that several genes controlling nucleotide synthesis are downregulated in tissue from E2f1/E2f2-deficient mice, which could account for the degenerative phenotype observed in these mice. We wondered whether increasing nucleotide synthesis in DKO mice could alleviate replication stress and prevent pancreatic atrophy in this model. The group of Fernández-Capetillo has demonstrated that increasing *Rrm2* gene dosage potentiates nucleotide synthesis and prolongs survival of an ATR-hypomorph mutant mouse model undergoing replication stress and subsequent tissue atrophy (Lopez-Contreras et al., 2015). *Rrm2* encodes a regulatory subunit of ribonucleotide reductase (RNR), a key enzyme that mediates the synthesis of deoxyribonucleotides from ribonucleotides.

To check this possibility, we introduced an extra allele of *Rrm2* in *E2f1/E2f2* DKO mice by breeding the mice with *Rrm2* transgenic mice (*Rrm2*$^{TG}$, kindly provided by Dr. Fdez-Capetillo). As shown in Figure 20A, DKO;*Rrm2*$^{TG}$ mice have a survival rate that is similar to that of DKO mice. In female mice, DKO;*Rrm2*$^{TG}$ mouse survival is even lower than that of DKO mice. The levels of serum glucose in DKO;*Rrm2*$^{TG}$ were as high as in non-transgenic DKO mice (Figure 20B). Regarding the pancreas, a similar reduction of pancreas weight was observed in DKO and DKO;*Rrm2*$^{TG}$ mice (Figure 20C). Therefore, introducing an extra *Rrm2* allele in DKO mice does not rescue the poor survival rate, hyperglycemia and pancreatic atrophy of *E2f1/E2f2* DKO mice.

**A**

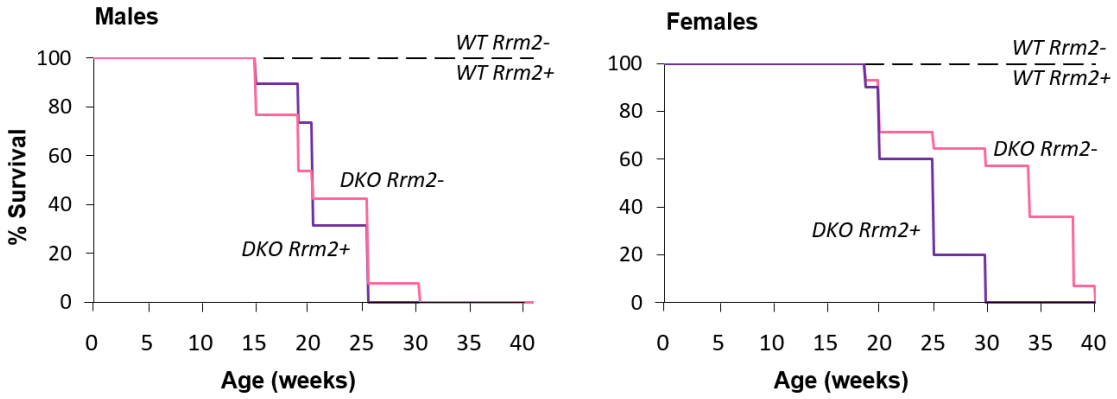

**B**

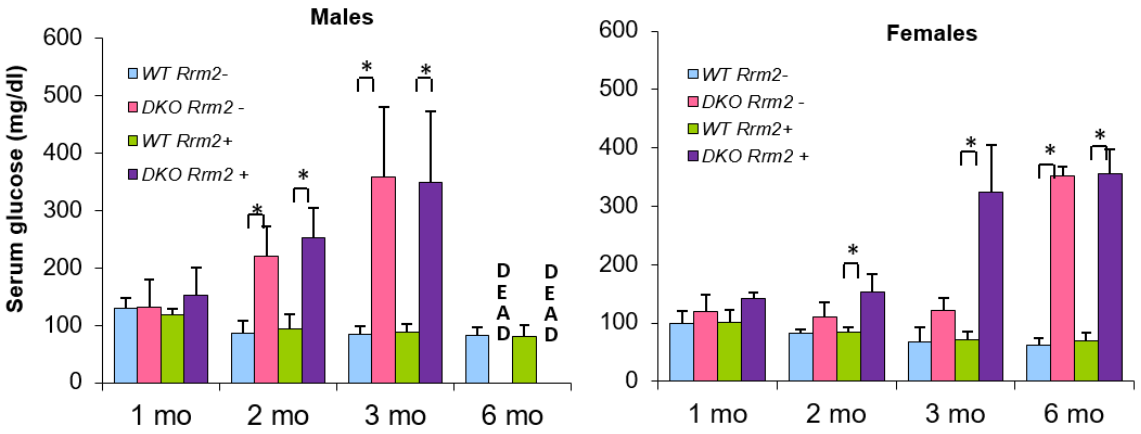


**C**

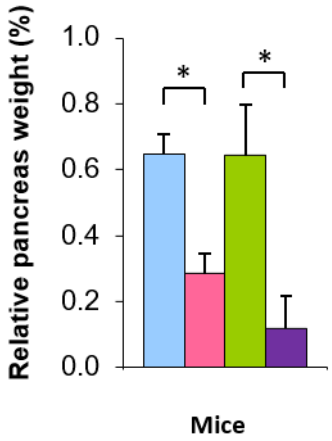


Figure 20. **Increasing allelic dose of *Rrm2* in *E2f1/E2f2* DKO mice does not prevent premature death, hyperglycemia and pancreatic atrophy**. A) Life spans of WT, WT;*Rrm2*$^{TG}$, DKO and DKO;*Rrm2*$^{TG}$ mice (n=14-20/genotype) analyzed using a non-parametric test and expressed as Kaplan-Meier survival curves (DKO;*Rrm2*$^{TG}$ *vs.* DKO, not significant in males and $p<0.001$ in females. DKO;*Rrm2*$^{TG}$ or DKO *vs.* WT, $p<0.0001$ in both males and females). B) Spot blood glucose levels were determined at the indicated times. Results are the means ± SD for 10 animals per sex group and genotype. *$p<0.0001$. C) Pancreas weight expressed as the fraction of total body weight of 3 to 4 month-old animals. Shown are means ± SD for 5 mice per genotype. *$p<0.0001$.

Thus, enhancing nucleotide metabolism by increasing the expression of the rate-limiting enzyme RNR does not prevent DNA replication stress and damage in DKO pancreas.

### 1.3.2. Effect of an exogenous nucleoside supply on the genomic stability of E2f1/E2f2 DKO pancreas

One possibility that may account for the failure to revert the aberrant phenotype of DKO pancreas after introducing an extra *Rrm2* allele is that animals lacking E2f1/E2f2 could have a deficiency of ribonucleotide precursors. If this were the case, overexpressing Rrm2 would not help increase the production of deoxyribonucleotides due to lack of substrates. To examine this possibility, we sought to assess the effect of administering exogenously a mixture of nucleosides to the mice. In fact, Kerem's group has shown that replication stress elicited by oncogenes, which is a consequence of nucleotide deficiency, can be restored by exogenously supplied nucleosides (Bester et al., 2011). We examined whether administration of a cocktail of nucleosides to DKO mice could have a similar rescue effect in the DNA damage response of pancreatic cells.

To this end, we designed an *in vivo* experiment in which we injected intraperitoneally young DKO and WT mice with increasing concentrations of nucleosides (0, 8, 16, 40 μg/ml; Embryomax) for 6 days (Figure 21A). Subsequently, we analyzed the levels of markers of DNA damage and apoptosis (γ-H2AX, p53, Bax), as well as a marker of DNA replication activity (Mcm2) in pancreatic tissues by western blot analysis. We compared the accumulation of these proteins in WT and DKO extracts upon treatment with the nucleosides *versus* the untreated samples (Figure 21B).

Treatment with nucleosides did not affect significantly the levels of γ-H2AX, p53 and Bax proteins in WT pancreas, except at the highest dose of nucleosides, which may be toxic for the cells (Figure 21B). Interestingly, we found a substantial reduction in γ-H2AX, p53 and Bax protein levels in pancreatic samples derived from DKO mice treated with nucleosides relative to untreated DKO samples, to levels similar to those in untreated WT mice (Figure 21B). By contrast, the treatment with nucleosides did not affect the aberrant accumulation of Mcm2 (not a DNA damage marker) in DKO pancreas.

**A**

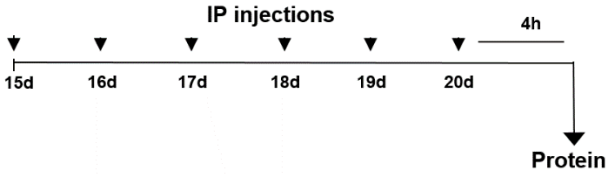


**B**

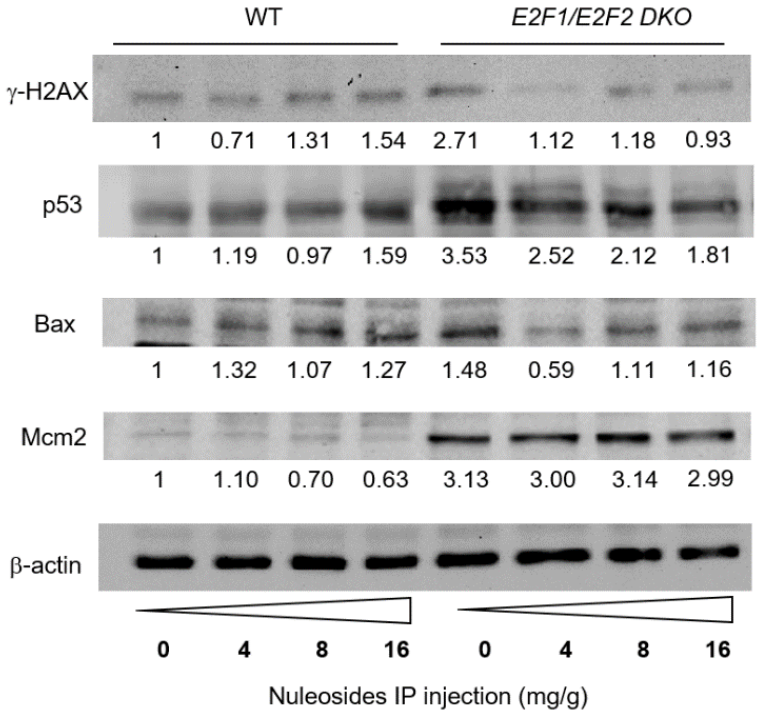


Figure 21. **Exogenous supply with nucleosides *in vivo* ameliorates replication stress in DKO mice.** A) Schematic representation of the experimental design.15 days-old WT and DKO were injected intraperitoneally with increasing concentrations of Embryomax (0, 8, 16, 40 μg/ml) for 6 days. The pancreas was isolated and pancreatic extracts were prepared for western blot analysis. B) Western blot analysis of γ-H2AX, p53, Bax and Mcm2 in extracts prepared from pancreas treated with the indicated concentrations of nucleoside. Expression of β-actin was used as loading control. Numbers below the blots correspond to the densitometric values of a representative experiment, expressed as fold over untreated WT.

Taken together, the observed phenotypic rescue triggered by addition of nucleosides suggests that DNA damage response activation and p53-dependent apoptosis in mice lacking E2f1 and E2f2 could result from an untimely nucleotide exhaustion, underlying the relevance of E2F in the regulation of cellular nucleoside pools.

# Objective 2. Assessment of the relevance of E2F1/E2F2-regulated nucleotide metabolism in prostate cancer

Nucleotide biosynthesis is central to the capacity of a cell to proliferate, and, therefore, cancer cells are exquisitely sensitive to nucleotide pool levels for their growth. The aberrant E2F activity that characterizes tumor cells with an inactive Retinoblastoma pathway is thought to supply the nucleotides that are required for their exacerbated DNA replication and cellular proliferation (Villa et al., 2019). At the same time, this feature of E2F biology could be exploited therapeutically in cancer cells to induce replication stress and genomic instability upon inhibition of E2F activity, either alone or in combination with other therapeutic strategies.

## 2.1 *In silico* analyses of cancer databases

### 2.1.1. E2F1/E2F2 and target gene expression in cancer databases

We aimed to identify the type of cancer that would be the most suitable target to E2F inhibition therapy, and focused our study in four major cancer types: colorectal, pancreatic, breast and prostate cancers. To investigate *in silico* the possible correlation between the expression of *E2F1* and *E2F2* genes and disease-free survival (DFS), we performed bioinformatic analyses using cBioportal (Cerami et al., 2012a; Gao et al., 2013) and *KM plotter* (Nagy et al., 2021) online tools, open-access resources for performing correlations between gene expressions in many cancer patients, using samples obtained from TCGA database (Figure 22).

As shown in figure 22, prostate, pancreatic and breast cancers showed an inverse correlation between *E2F1* and *E2F2* gene expression and DFS, that is, high expression of these genes correlated significantly with a worse prognosis. These results suggest that these types of cancers would be suitable for the design of therapies based on E2F inhibition. By contrast, colorectal cancer did not show such inverse correlation.

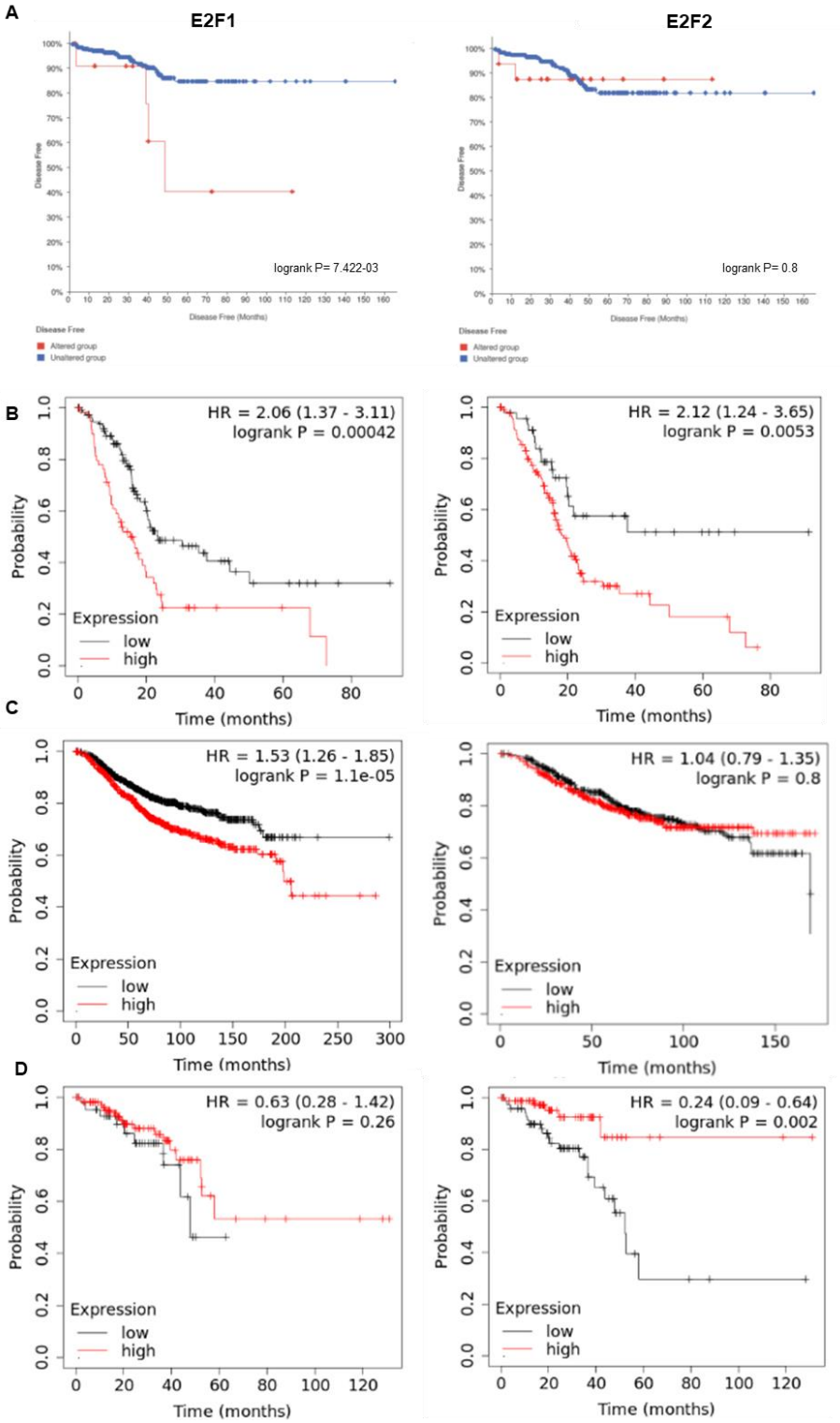


Figure 22. ***In silico*** **analysis of the correlation between expression of *E2F1* and *E2F2* genes and disease-free survival (DFS) in cancer.** Kaplan-Meier curves representing the disease-free survival (DFS) of patient groups selected in the Pan Cancer TCGA samples of prostate (A) (cBioportal), pancreatic (B), breast (C) and colorectal cancer (D) (KM-plotter) patients.

We next examined whether the negative correlation shown in prostate, pancreatic and breast cancer between E2F expression and DFS was also detected when E2F target genes involved in nucleotide biosynthesis were examined. For these analyses, and based on our previous results, we selected TK1 and DCK genes of the nucleotide salvage pathway. We also included TYMS, key player in *de novo* pathway that harbors several E2F binding sites in its promoter sequence (based on analysis with *ConSite*). Indeed, an equivalent negative correlation was observed for these genes (Figure 23), consistent with the existence of a common regulatory pathway for their expression.

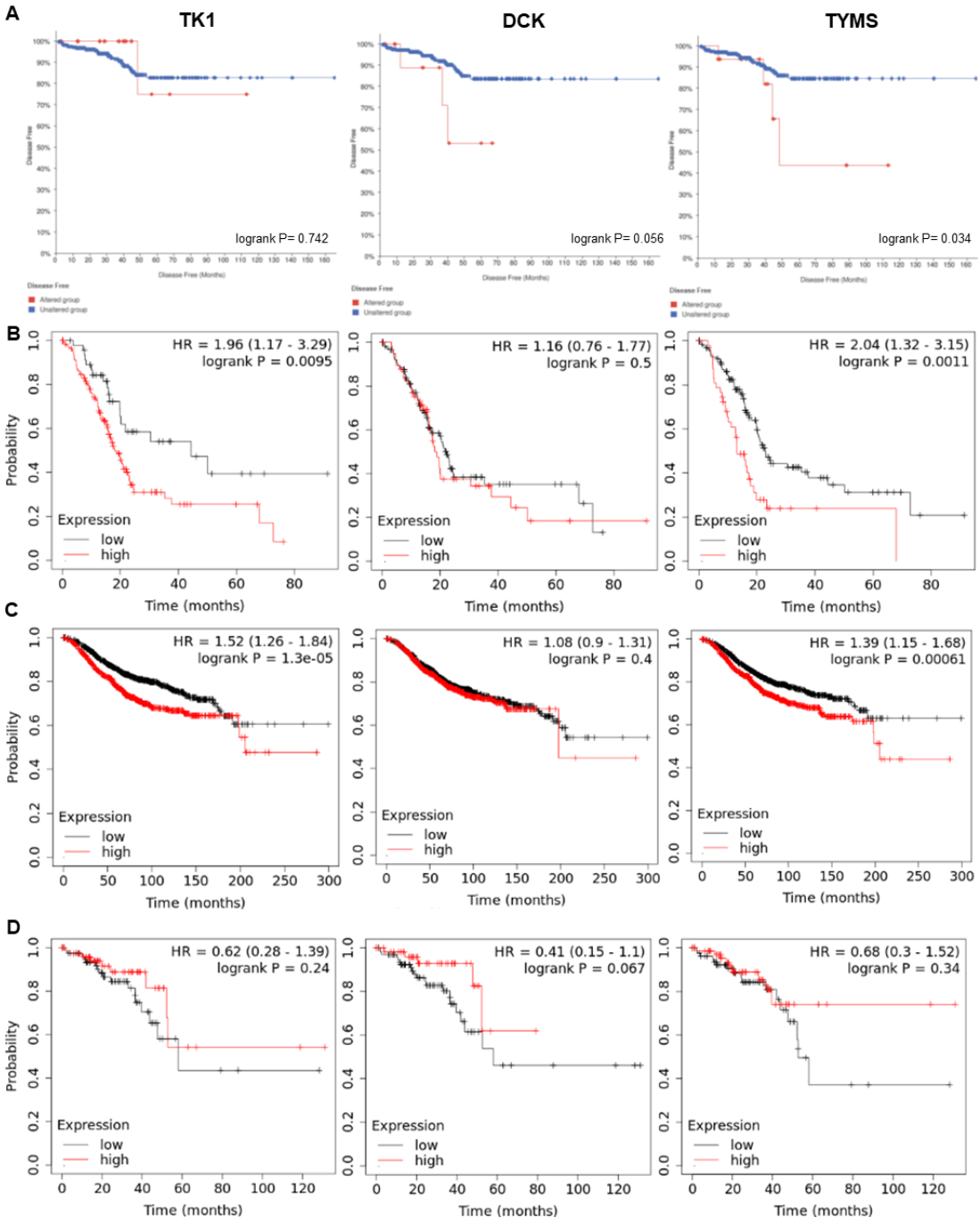

Figure 23. ***In silico* analysis of the correlation between expression of *TK1*, *DCK* and *TYMS* genes and disease-free survival (DFS) in cancer.** Kaplan-Meier curves representing the disease-free survival (DFS) of patient groups selected in the Pan Cancer TCGA samples of prostate (A) (cBioportal), pancreatic (B), breast (C) and colorectal cancer (D) (KM-plotter) patients.

Given the availability of prostate-derived cell lines with different degrees of malignancy in our laboratory (kindly provided by Dr. Carracedo), we decided to focus on prostate cancer as the paradigm in which to study the relevance of E2F1/2 in the malignant progression of this type of neoplasia, and to explore the usefulness of E2Fs as therapeutic targets.

### 2.1.2. Relationship between E2F-dependent gene expression and malignancy in prostate cancer

To study further the correlation between *E2F1*, *E2F2*, *TK1*, *DCK* and *TYMS* gene expression and tumor malignancy in prostate cancer, we performed bioinformatics analyses making use of the Cancertool webtool, an open-access resource for performing detailed correlation studies between gene expression data in many cancer patients (Cortazar et al., 2018). We first studied the relative gene expression in prostate cancer specimens (PCa) compared to non-tumoral (N) samples. Interestingly, expression of the five genes under study appeared to be increased in PCa compared to N samples (Figure 24A), although the fold increase in expression was not significant, or was only slightly significant for most of the genes analyzed. Interestingly, the p-value became highly significant when samples were divided into two subsets based on their progression stage (Figure 24B). This analysis showed that expression of the genes was moderately increased in primary tumor (PT) compared to non-tumoral (N) samples, but it was dramatically increased in metastatic PCa (M) specimens compared to N and PT samples, suggesting that the aberrant expression of *E2F1*, *E2F2*, *TK1, DCK* and *TYMS* genes might be a feature of malignant cells. Consistent with this notion, samples with the highest score in dedifferentiation stablished by Gleason grade (GS) showed the highest expression of *E2F1*, *E2F2*, *TK1, DCK* and *TYMS* genes (Figure 24C).

We next analyzed the correlation between different gene expression levels and survival. To this end, we plotted Kaplan-Meier curves representing the disease-free survival of patient groups selected according to the quartile expression of each gene (Figure 24D). Importantly, patients grouped in the fourth quartile, in red, showing the highest expression of *E2F1*, *E2F2*, *TK1, DCK* and *TYMS* genes, exhibited the lowest survival rate. The correlation between *E2F1*, *E2F2*, *TK1*, *DCK* and *TYMS* gene expression and tumor malignancy, Gleason state and poor survival suggest that the mechanism governed by E2F1 and E2F2 to promote nucleotide biosynthesis might be crucial to increase prostate cancer aggressiveness.

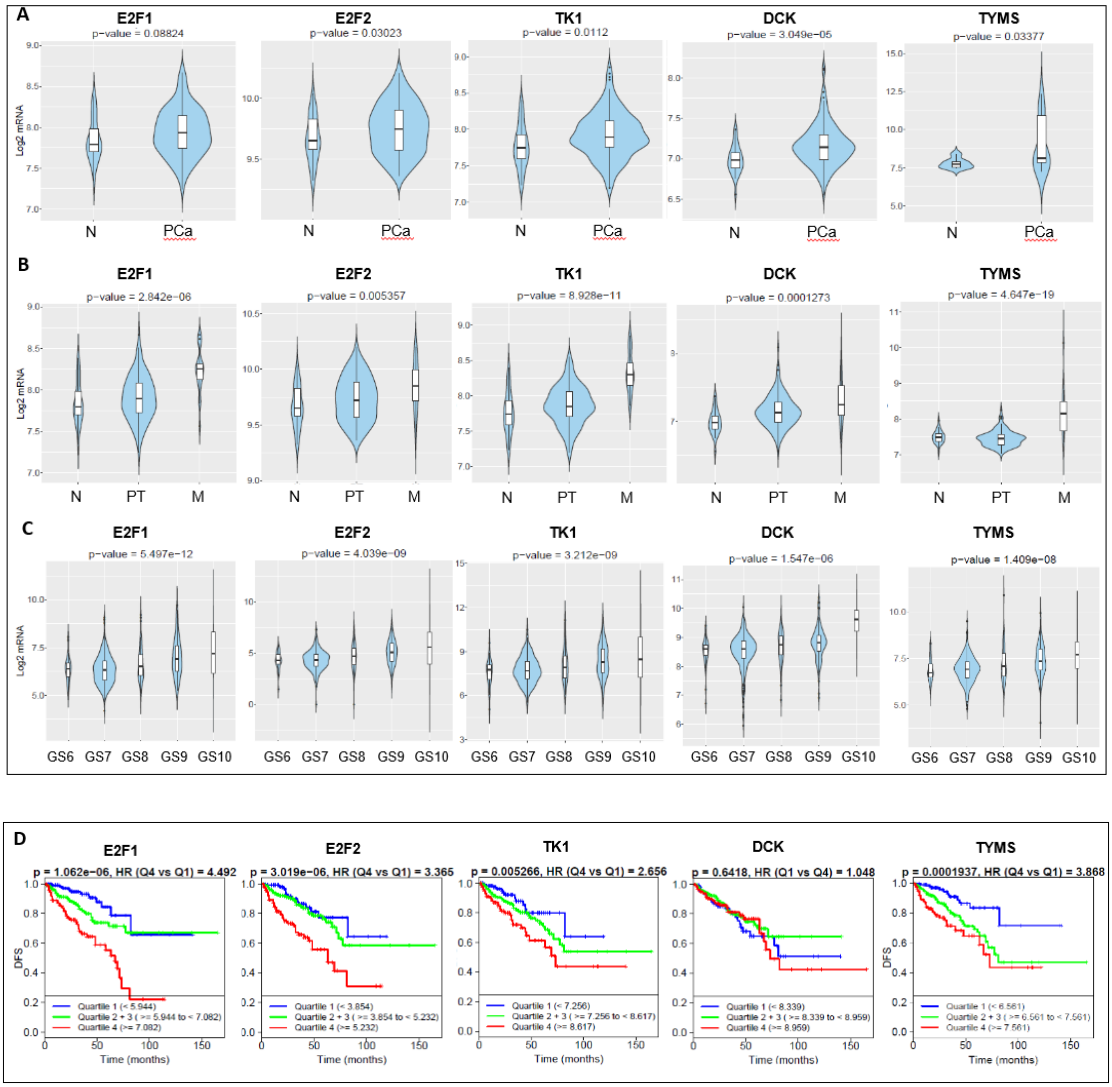


Figure 24. **Increased expression of *E2F1*, *E2F2*, *TK1*, *DCK* and *TYMS* correlates with malignancy, Gleason grade and poor survival in prostate cancer.** A) Violin plots depicting the expression of the gene of interest between non-tumoral (N) and prostate cancer specimens (PCa) in the Taylor (n=176) dataset. The Y-axis represents the Log2-normalized gene expression (fluorescence intensity values for microarray data, or sequencing reads values obtained after gene quantification with RSEM and normalization using Upper Quartile in case of RNAseq). A Student T-test was performed in order to compare the mean gene expression between two groups. B) Violin plots depicting the expression of the gene of interest among non-tumoral (N), primary tumor (PT) and metastatic (M) PCa specimens in the Taylor (n=176) dataset. An ANOVA test was performed in order to compare the mean gene expression among 3 groups. C) Violin plots depicting the expression of the indicated gene among PCa specimens of the indicated Gleason grade in the TCGA (n=496). Gleason grade is indicated as GS6, GS7, GS8, GS8+9, GS9, GS10. An ANOVA test was performed in order to compare the mean among groups. D) Kaplan-Meier curves representing the disease-free survival (DFS) of patient groups selected according to the quartile expression of the indicated gene in the TCGA (n=496) dataset. Quartiles represent ranges of expression that divide the set of values into quarters. Quartile color code: Q1 (Blue), Q2 + Q3 (Green), Q4 (Red). Each curve represents the percentage (Y-axis) of the

population that exhibits recurrence of the disease along time (X-axis, in months) for a given gene expression distribution quartile. Vertical ticks indicate censored patients. A Mantel-Cox test was performed in order to compare the differences between curves, while a Cox proportional hazards regression model was performed to calculate de Hazard Ratio (HR) between the indicated groups.

We next estimated the extent of positive correlation between expression levels of E2F1/E2F2 and expression levels of nucleotide synthesis regulator genes (*TK1*, *DCK* and *TYMS*) in each individual prostate tumor sample. To this end, we plotted the values corresponding to gene expression for *E2F1* or *E2F2* genes (X-axis) and the values for *TK1*, *DCK* or *TYMS* genes (Y-axis) for each patient, represented a linear regression and calculated the Person´s correlation coefficient (Figure 25). Importantly, a positive correlation between *E2F1*/*E2F2* and *TK1*, *DCK* and *TYMS* was observed, being this correlation strong for *TK1* and *TYMS.*

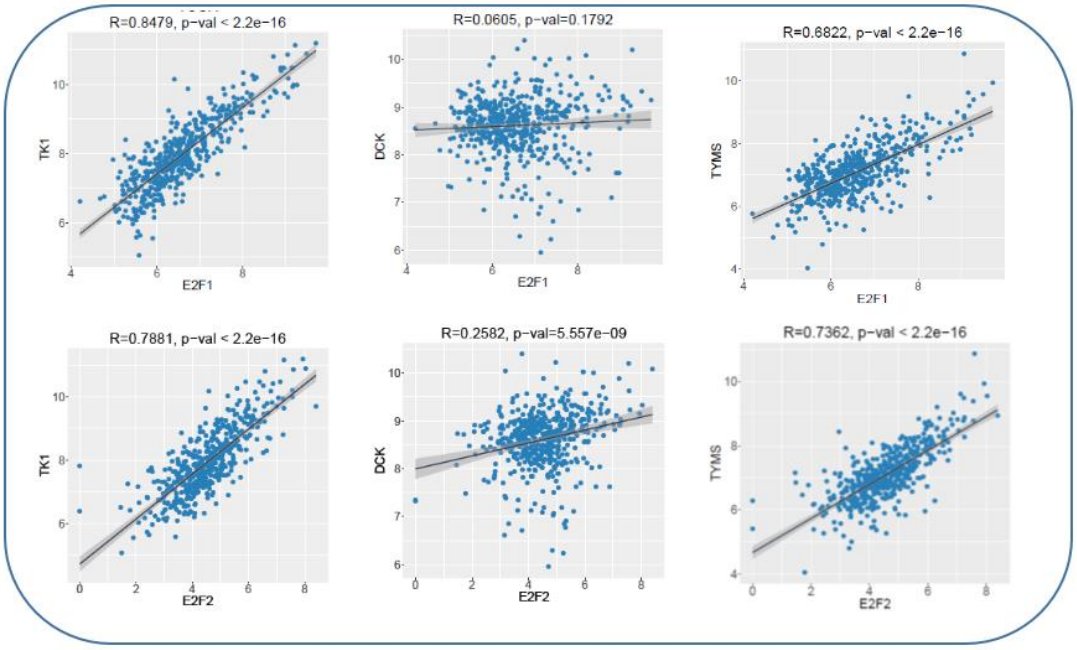


Figure 25. **Expression of *E2F1* and *E2F2* is positively correlated to expression of *TK1*, *DCK* and TYMS genes in individual prostate tumor samples.** Plotted values correspond to the log2-normalized gene expression values (fluorescence intensity or RSEM-UQ) for two genes (in X and Y-axis) for each patient in the TCGA (n=496) dataset. Black line represents linear regression, the grey area indicates the limits of the confidence intervals and R and p indicate Pearson´s correlation coefficient and statistical significance, respectively.

Taken together, *in silico* analyses of human samples point towards a role for *E2F1*/*E2F2* and their targets *TK1*, *DCK* and *TYMS* in malignancy and aggressiveness in prostate cancer.

## 2.2. Role of E2F1/E2F2 in prostate cancer cell function

### 2.2.1. Gene expression analysis of E2F1/E2F2 and nucleotide biosynthetic genes in prostate cell lines

The data obtained from the *in silico* analyses in human samples support the notion that expression of *E2F1*, *E2F2*, *TK1*, *DCK* and *TYMS* is correlated with the aggressiveness and malignancy of prostate cancer. Consequently, we wondered whether this correlation was recapitulated in our available prostate cell lines with different degrees of malignant progression status. To this end, we evaluated gene expression levels in a non-cancerous prostate cell line, BPH1, a cancerous non-metastatic prostate cell line, 22RV1, and three prostate cancer cell lines with low, moderate and high metastatic potential, respectively, namely, LNCaP, DU145 and PC3 (Stice et al., 2017).

RT-QPCR showed that, in general, expression of *E2F1*, *TK1*, *DCK* and *TYMS* is higher in prostate cancer cells compared to non-tumoral cells (Figure 26). Furthermore, the most malignant PCa cell line, PC3, exhibits the highest differential gene expression levels for most of the analyzed genes (Figure 26).

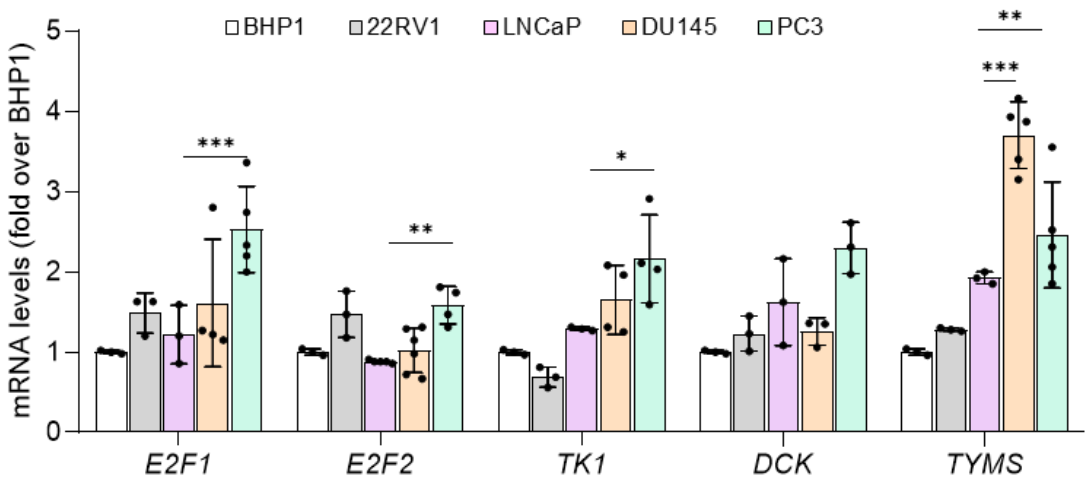


Figure 26. **Expression of *E2Fs* and its target genes *TK1*, *DCK* and *TYMS* correlates with malignancy of prostate cell lines**. RT-QPCR was carried out to analyze the expression of E2Fs and its indicated target genes in BHP1, 22RV1, LNCaP, DU145 and PC3 cell lines. *L19* was used as a normalization control. Results are expressed as fold over BHP1 cell line (mean±SD) from 3 to 7 independent experiments. ***p<0.0001, **p<0.005, *p<0.05.

These data are consistent with our *in silico* data, in that the increased expression of E2Fs and their downstream target genes controlling nucleotide biosynthesis may play a role in the malignancy of prostate cancer.

### 2.2.2. Role of E2F1 and E2F2 in the regulation of nucleotide biosynthetic gene expression in prostate cell lines

In order to analyze the contribution of E2F1 and E2F2 to the expression of their downstream target genes controlling nucleotide biosynthesis in prostate cancer cell lines we performed mRNA expression analyses 96h after individual and combined silencing of E2F1 and E2F2 with two sets (#1 and #2) of specific siRNA oligonucleotides in PC3 cells (Figure 27).

We first checked silencing efficiency of *E2F1* and *E2F2* by RT-QPCR (Figure 27A, left panel). The silencing efficiency of siE2F1 #1 was of 85% for *E2F1* expression relative to siRNA control. siE2F1 #1 molecules also reduced the expression of E2F2. This effect is probably not the result of a non-specific effect of the siE2F1 #1 molecules. Instead, it may reflect a well-known role for E2F1 in the transcriptional induction of E2F2 (Chen et al., 2009). The silencing efficiency of siE2F2 #1 was of 80% for *E2F2* expression, and siE2F2 molecules had no effect on the expression of E2F1. The silencing efficiency increased to 95% when both siE2F1 #1 and siE2F2 #1 oligos were combined. This result was repeated with the set #2 of siRNA molecules specific for E2F1 and E2F2 (Figure 27B, left panel).

We next analyzed the expression of *TK1*, *DCK* and *TYMS* after the silencing with the set #1 of siE2F1 and siE2F2 (27A, right panel). Individual silencing of E2F1 significantly reduced the expression *TK1* and *TYMS*, but only slightly the expression of *DCK*. Silencing of E2F2 significantly reduced the expression TK1, and less the expression of DCK and TYMS. Interestingly, combined silencing of E2F1 and E2F2, drastically reduced the expression levels of *TK1*, *DCK* and *TYMS*. Similar results were obtained with the set #2 of siRNA molecules specific for E2F1 and E2F2 (Figure 27B, right panel). Furthermore, the mPCa cell line DU145 treated with siE2F1 #1 and siE2F2 #1 also exhibited a similar reduction in target gene expression (Figure 28), indicating that the observed regulation of *TK1*, *DCK* and *TYMS* by E2F1 and E2F2 is not restricted to a particular cell line or silencing oligonucleotide.

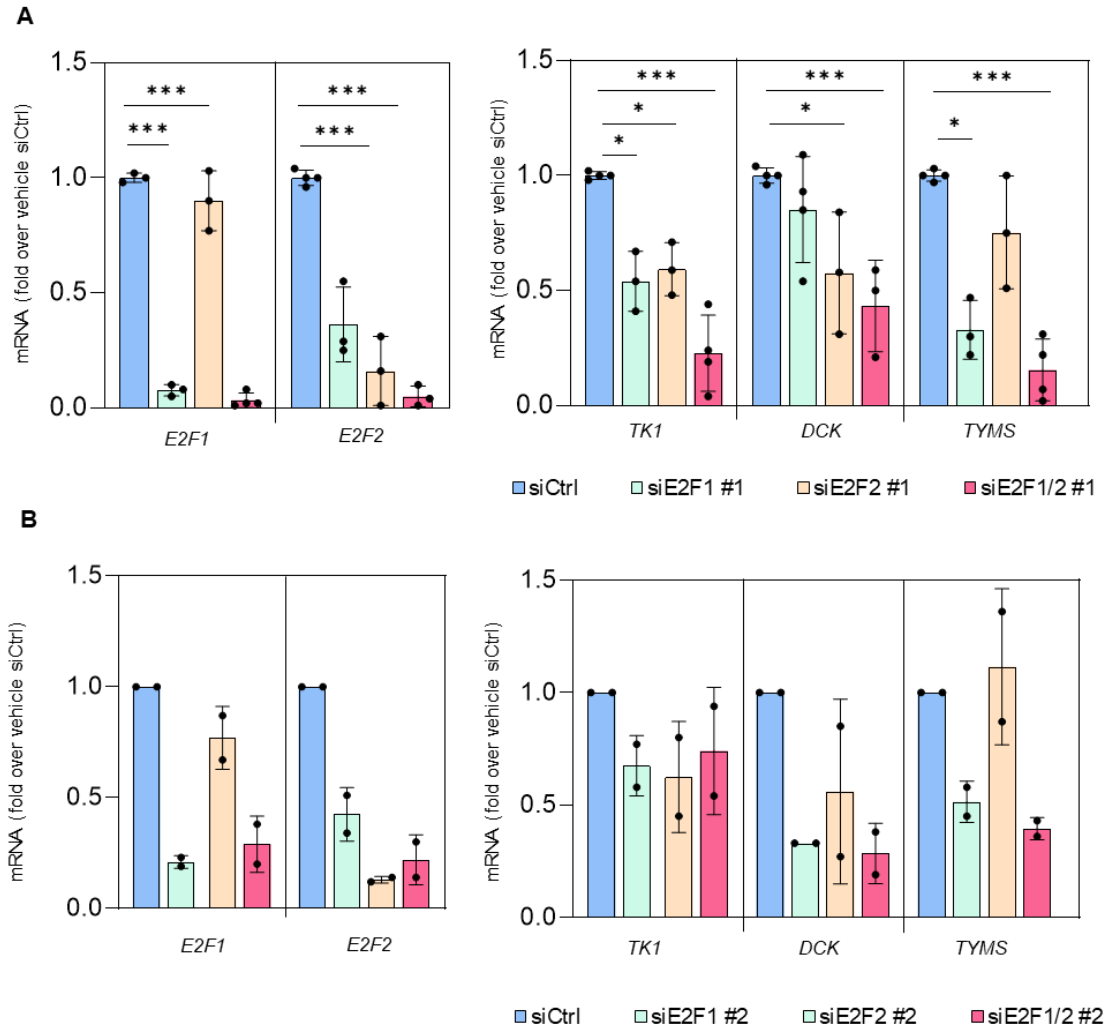


Figure 27. **Effect of silencing E2F1 and E2F2 on the expression of their targets genes *TK1*, *DCK* and *TYMS* in PC3 cells.** A) PC3 cells were reverse transfected with siRNAs specific for E2F1 (siE2F1 #1), E2F2 (siE2F2 #1) or with their combination (siE2F1/2 #1). Transfection with non-target control siRNA (siCTRL) was used as silencing control. 96h later, RNA was extracted and mRNA expression was analyzed by RT-QPCR. mRNA expression of *E2F1* and *E2F2* (left panel) and *TK1*, *DCK* and *TYMS* (right panel) values were normalized to the expression of *EIF2C2*, used as standard control. Data are represented as fold-change relative to siRNA control treated with vehicle (vehicle siCTRL). **p<0.0001, *p<0.05 vs. siCTRL. B) PC3 cells were reverse transfected with other set of siRNAs specific for E2F1 (siE2F1 #2), E2F2 (siE2F2 #2) or with their combination (siE2F1/2 #2).

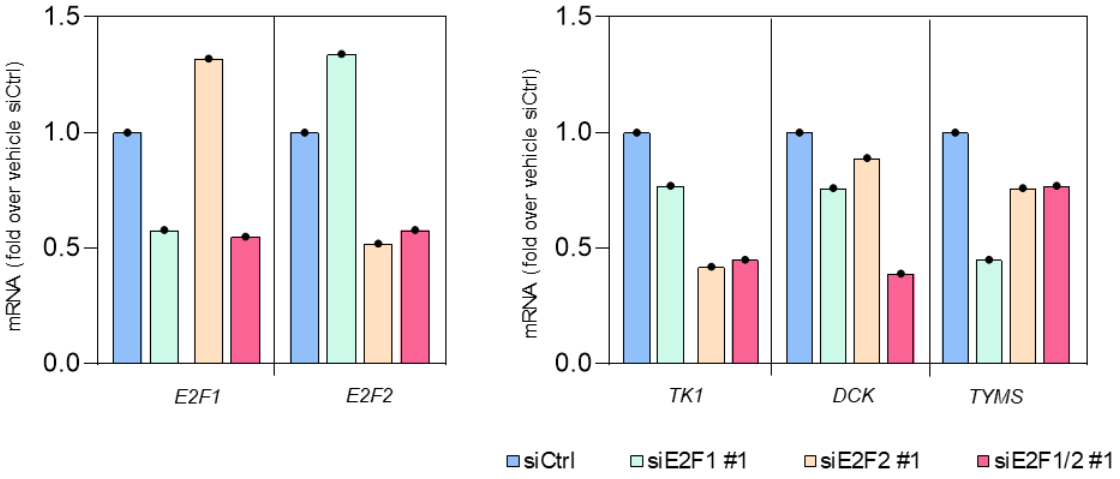


Figure 28. **Effect of silencing E2F1 and E2F2 on the expression of their targets genes *TK1*, *DCK* and *TYMS* in DU145 cells.** DU145 cells were reverse transfected with siRNAs specific for E2F1 (siE2F1 #1), E2F2 (siE2F2 #1) or with their combination (siE2F1/2 #1). Transfection with non-target control siRNA (siCTRL) was used as silencing control. 96h later, RNA was extracted and mRNA expression was analyzed by RT-QPCR. mRNA expression of *E2F1* and *E2F2* (left panel) and *TK1*, *DCK* and *TYMS* (right panel) values were normalized to the expression of *EIF2C2*, used as standard control. Data are represented as fold-change relative to siRNA control treated with vehicle (vehicle siCTRL).

In order to test whether the changes observed at the mRNA level in PC3 cells were translated to differences in the expression of the corresponding proteins, we analyzed TK1, DCK and TS (encoded by *TYMS* gene) proteins 96h after the silencing with #1 set of oligos. As shown in Figure 29, silencing of E2F1 and double silencing of E2F1 and E2F2 efficiently reduced the accumulation of TK1, DCK and TS proteins.

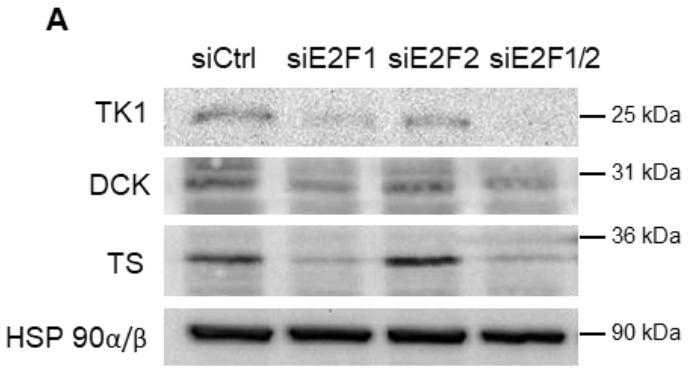

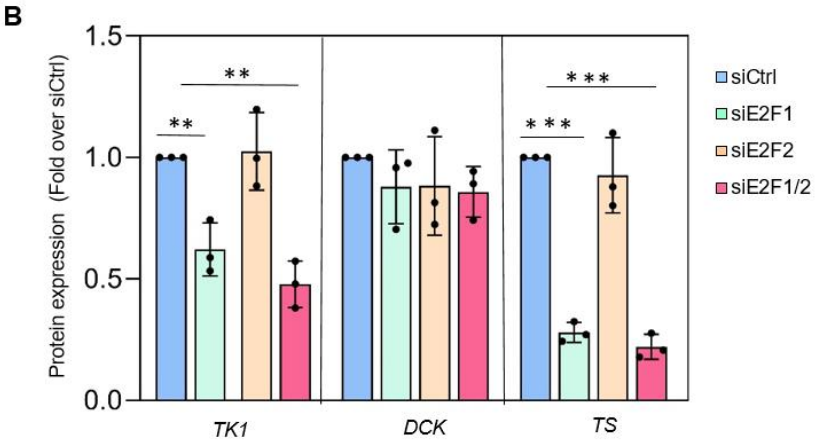


Figure 29. **Silencing of E2F1 and combined silencing of E2F1/2 reduces steady-state levels of TK1, DCK and TS.** A) PC3 cells were reverse transfected with siRNAs specific for E2F1 (siE2F1 #1), E2F2 (siE2F2 #1) or with their combination (siE2F1/2 #1). Transfection with non-target control siRNA (siCTRL) was used as silencing control. 96h later, protein was extracted and analyzed by Western blot. Representative western blots of 3 different experiments are shown. HSP90 was used as loading control. B) Densitometry values were obtained from 3 independent experiments. Values were normalized to the expression of HSP90, used as standard control. Data are represented as fold-change relative to siRNA control treated with vehicle (vehicle siCTRL).

The results observed at the protein level resemble those obtained at the mRNA level, implying that the control of TK1, DCK and TS (*TYMS*) expression by E2F1 and E2F2 occurs primarily at the transcriptional level. Taken together, these findings suggest that E2F1 and E2F2 are critical for the expression of the nucleotide biosynthetic genes TK1, DCK and TYMS in mPCa cell lines.

### 2.2.3. Role of E2F1 and E2F2 in cell cycle progression of mPCa cells

In order to understand the functional role of E2F1 and E2F2 in prostate cancer biology, we analyzed their contribution to the control of cell cycle progression in PCa cells. The fact that E2F1 and E2F2 are necessary for the expression of genes involved in nucleotide biosynthesis in mPCa cells, led us to speculate that E2F1 and E2F2 would be necessary for their normal progression through the cell cycle. We analyzed cell cycle distribution in PC3 cells in a time-course after individual and combined silencing of E2F1 and E2F2 #1 siRNA oligonucleotides (Figure 30).

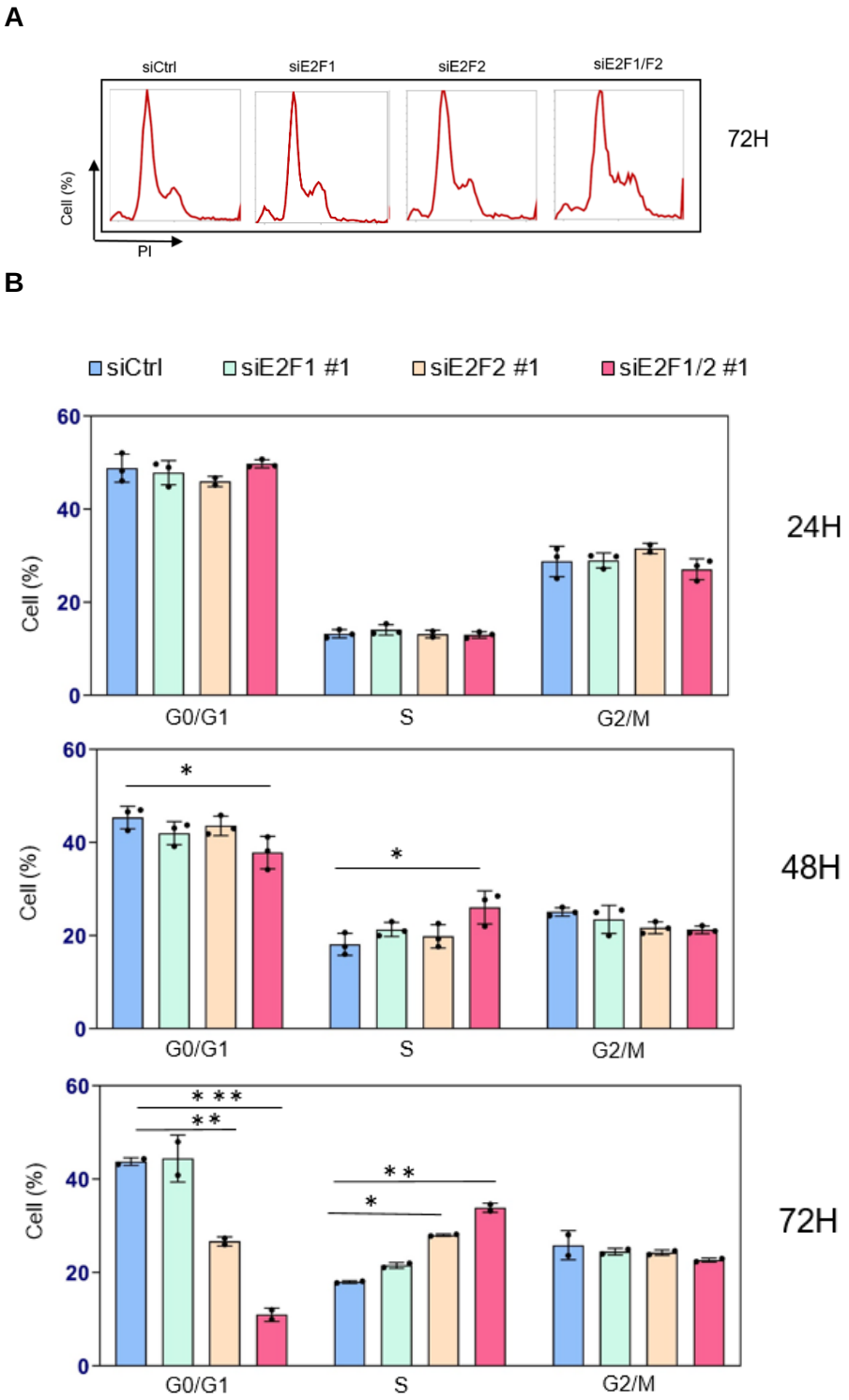


Figure 30. **Combined silencing of E2F1 and E2F2 leads to the accumulation of PC3 cells in S phase.** A) Representative histograms with cell cycle profiles. B) Percentage of viable cells in different stages of the cell cycle according to DNA content after transfection with non-target control siRNAs (siCTRL), with siRNAs specific for E2F1 (siE2F1 #1), E2F2 (siE2F2 #1) or with their combination (siE2F1/2 #1) for 24, 48 and 72 h. after. Data shows the average ±SD from 3 independent experiments. ***p<0.0001, **p<0.005, *p<0.05, *vs.* siCTRL.

We observed that individual silencing of E2F1 did not have any effect on the cell cycle distribution of PC3 cells, whereas single silencing E2F2 moderately increased the percentage of cells in S phase at 72h. Importantly, combined silencing of E2F1 and E2F2 lead to a mild accumulation of the cells in S phase at 48 hours, which became highly significant after 72 hours (Figure 30). Given the accumulation of the cells in S phase upon depletion of E2F1/E2F2, we asked whether knockdown of these E2Fs might be blocking the cells from entering into mitosis. To check this possibility, we analyzed the phosphorylation levels of histone H3 on Ser10 (pH3), widely used as a mitotic marker (Crosio et al., 2002), at several time-points (24-48-72h) after silencing of E2F1 and E2F2 individually or in combination.

As shown in Figure 31, individual silencing of E2F1 and E2F2 did not significantly modify the percentage of pH3+ cells, whereas combined silencing resulted in a significantly decreased percentage of pH3+ cells at 48-72 hours.

**A**

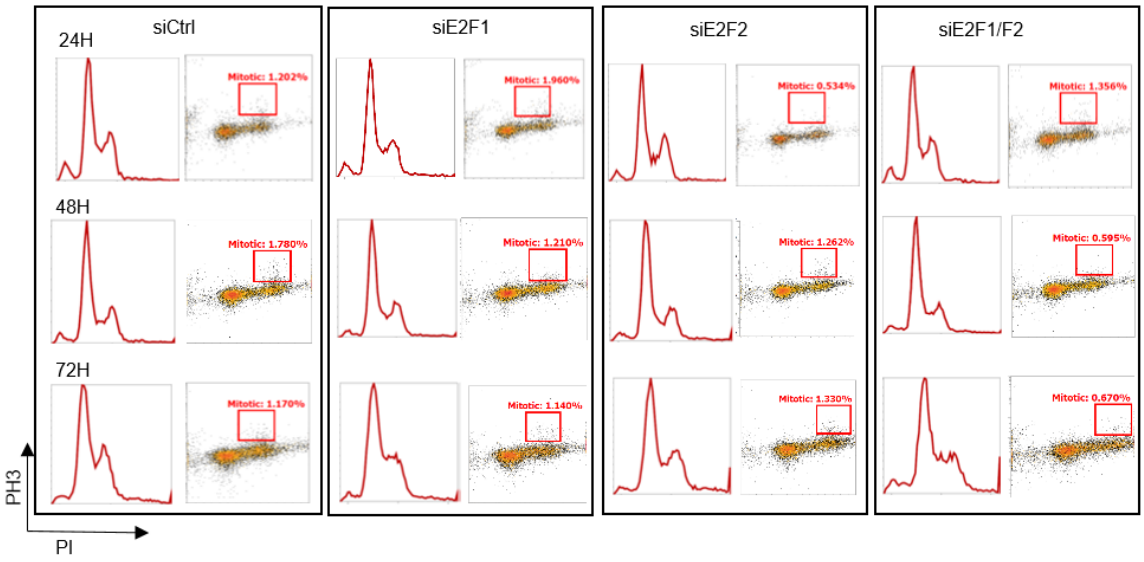


**B**

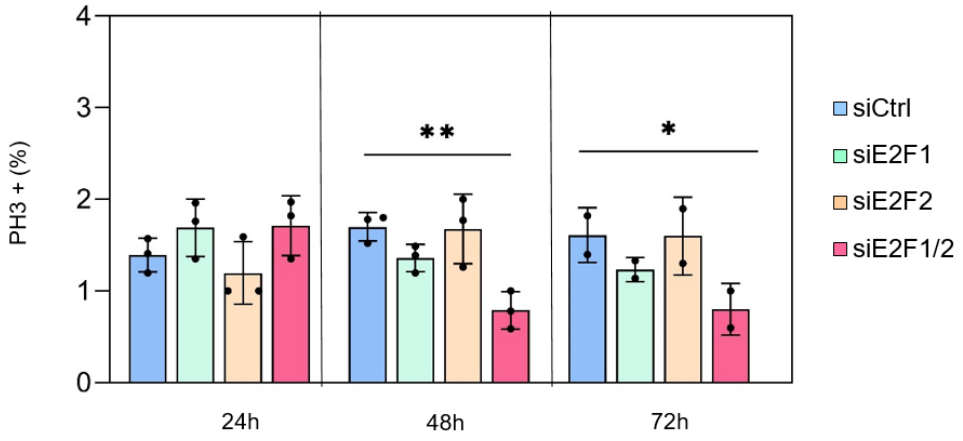

Figure 31. **Combined silencing of E2F1 and E2F2 prevents mitotic entry of PC3 cells.** A) Representative histograms with cell cycle profiles (left panels) and dot plots showing the percentage and cell cycle distribution of PH3-positive cells (right panels) of PC3 cells 24, 48 and 72 h after the transfection with non-target control siRNAs (siCtrl), with siRNAs specific for E2F1 (siE2F1 #1), E2F2 (siE2F2 #1) or with their combination (siE2F1/2 #1). B) Percentage of PH3-positive cells at the indicated time point. Data shows the average ±SD from 3 independent experiments. *p<0.05, **p<0.005, vs. siCtrl.

These data suggested that E2F1 and E2F2 are required for the correct progression of PC3 cells in the cell cycle, because lack of these factors led to an accumulation of cells in S-phase and a reduction of cells entering mitosis.

### 2.2.4. Role of E2F1 and E2F2 in the genomic stability of mPCa cells

The aberrant cell cycle profile of PC3 cells upon E2F1/E2F2 knockdown, and especially their accumulation in S phase, suggested that these cells could be undergoing replication stress. To analyze the individual and shared contribution of E2F1 and E2F2 in the control of genomic stability, we analyzed the percentage of γH2AX-positive cells by FACS at several time-points (24-48-72-96h) after silencing of E2F1 and E2F2 (Figure 32). The flow cytometry data showed a mild increase in the percentage of γH2AX-positive cells 48 hours after double-silencing of E2F1 and E2F2. This increase was more robust at the 72h time-point (Figure 32), coinciding with the accumulation of E2F1/E2F2 knockdown cells in S phase (Figure 30). Moreover, according to the dot-plots obtained in the FACS analysis, γ-H2AX positive cells had a DNA content compatible with an S phase, implying that knockdown of E2F1/E2F2 triggers replication stress in PCa cells undergoing DNA synthesis, thereby blocking their progression in the cell cycle, and inducing their apoptosis.

**A**

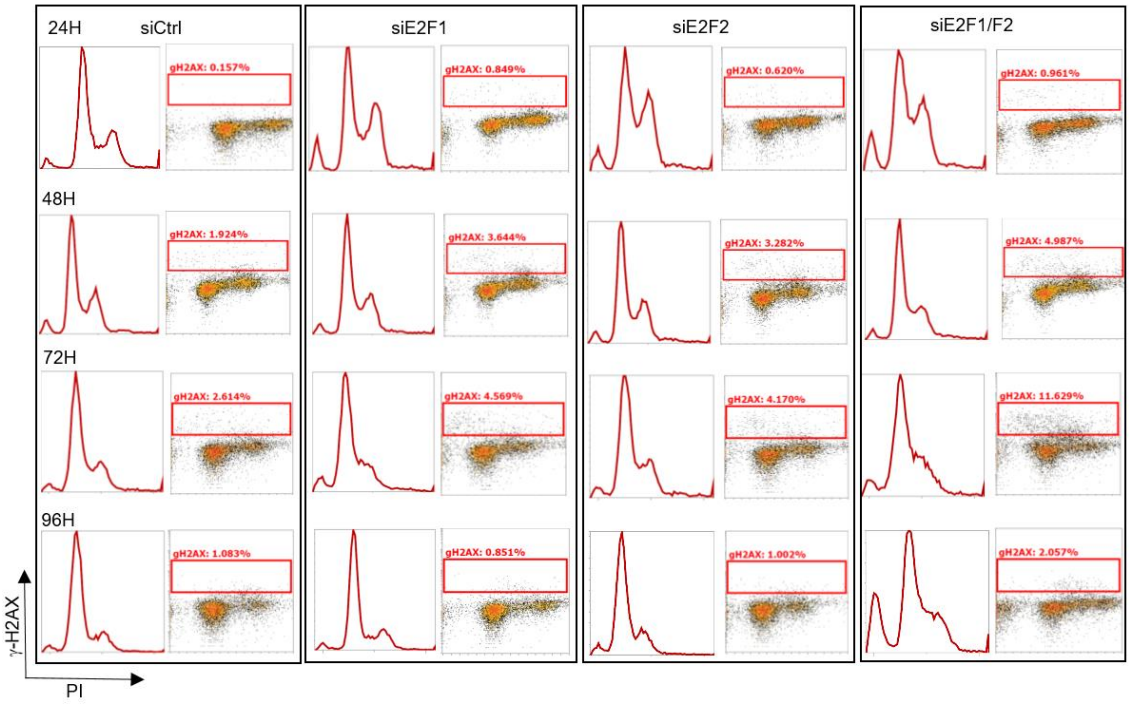


**B**

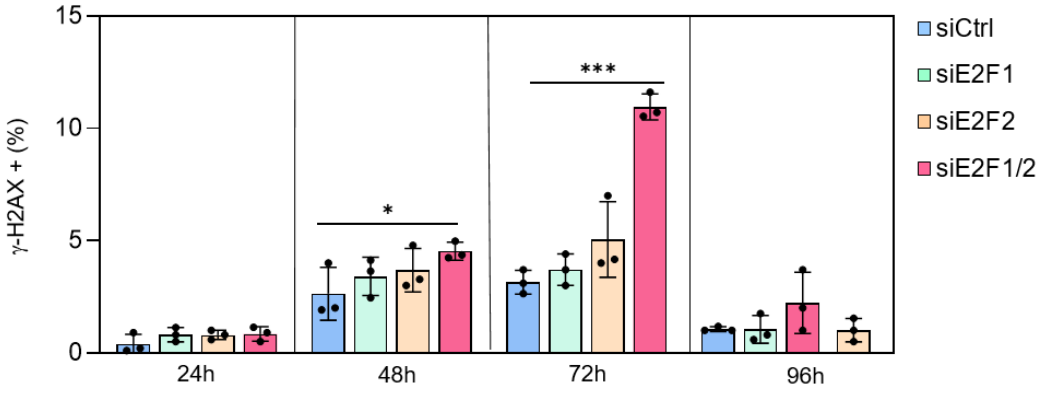


Figure 32. **Combined silencing of E2F1 and E2F2 leads to replication stress in PC3 cells.** A) Representative histograms with cell cycle profiles (left panels) and dot plots showing the percentage and cell cycle distribution of γ-H2AX-positive cells (right panels) of PC3 cells 24, 48, 72, 96 h after the transfection with non-target control siRNAs (siCtrl) or with siRNAs specific for E2F1 and E2F2. B) Percentage of γ-H2AX- positive cells at the indicated time point. Data shows the average ±SD from 3 independent experiments. *p<0.05, ***p<0.0001 *vs.* siCtrl.

Genome integrity during S phase requires the scheduled control of CDK activity (Beck et al., 2010). Specifically, restraining CDK1 activity during S phase is key to prevent replication stress (Szmyd et al., 2019). It has been established that restriction of CDK1 activation during S phase is accomplished by the inhibitory phosphorylation of CDK1 in

Tyr15 (Akopyan et al., 2014; Deng et al., 2019; Lemmens et al., 2018). Importantly, cells with decreased pCDK1 levels undergo replication stress when nucleotide levels are reduced (Beck et al., 2012). We asked whether E2F1/E2F2 knockdown cells exhibited improper activation of CDK1 by analyzing the levels of pCDK1 (Tyr15). To this end, 96h after silencing of E2F1 and E2F2 with #1 set of oligos, we studied the accumulation of total and phosphorylated CDK1 by western blot analysis (Figure 33).

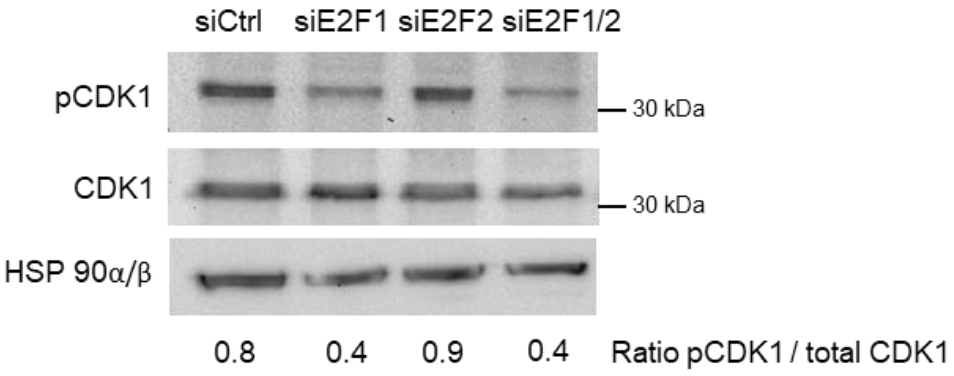


Figure 33. **Silencing of E2F1, and more potently, combined silencing of E2F1 and E2F2 decreases the inhibitory phosphorylation of CDK1.** 96h after transfection of PC3 with non-target control siRNAs (siCTRL), with siRNAs specific for E2F1 (siE2F1 #1) or E2F2 (siE2F2 #1) or for E2F1 and E2F2 (siE2F1/2 #1), accumulation of CDK1 and pCDK1 (Tyr15) was measured by western blot analysis. Results of one experiment are shown as representative. HSP90α/β was used as standard control. Numbers below the blots correspond to the relative densitometric values of pCDK1/ total CDK1. Similar results were obtained in more than 2 experiments.

Strikingly, silencing of E2F1 decreased the relative pCDK1/CDK1 levels (Figure 33), suggesting that E2F1 plays a role promoting the inhibitory phosphorylation of CDK1 in order to maintain genomic stability. The dependency of prostate cancer cells on E2F activity for their correct progression in the cell cycle that we have uncovered represents a vulnerability that could be exploited therapeutically.

# Objective 3. Assessment of the use of E2F1/E2F2 as targets for prostate cancer treatment

## 3.1 Therapeutic approaches to inhibit nucleotide synthesis in metastatic prostate cancer

Inhibition of nucleotide synthesis by nucleotide analogs such as 5-FU is considered a treatment option for several types of cancer, including prostate cancer (Yagoda & Petrylak, 1993). 5-FU was rationally designed to target TS enzyme, encoded by the E2F target gene *TYMS*, which is essential for *de novo* synthesis of nucleosides. Nevertheless, treatment with 5-FU commonly becomes refractory in malignant cells. A mechanism for 5-FU resistance relies on the alternative nucleoside salvage pathway to compensate for the nucleotide deficiency following treatment with the drug (Fanciullino et al., 2006). Based on our findings on PCa cell lines, whereby depletion of E2F1/E2F2 downregulates the expression of several key genes of nucleotide synthesis, we reasoned that therapies based on the combination of 5-FU and E2F inhibition could fully prevent nucleoside biosynthesis, and thereby, induce high levels of replication stress and apoptosis in tumor cells.

We first investigated whether the malignancy of metastatic prostate cancer cells was associated with differences in response and in resistance to 5-FU, by examining their viability upon 5-FU addition. To this end, LNCaP, DU145 and PC3 cell lines were treated with increasing doses of 5-FU, and cell viability was analyzed 72h later using crystal violet staining (Figure 34A). We found that IC50 values (figure 34B) correlated nicely with their metastatic potential, such that PC3, the cell line with the highest metastatic potential, showed the highest resistance to 5-FU induced apoptosis.

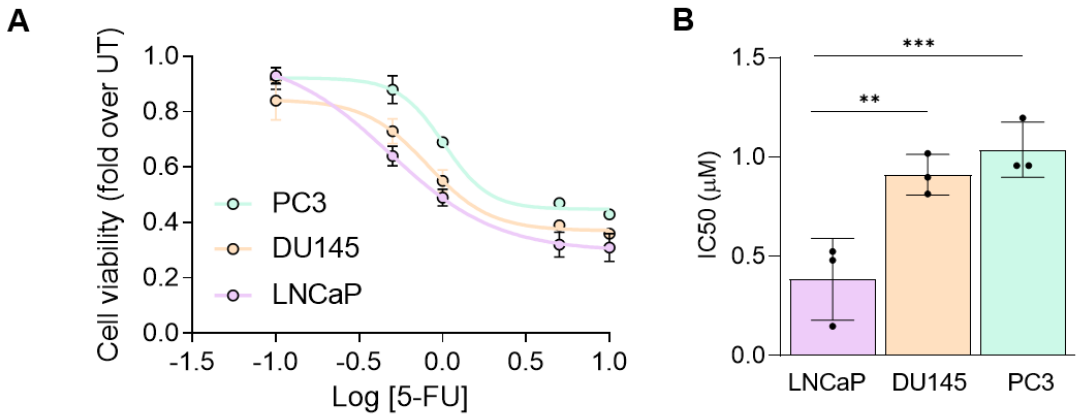


Figure 34. **Metastatic potential in mPCa correlates with the resistance to 5-FU-induced apoptosis.** A) The graph represents growth inhibition of LNCaP, DU145 and PC3 cell lines. 24 hours after seeding, cells were treated with increasing concentrations (0, 0.1, 0.5, 1, 5, 10 µM) of 5-FU. 72hours later, cells were fixed and stained with crystal violet. Subsequently, crystal violet was dissolved with acetic acid and the absorbance was measured by spectrophotometry. Cell survival ratio was calculated by normalizing the absorbance of each condition using their untreated controls. Dose-response data points represent the mean value (±SD) of 3 experiments. RSDR<0, 05. B) IC50 values obtained from the graphs in (A), using GraphPad software. ***p<0.0001, **p<0.005 *vs.* LNCaP.

## 3.2. Effect of 5-FU on the expression of E2F target genes encoding enzymes of nucleotide biosynthesis pathways

The fact that PC3 cells express high levels of E2F1 and E2F2, and are resistant to 5-FU lead us to speculate that PC3 cells could overcome the reduction of nucleotide pools imposed by 5-FU by activating the expression of E2F target genes coding for enzymes responsible for the synthesis of nucleosides. To analyze whether E2F target genes are deregulated in PC3 cells upon 5-FU treatment, we evaluated the expression by RT-QPCR of E2F1/2 themselves and their target genes encoding rate-limiting enzymes responsible for the synthesis of nucleosides in PC3 cells after 5-FU treatment.

RT-QPCR showed that expression of *E2F1* and *E2F2* is not significantly altered by exposure to 5-FU, although there is substantial variability among experiments. The expression of *TK1*, *DCK*, and *TYMS* is significantly induced by 5-FU (Figure 35), hinting that the enhanced expression of these E2F targets may be involved in the resistance of PC3 to 5-FU.

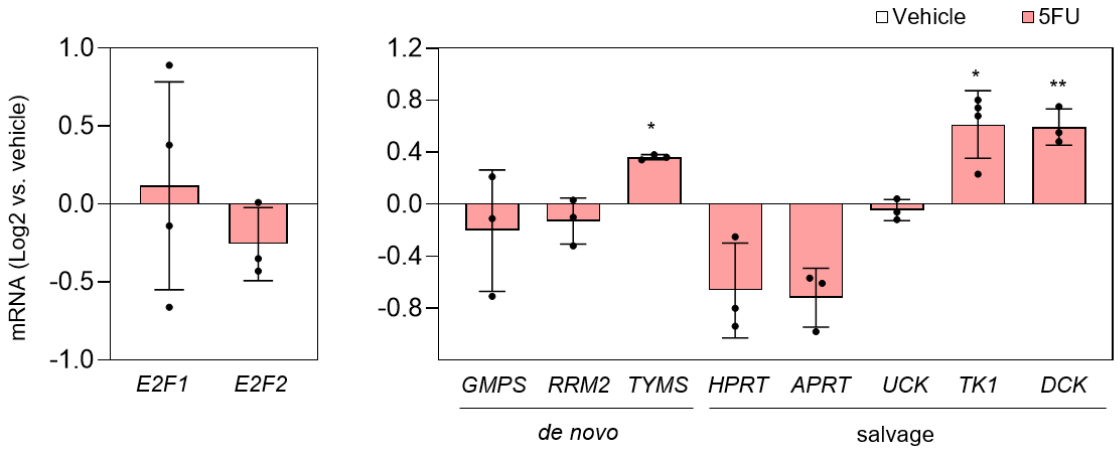


Figure 35. **Expression of E2F targets *TK1*, *DCK*, and *TYMS* is induced (70%, 30% respectively) upon treatment with 5-FU in PC3 cells.** RT-QPCR was carried out to analyze the expression of E2Fs and their target genes encoding enzymes involved in salvage and *de novo* pathway of biosynthesis of nucleotide in PC3 cells after 72h of 5FU (5 μM) treatment compared with sample treated with vehicle. *L19* was used as the normalization control. The values are expressed as Log2 ratio *vs.* vehicle control and are the results (mean±SD) of three independent experiments. **p<0.005, *p<0.05 *vs.* vehicle control.

Moreover, the fact that the expression of E2F targets *TK1*, *DCK*, and *TYMS* was enhanced upon 5-FU exposure in PC3 cells suggested the possibility that E2F1 and E2F2 were not only maintaining the steady state expression of these genes, but that they were promoting their expression to overcome the reduction of nucleotide pools imposed by 5-FU.

To check this possibility, we silenced E2F1 and E2F2 alone or in combination with set #1 of siRNAs. 24h later, we treated the cells with 5-FU or vehicle control and 72h later, we extracted mRNA for gene expression analyses (Figure 36A). We confirmed knockdown of E2F1 and E2F2 in cells transfected with siRNA molecules and treated with 5-FU (Figure 36B). Importantly, silencing of E2F1 and more potently, combined silencing of E2F1 and E2F2, prevented 5-FU-induced upregulation of *TK1*, *DCK* and *TYMS* (Figure 36C).

These results were confirmed using set #2 of silencing oligos for *E2F1* and *E2F2* in PC3 cells (Figure 37). Furthermore, the mPCa cell line DU145 behaved similarly to PC3 cells when cells were treated with siE2F1 and siE2F2 in the presence of 5-FU (Figure 38), indicating that the observed phenotype is not restricted to a particular cell line or silencing oligonucleotide.

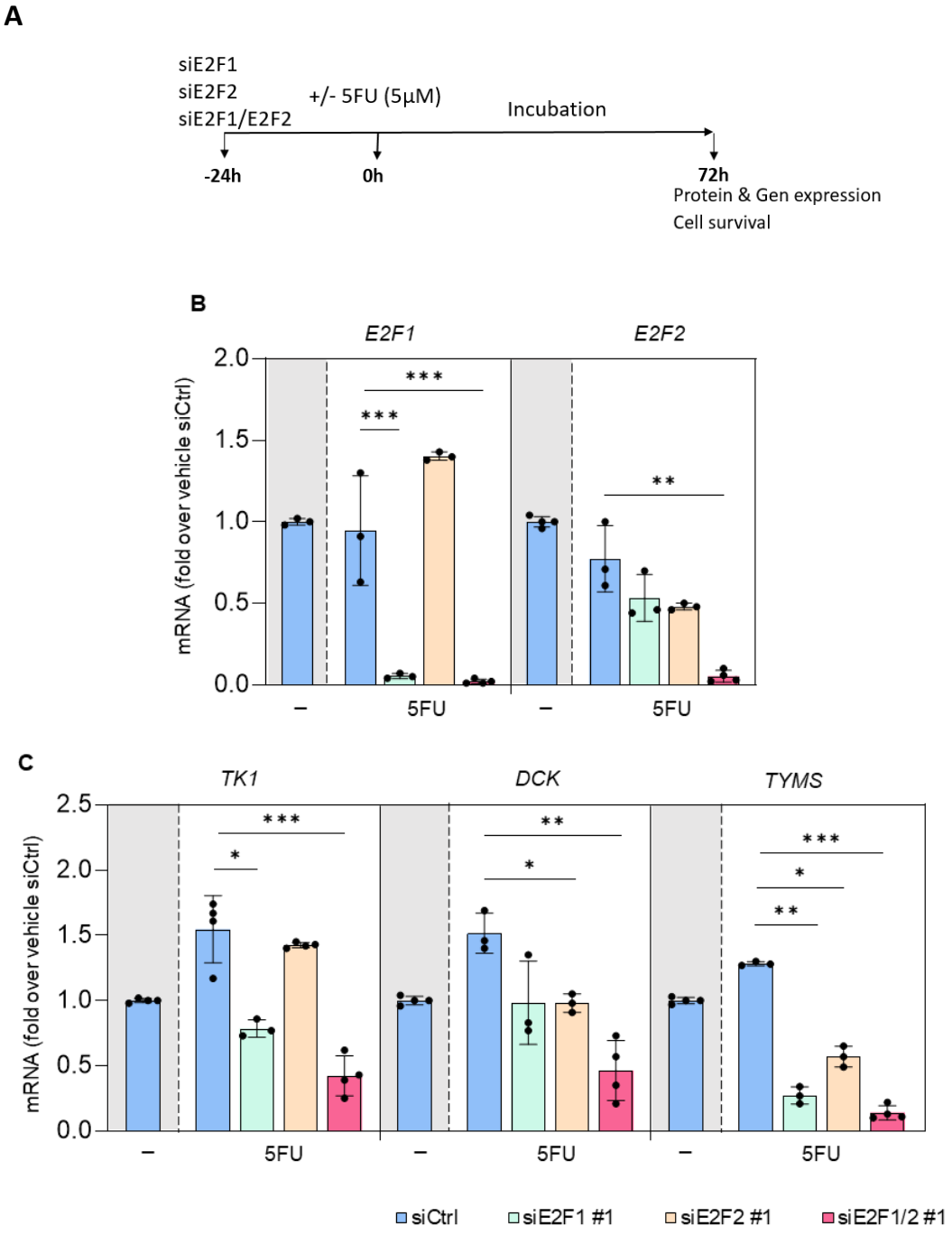


Figure 36. **Silencing of E2F1 alone, or more pronouncedly, combined silencing of E2F1 and E2F2 reduces steady-state levels of *TK1*, *DCK* and *TYMS* and prevents their induction by 5-FU.** A) PC3 cells were reverse transfected with siRNAs specific for *E2F1* (siE2F1 #1), *E2F2* (siE2F2 #1) or with their combination (siE2F1/2 #1). Transfection with non-target control siRNA (siCTRL) was used as silencing control. After 24h, 5 uM of 5-FU or vehicle control was added. 72h later, RNA was extracted and mRNA expression was analyzed by RT-QPCR. mRNA expression of *E2F1* and *E2F2* (B) and *TK1*, *DCK* and *TYMS* (C) values were normalized to the expression of *EIF2C2*, used as standard control. Data are represented as fold-change relative to siRNA control (siCtrl) treated with vehicle (-) shown in grey panel. * **p<0.0001, **p<0.005, *p<0.05 *vs.* siCTRL.

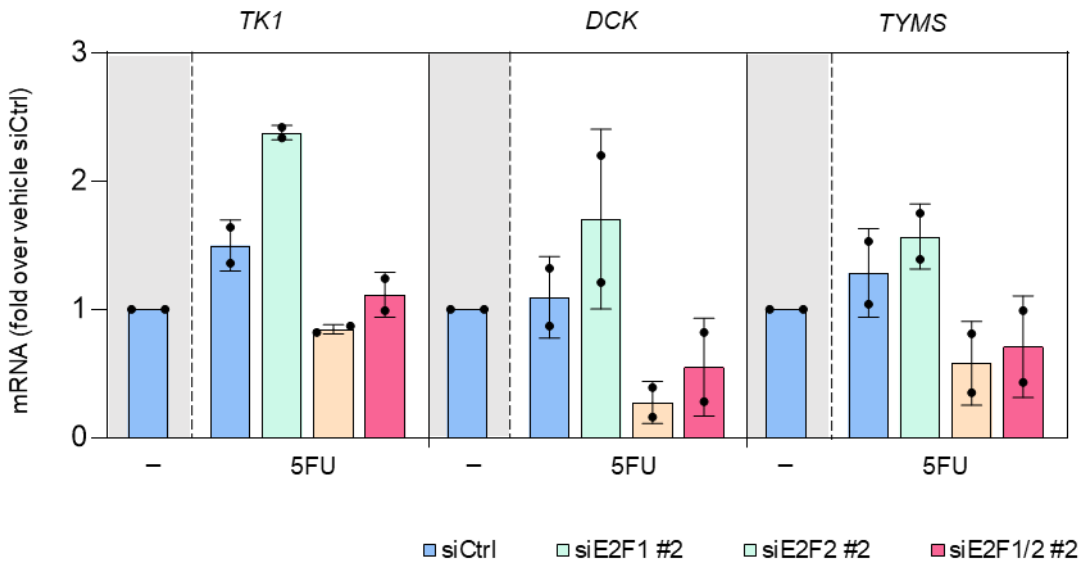


Figure 37. **Gene expression at the mRNA level in PC3 cells with set #2 of silencing oligos for E2F1 and E2F2.** PC3 cells were reverse transfected with siRNAs specific for *E2F1* (siE2F1 #2), *E2F2* (siE2F2 #2) or with their combination (siE2F1/2 #2). Transfection with non-target control siRNA (siCTRL) was used as silencing control. After 24h, 5 uM of 5-FU or vehicle control was added. 72h later, RNA was extracted and mRNA expression was analyzed by RT-QPCR. mRNA expression of *TK1*, *DCK* and *TYMS* values from 2 independent experiments were normalized to the expression of *EIF2C2*, used as standard control. Data are represented as fold-change relative to siRNA control (siCTRL) treated with vehicle (-) shown in grey panel.

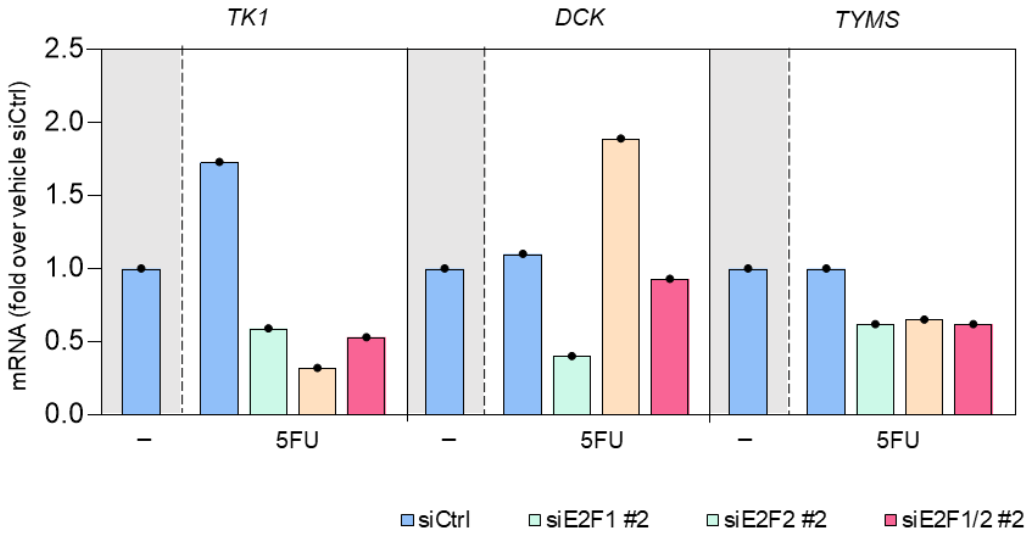


Figure 38. **Silencing of E2F1 and E2F2 in DU145 results in the downregulation of *TK1*, *DCK* and *TYMS*.** DU145 cells were reverse transfected with siRNAs specific for *E2F1* (siE2F1 #2), *E2F2* (siE2F2 #2), or with their combination (siE2F1/2 #2). Transfection with non-target control siRNA (siCTRL) was used as silencing control. After 24h, 5 uM of 5-FU or vehicle control was added. 72h later, RNA was extracted and mRNA expression was analyzed by RT-QPCR. mRNA expression of *TK1*, *DCK* and *TYMS* values from 1 experiment were normalized to the expression

of *EIF2C2*, used as standard control. Data are represented as fold-change relative to siRNA control (siCTRL) treated with vehicle (-) shown in grey panel.

In order to test whether the changes observed at mRNA level in PC3 cells were translated to differences in the accumulation of the corresponding proteins, we analyzed TK1, DCK and TS proteins in cells silenced with #1 oligos. As shown in Figure 39, 5-FU treatment induced the accumulation of TK1, DCK and TS. Consistent with previously reported evidences (Ligabue et al., 2012), an additional band of ternary complexed TS appeared in 5-FU treated samples. Importantly, silencing of E2F1, or more dramatically, double silencing of E2F1 and E2F2 not only reduced the steady state levels of TK1, DCK and TS, as previously shown in Section 2, but also substantially reduced their 5-FU-dependent accumulation.

**A**

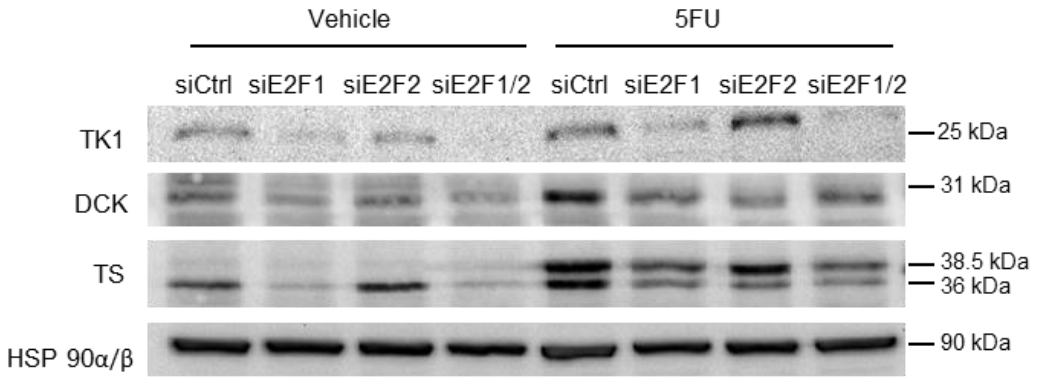


**B**

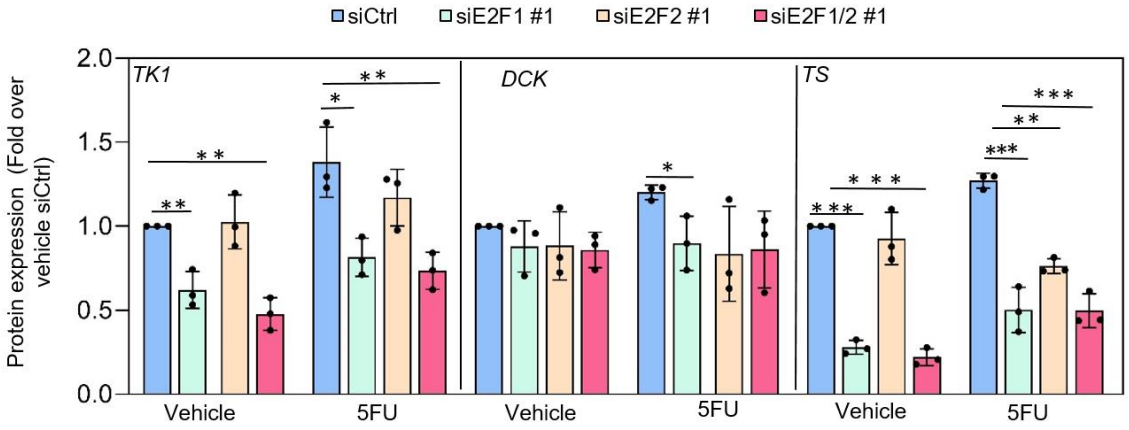

Figure 39. **Silencing of E2F1 alone, or more pronouncedly, combined silencing of E2F1/2 reduces steady-state levels of TK1, DCK and TS and prevents their induction by 5-FU.** A) PC3 cells were reverse transfected with siRNAs specific for *E2F1* (siE2F1 #1), *E2F2* (siE2F2 #1) or with their combination (siE2F1/2 #1). Transfection with non-target control siRNA (siCTRL) was used as silencing control. After 24h, 5 uM of 5-FU or vehicle control was added. 72h later, protein was extracted and analyzed by Western blot. Representative western blots of 3 different experiments done with the experimental setting shown in Figure 15. In TS blot, the band at 36 kDa corresponds to free TS, whereas the band at 38.5 kDa corresponds to ternary complexed TS. HSP90 was used as loading control. B) Densitometry values were obtained from 3 independent experiments. Values were normalized to the expression of HSP90, used as standard control. Data are represented as fold-change relative to siRNA control treated with vehicle (vehicle siCTRL).

The fact that the results observed at the protein level resemble those obtained at the mRNA level implies that the control of TK1, DCK and TS (*TYMS*) expression applied by E2F1 and E2F2 occurs primarily at the transcriptional level. Most importantly, these results suggest that E2F is required not only for the basal expression of TK1, DCK and TS (*TYMS*) in prostate cancer cells, but also for their upregulation by 5-FU.

## 3.3 Role of E2F1 and E2F2 in the resistance of mPCa cells to 5-FU-mediated cell death.

We next asked whether E2F1 and E2F2 are necessary for the resistance of mPCa cells to 5-FU. To address this question, we transfected cells with siE2F1 #1 and siE2F2 #1 alone or in combination, and 24h later treated them with 5-FU or vehicle control. After 72h, we measured cellular viability by counting live cells incubated with Trypan-blue vital exclusion colorant. As shown in figure 40A, silencing of E2F1, and more potently, combined silencing of E2F1 and E2F2, reduced to about 55% cellular viability of PC3 cells. Treatment with 5-FU reduced cellular viability to about 50%. Remarkably, combined treatment of 5-FU and siE2F had a dramatic effect, as cell viability was reduced to about 10%. Transfection with set #2 siRNA oligos produced similar results, although less strongly. In this case, cell viability was measured by FACS analysis after cell fixation and PI staining to detect DNA content. Cells that were not in SubG0/G1 were considered viable (Figure 40B). Using this experimental approach, we also confirmed that combined silencing of E2F1/E2F2 sensitizes DU145 cells to 5-FU mediated cell death (Figure 41).

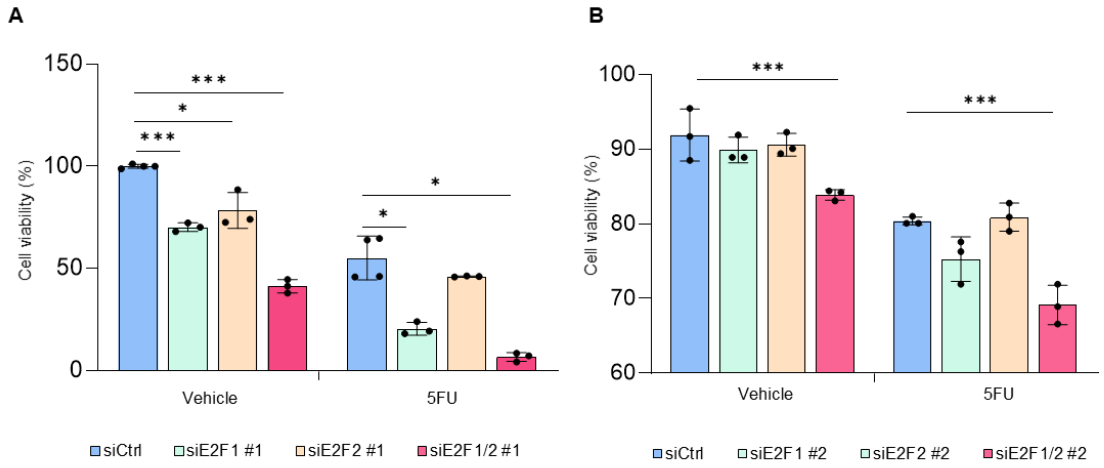


Figure 40. **Silencing of E2F1 alone, or more pronouncedly combined silencing of E2F1/2 sensitize PC3 cells to 5-FU-mediated decrease in cellular viability.** A) Quantification of cell number using Trypan blue exclusion colorant 96h after transfection with non-target control siRNAs (siCTRL), with siRNAs specific for E2F1 (siE2F1 #1) or E2F2 (siE2F2 #1) or for E2F1 and E2F2 (siE2F1/2 #1) and 72h after treatment with vehicle or 5-FU (5 μM). Results of cell viability are expressed as percentage of viable cells over the siCtrl vehicle sample. B) PC3 cells treated as in A, but with set #2 of silencing oligos for *E2F1* and *E2F2*. Cellular viability was measured by FACS analysis after cell fixation and PI staining to detect DNA content and determined as the percentage of all the cells that were not in SubG0/G1. Data shows the average ±SD from 3 independent experiments. ***p<0.0001, **p<0.005, *p<0.05, *vs.* siCTRL and 5FU sample.

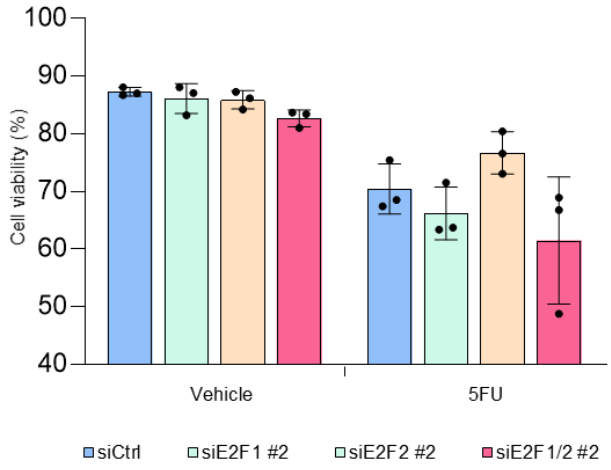


Figure 41. **Silencing of E2F1 alone, or more pronouncedly combined silencing of E2F1/2 sensitize DU145 cells to 5-FU-mediated cell death.** Cellular viability estimated by PI staining and FACS analysis of 96h after transfection with non-target control siRNAs (siCTRL), with siRNAs specific for E2F1 (siE2F1 #2) or E2F2 (siE2F2 #2) or for E2F1 and E2F2 (siE2F1/2 #2) and 72h after treatment with vehicle or 5-FU (5 μM). Data shows the average ±SD from 3 independent experiments.

These data suggested that E2F1 and E2F2 are involved in the resistance of mPCa to 5-FU. To further explore the impact of E2F1/E2F2 on 5-FU responses, we examined cell cycle distribution in PC3 cells transfected with siE2F1/siE2F2 and subsequently treated with 5-FU for 72h. We analyzed cell cycle distribution using PI staining and FACS analysis after 96h.

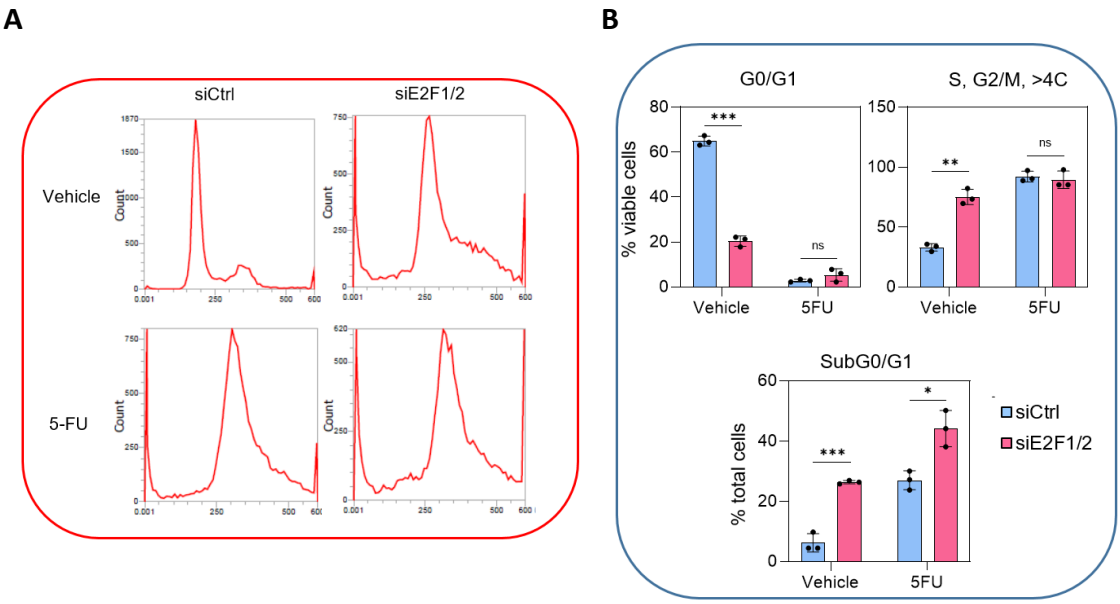


Figure 42. **Cell cycle distribution in cells after silencing of E2F1/2 and treatment with 5FU.** A) Representative cell cycle profiles obtained from PC3 cells 96h after transfection with non-target control siRNAs (siCTRL) or with siRNAs specific for E2F1 and E2F2 (siE2F1/2 #1) and 72h after treatment with vehicle or 5FU. Cells were stained with PI and analyzed by flow cytometry to determine their relative DNA content. B) Percentage of total cells with DNA content compatible with apoptosis (upper panel), and percentage of viable cells in different stages of the cell cycle according to DNA content (lower panels), after the indicated treatments. Data shows the average ±SD from 3 independent experiments. ***p<0.0001, **p<0.005, *p<0.05, *vs.* siCTRL and 5FU sample, ns=not significant.

Silencing of E2F1/E2F2 for 96h resulted in an accumulation of viable cells in S and G2/M phases concomitant to a reduction of cells in G1 phase (Figure 42), consistent with the results described in section 2 (Figure 30). Treatment with 5-FU led to an even higher accumulation of viable PC3 cells in S phase and a strong reduction in G1 phase (Figure 42), consistent with the induction of replication stress previously reported in the literature (de Angelis et al., 2006). In parallel, we detected an increased percentage of cells undergoing apoptosis (subG0/G1) to around 25% of the total cell population in each treatment. Importantly, the combination of siE2F1/siE2F2 and 5-FU treatment led to an approximately 50% of cells undergoing apoptosis.

## 3.5 Studying the contribution of TK1 and DCK to the resistance of PC3 cells to 5-FU

Based on our findings, we hypothesized that E2F1 and E2F2 could promote resistance of PC3 cells to 5-FU by inducing the expression of the nucleotide salvage pathway target genes TK1 and DCK. If that was the case, silencing of TK1 and DCK in PC3 cells should recapitulate the phenotypes that we observed after silencing E2F1 and E2F2.

In order to test this, we performed a series of experiments that were similar to those performed above, but in this case, we silenced TK1 and DCK. We first confirmed that two different sets of silencing oligos for TK1 and DCK were efficient at reducing the levels of TK1 and DCK expression (Figure 43). siDCK #1,2 molecules also reduced the expression of TK1.

Importantly, combined silencing of TK1 and DCK with both sets of oligos reduced cellular viability and potentiated the effect of 5-FU at a level that was similar to that observed after combined silencing of E2F1 and E2F2 (Figure 44). Flow cytometry analysis showed that silencing of TK1/DCK sensitized cells to apoptosis, as shown by the increased proportion of the subG0/G1 population of about 40% of the total number of cells (Figure 44-45). When analyzing the viable cells, we noticed that silencing of TK1/DCK resulted in a mild accumulation of cells in S and G2/M phases (Figure 45), suggestive of replication stress and cell cycle arrest. The combination of siTK1/siDCK and 5-FU treatment led to a dramatic arrest of cells in S and G2/M, which was associated with a significant increase of cells undergoing apoptosis (Sub G0/G1 population).

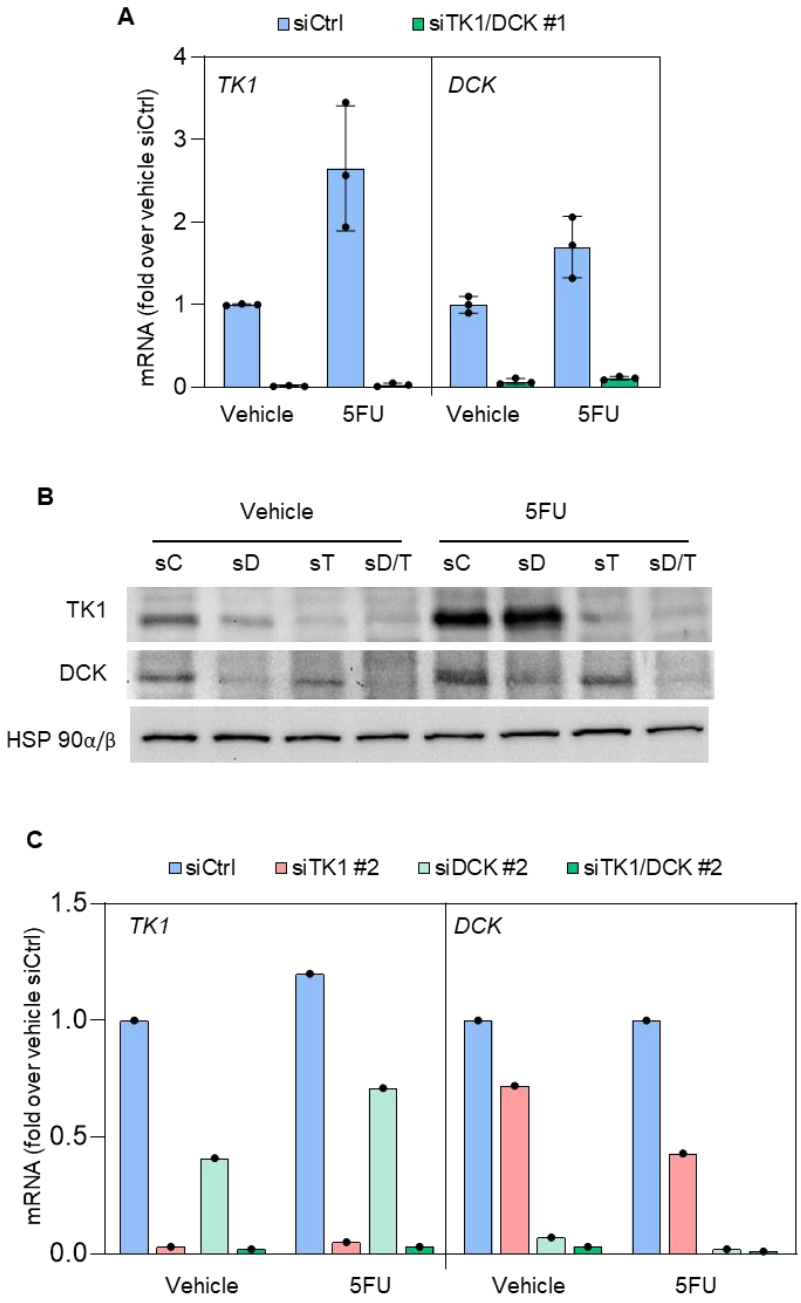


Figure 43. **Silencing efficiency of TK1 and DCK in PC3 cells with two different sets of silencing oligos after treatment with vehicle or 5-FU.** Efficiency of silencing with #1 set of oligos, analyzed by RT-QPCR (A) and western blot (B) 96 h after transfection of siRNAs specific for TK1, DCK or combined TK1 and DCK and non-target control siRNAs (siCTRL), and 72h after 5FU (5µM) treatment. C) Efficiency of silencing with the #2 set of oligos, analyzed by RT-QPCR.

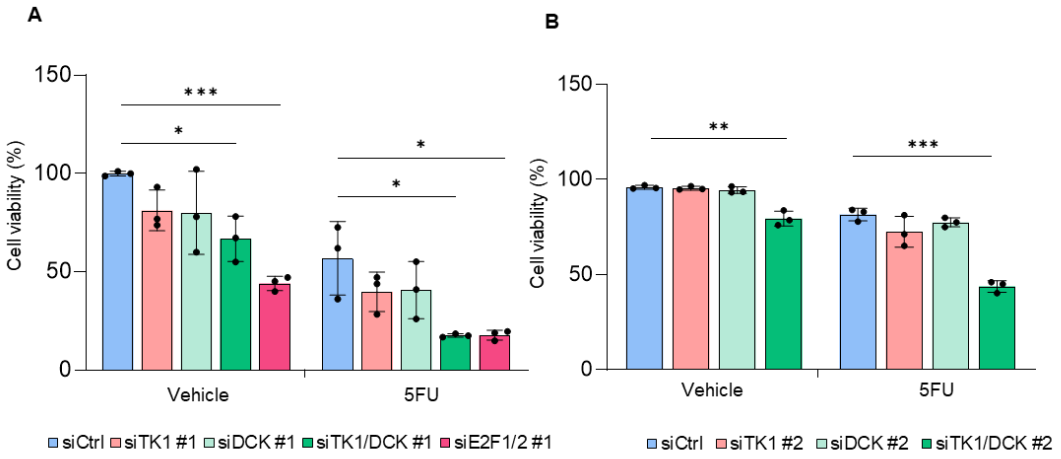


Figure 44. **Combined silencing of TK1 and DCK sensitizes PC3 cells to 5-FU-mediated decrease in cellular viability.** A) Quantification of cell viability using Trypan blue staining 96h after transfection with non-target control siRNAs (siCTRL), with siRNAs specific for TK1 (siTK1 #1) or DCK (siDCK #1) or for TK1 and DCK (siTK1/DCK #1), or for E2F1 and E2F2 (siE2F1/2 #1) and 72h after treatment with vehicle or 5-FU. B) Cellular viability estimated by PI staining and FACS analysis of PC3 cells treated as in B, but with set #2 of silencing oligos for TK1 and DCK. Data shows the average ±SD from 3 independent experiments. ***p<0.0001, **p<0.005, *p<0.05, *vs.* siCTRL and 5FU sample.

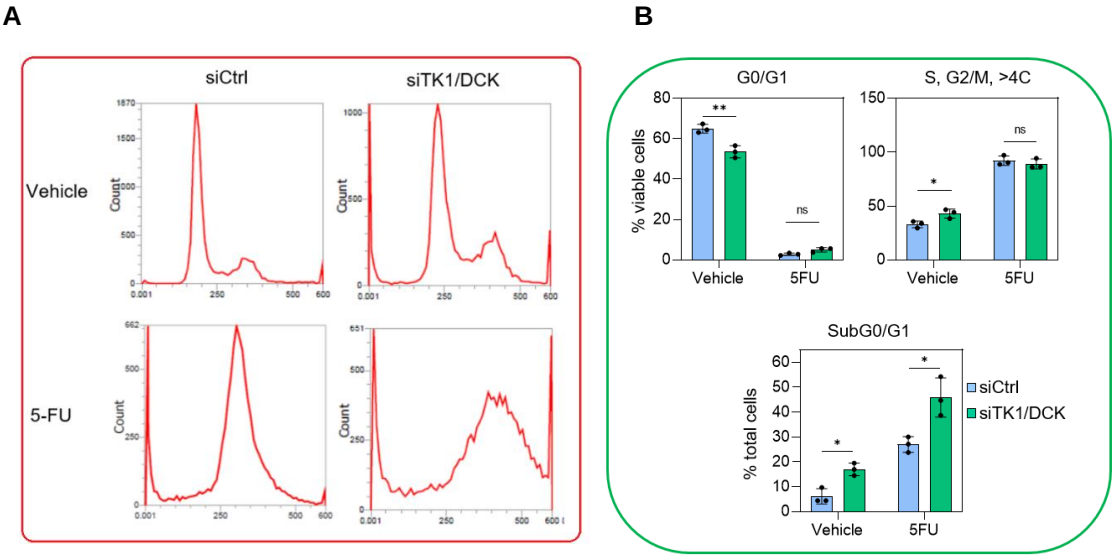


Figure 45. **Combined silencing of TK1 and DCK sensitize cells to 5FU-induced cell death and results in the accumulation of cells throughout the cell cycle.** A) Representative cell cycle profiles obtained from PC3 cells 96h after transfection with non-target control siRNAs (siCTRL) or with siRNAs specific for TK1 and DCK (siTK1/DCK #1) and 72h after treatment with vehicle or 5FU. Cells were stained with PI and analyzed by flow cytometry to determine their relative DNA content. B) Percentage of total cells with DNA content compatible with apoptosis (upper panel), and percentage of viable cells in different stages of the cell cycle according to DNA

content (lower panels), after the indicated treatments. Data shows the average ±SD from 3 independent experiments. **p<0.005, *p<0.05, *vs.* siCTRL and 5FU sample, ns=not significant.

Taken together, the results suggested that depletion of the E2F targets TK1 and DCK recapitulates the increased apoptotic rate and cell cycle arrest obtained after silencing of E2F1 and E2F2. This led us to ask whether silencing of TK1 and DCK also results in DNA replication stress similarly to silencing E2F1 and E2F2. We analyzed the percentage of γH2AX-positive cells after silencing of TK1 and DCK individually or in combination with #1 oligos, and stained with PI by FACS at 48-72H time point (Figure 46). Flow cytometry data showed an increase in the percentage of γH2AX-positive cells 48 hours after double silencing of TK1 and DCK. This increase was more robust at the 72h time-point (Figure 46). Thus, inactivation of TK1 and DCK recapitulates the DNA replication stress and subsequent activation of DNA damage response observed after silencing of E2F1 and E2F2. Altogether, our findings provide strong support for a critical role of the E2F1/2-TK1/DCK pathway in lowering replication stress levels and preventing apoptosis of PC3 cells. This activity would facilitate the development of resistance to a treatment, such as 5-FU, which impacts nucleotide levels.

**A**

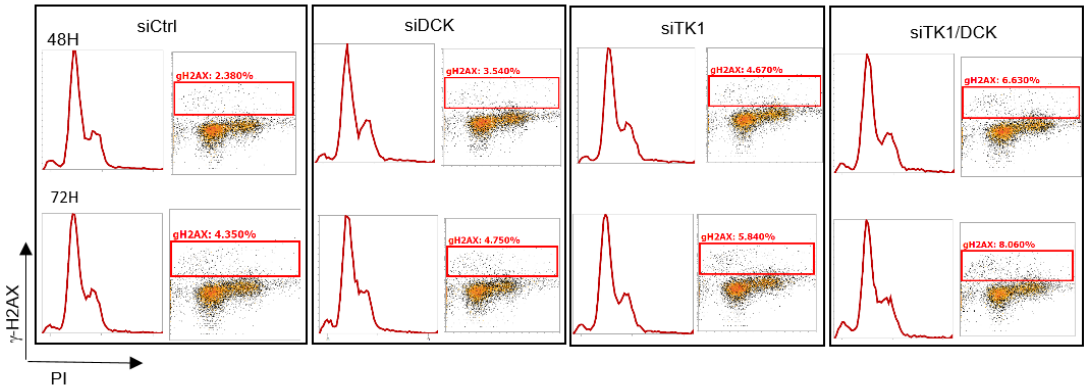


**B**

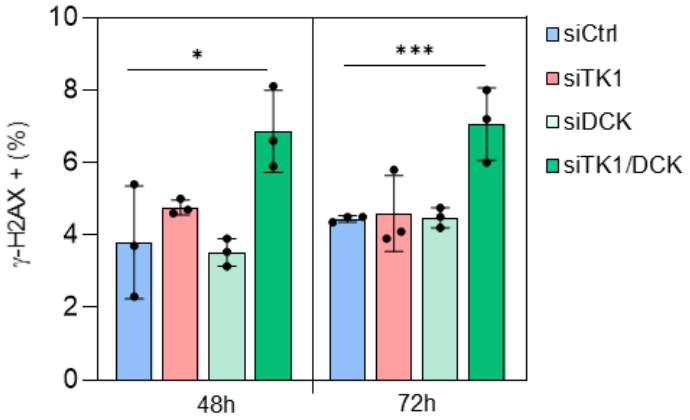

Figure46.**Combined silencing of TK1 and DCK leads on replication stress in PC3 cells.** A) Cell cycle profiles and the percentage of g-H2AX determined by g-H2AX positivity and FACS analysis obtained from PC3 cells at 48, 72 hours after transfection with non-target control siRNAs (siCtrl) or with siRNAs specific for TK1 and DCK. B) The percentage of g-H2AX positivity from indicated time point. The result are representative of 3 independent experiment. . *p<0, 05, **p<0,005, vs. siCtrl.

We also asked whether TK1/DCK knockdown cells exhibited improper activation of CDK1, by analyzing the levels of pCDK1 (Tyr15) by western blot analysis. However, the relative pCDK1/CDK1 levels were similar in knockdown cells and their respective siCtrl controls (Figure 47), suggesting that TK1 and DCK do not contribute to the regulation of the inhibitory phosphorylation of CDK1 exerted by E2F1 and E2F2 in order to maintain genomic stability. More probably, the role of TK1 and DCK would be restricted to maintaining nucleotide production.

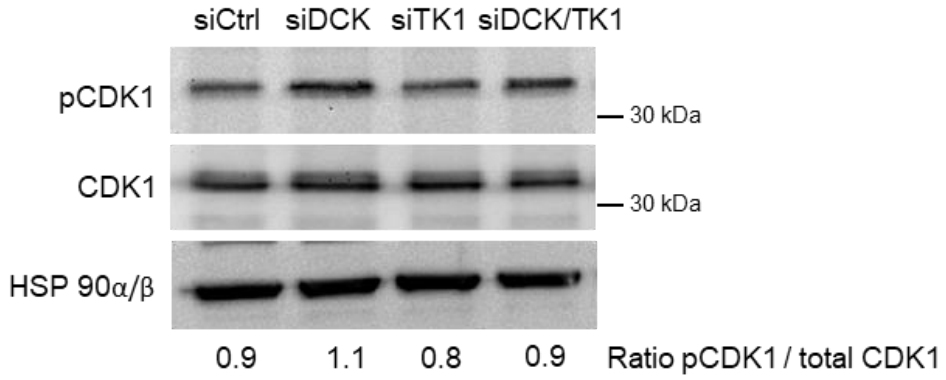


Figure 47. **Silencing of TK1 and DCK does not modify the levels of inhibitory phosphorylation of CDK1.** 96h after transfection of PC3 with non-target control siRNAs (siCTRL), with siRNAs specific for TK1 (siTK1 #1) or DCK (siDCK #1) or for TK1 and DCK (siTK1/DCK #1), accumulation of CDK1 and pCDK1 (Tyr15) was measured by western blot analysis. Results of one experiment are shown as representative. HSP90α/β was used as standard control. Numbers below the blots correspond to the relative densitometric values of pCDK1/ total CDK1. Similar results were obtained in more than 2 experiments.

## 3.5 Studying the contribution of nucleosides to the resistance of PC3 cells to 5-FU

Our findings suggest that the activation of the E2F1/2-TK1/DCK pathway could be involved in maintaining genomic stability and preventing 5-FU-induced apoptosis in PC3 cells. The following lines of evidence led us to hypothesize that the E2F1/2-TK1/DCK pathway promotes the production of nucleosides to overcome 5-FU-imposed depletion: i) The fact that TK1 and DCK are necessary for the biosynthesis of nucleosides, ii) that they are E2F target genes, iii) are upregulated after 5-FU treatment, iv) and are necessary for the resistance of PC3 cell to 5-FU. If this hypothesis is correct, exogenous supply of nucleosides, or the products of TK1 and DCK activities should prevent the reversion of resistance to 5-FU observed upon silencing of E2F1 and E2F2.

To formally prove this hypothesis, rescue experiments were designed, in which exogenous nucleosides (Embryomax) or deoxynucleotide monophosphate (dNMP) products of TK1 and DCK activities were added to cells 4 hours after silencing of E2F1 and E2F2. 24 hours later, cells were treated with 5-FU. Cell viability was assessed 48 hours later (Figure 48A) by trypan blue staining in the rescue experiments with nucleosides and by PI-staining and FACS analysis in the rescue experiments with dNMPs.

Adding nucleosides (Figure 48B) or dNMPs (Figure 48C) to siCTRL-treated PC3 cells did not significantly increase cell viability. By contrast, addition of nucleosides increased by 25% the viability of $E2F1^{low}/E2F2^{low}$ cells. Similarly, dNMPs treated cells partially improved their viability, although to a lesser degree. In 5-FU treated cells, addition of nucleosides or dNMPs to PC3 cells helped improve the survival in siCTRL condition and enhanced by nearly 35 % the viability of $E2F1^{low}/E2F2^{low}$ cells. Thus, nucleosides hinder the sensitization to 5-FU-induced cell death observed after silencing of E2F1 and E2F2.

Taken together, these results highlight the relevance of E2F1/2-TK1/DCK pathway to provide nucleotide intermediates necessary to maintain genomic integrity.

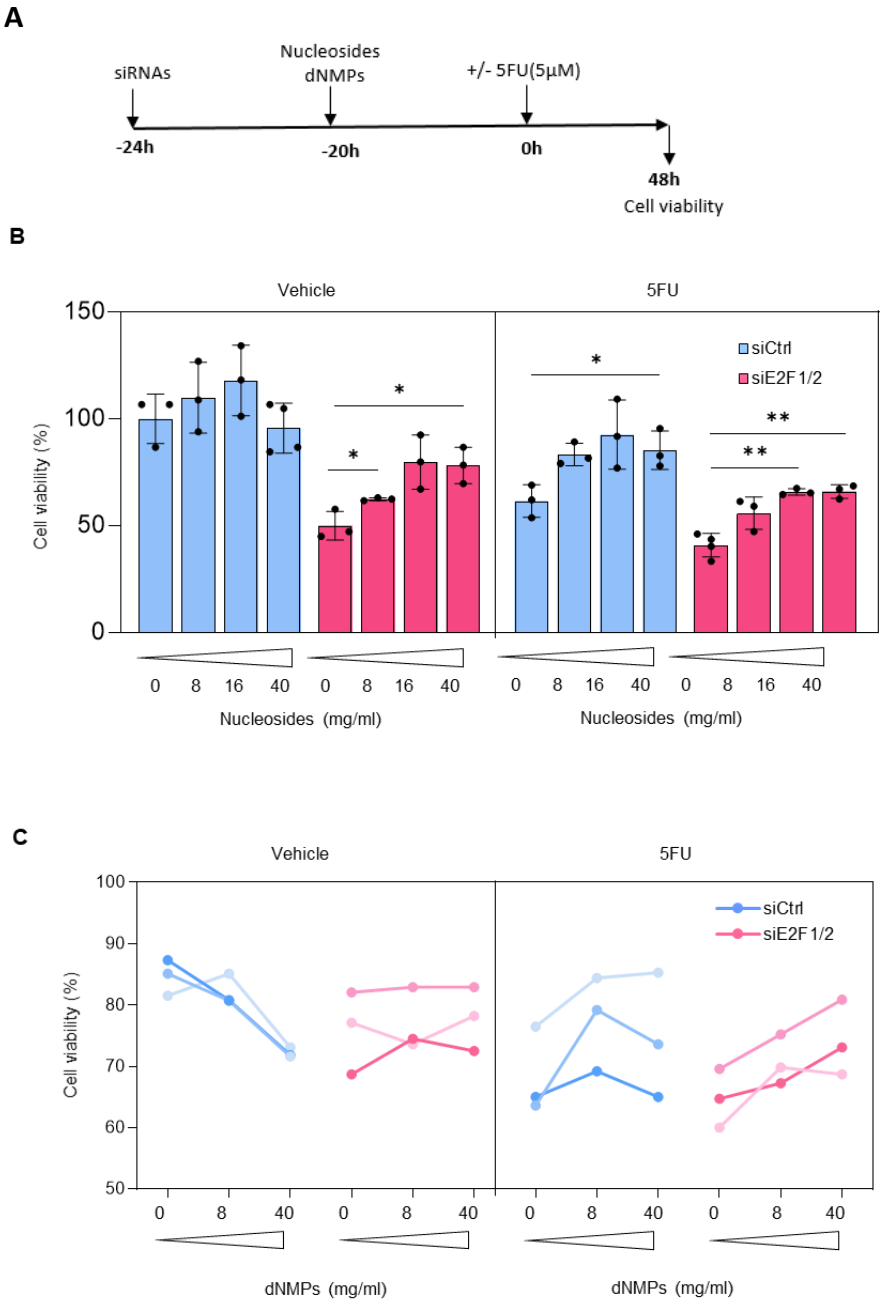


Figure 48. **Exogenous supply with nucleosides or the sole dNMP products of TK1 and DCK increase the cell viability in PC3 cells treated with siE2F1 and siE2F2.** A) Schematic representation of the experimental design. PC3 cells were co-transfected with siE2F1 and siE2F2 with set #1 oligos. 4 hours later, cells were treated with 0, 8, 16, 40 µg/ml of nucleoside mixture Embryomax or dNMP, and 24 hours later, treated with 5FU (5µM). Cell viability was analyzed 48 h later. B) Quantification of PC3 cell number 72h after combined silencing of E2F1 and E2F2 and 48 hours after 5-FU treatment by trypan blue staining. Data is presented as percentage of viable cell over the viable cells in untreated siCtrl sample. *p<0.05, **p<0.005, *vs.* vehicle siCtrl and 5FU. C) Percentage of viable cells, according to PI staining and FACS analysis, after the indicated treatments. Results of 3 independent experiments are shown, where each color intensity represents one experiment.

# Objective 4. Studying a clinical approach to reverse resistance to 5-FU in PC3 cells using inhibitors of E2F activity

Based on our data on metastatic prostate cancer cells, inhibition of E2F1/E2F2 could be a promising strategy to fully prevent nucleotide biosynthesis and sensitize tumor cells to cell death after treatment with 5-FU. E2F proteins, similarly to most transcription factors, are not easily "druggable", and there are no E2F inhibitors in clinical use yet. We considered that an alternative possibility to inhibit E2F activity would be to use cyclin-dependent kinase 4/6 inhibitors (CDK4/6), which have entered the clinical setting for patients with metastatic breast cancer (palbociclib, ribociclib, and abemaciclib). They inhibit E2F activity by preventing pRB phosphorylation and subsequent E2F release (Roberts et al., 2020). These inhibitors are currently being tested in multiple tumor types, in most cases in combination with available drugs targeting other cellular pathways (Asghar et al., 2015; Salvador-Barbero et al., 2020).

To check any possible benefit on combining 5-FU and palbociclib, we performed a colony forming assay using increasing concentrations of palbociclib (0.25, 0.5, 1µM) alone or in combination with 5FU (5µM). 72 hours after the treatment, media containing drugs was replaced by fresh media, and the cells incubated for 10 days. Subsequently, cells were fixed with formaldehyde and stained with crystal violet (Figure 49A).

The additive effect of a combination of palbociclib and 5-FU can be nicely observed with the lowest concentration of palbociclib tested, 0.25 µM. Indeed, independent treatment with 5-FU or 0.25 µM palbociclib has minor effect in the colony formation, whereas the combination of both inhibitors potently reduced the viability of PC3 cells (Figure 49B-C). In conclusion, palbociclib and 5FU could be interesting candidates to be tested clinically to induce apoptosis of metastatic prostate cancer cells.

**A**

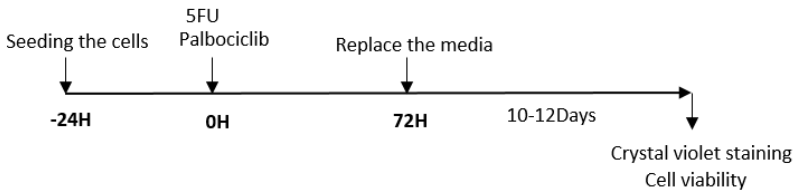


**B**

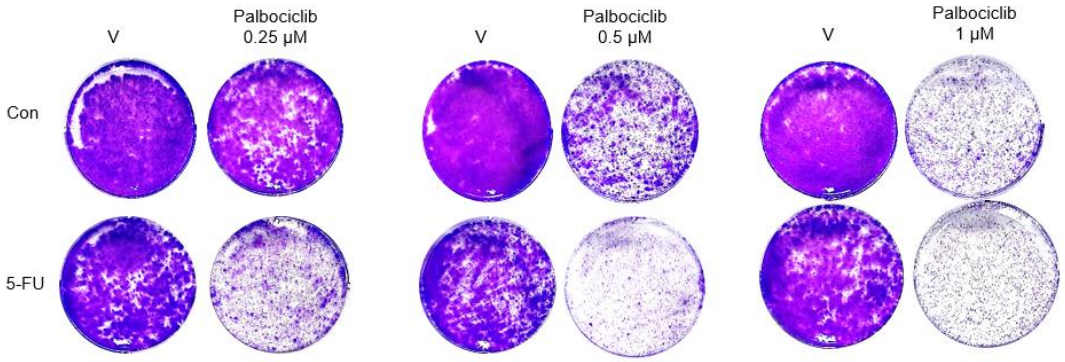


**C**

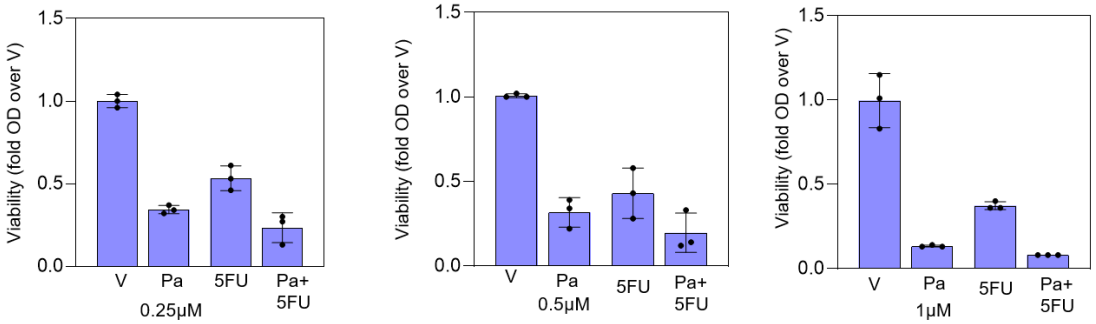


Figure 49. **Combination of palbociclib and 5-FU reduces colony formation of PC3 cells.** A) Schematic representation of the experimental design. 24 h after seeding PC3 cells, they were treated with 5FU (5µM) and palbociclib (0.25, 0.5, 1 µM) alone or in combination. 72hours later, drugs were wahed out and cells were incubated with fresh media additional 10-12 days. Then, cells were fixed and stained with crystal violet. B) Representative images of colony density in each condition. C) Crystal violet was dissolved with acetic acid and the absorbance was measured by Spectrophotometry. Relative cell viability was calculated by normalizing the absorbance of each condition using their vehicle (V) controls.

# Discussion

The pathway in which the tumor suppressor protein retinoblastoma (RB) regulates the activity of the E2F transcription factor (RB / E2F pathway) is critical for the controlled progression of the G1 phase to the S phase of the cell cycle, and its discovery allowed establish a cell cycle control model (Weinberg, 1995). E2F transcription factors (E2F1–8) are key downstream effectors of pRB. Hypophosphorylated pRb protein forms a complex with E2F members and blocks their transcriptional activity, preventing entry into the cell cycle (Trimarchi & Lees, 2002). E2F-dependent transcriptional network ensures the timely entry into S-phase through the regulation of genes involved in nucleotide biosynthesis and DNA replication (Hirschey et al., 2015; Ishida et al., 2001; Lane & Fan, 2015; Polager et al., 2002; Ren et al., 2002; Vernell et al., 2003). Remarkably, either a diminished or an elevated E2F activity negatively affects cellular homeostasis, leading to tissue atrophy or oncogenesis, depending on the context.

In non-tumoral cells, targeted depletion of *E2f1* and *E2f2* (DKO) in mice leads to the activation of DNA damage response and subsequent tissue atrophy and diabetes (Iglesias-Ara et al., 2010; 2015). However, the source of DNA damage in E2f1/E2f2-null pancreas has remained elusive. Given that, E2f factors' main role is to promote the expression of genes necessary for the duplication of DNA molecules, in this thesis work we speculated that the absence of E2f1/E2f2 might cause a downregulation of genes involved in the biosynthesis of nucleotides, which would induce replication stress and subsequent activation of DNA damage response. We reasoned that the restoration of nucleotide levels could attenuate genomic instability in the absence of E2f1/E2f2.

In tumor cells with an inactive Retinoblastoma protein, enhanced E2F activity is thought to supply the nucleotides required for their exacerbated DNA replication and cellular proliferation (Villa et al., 2019). Given that nucleotide biosynthesis is central to the capacity of a cell to proliferate, cancer cells are sensitive to nucleotide pool levels for their growth. For this reason, antimetabolite drugs blocking nucleotide production, such as 5-FU, have been widely used to treat different types of cancer, including prostate cancer (Longley et al., 2003). 5-FU irreversibly binds to and blocks the activity of TS, an E2F target involved on *de novo* synthesis of thymidine (Sethy & Kundu, 2021), resulting in apoptosis of prostate cancer cells (Yee et al., 1998). However, metastatic prostate cancer cells show resistance to 5-FU. We hypothesized that other E2F target genes involved in the *de novo* or salvage nucleotide biosynthesis pathways could account for the resistance to 5-FU. Thus, targeting E2F could be an approach to sensitize cells to 5-FU treatment.

In this work, we investigated the role of E2F1 and E2F2 in the metabolism of nucleosides and the implications that their function might have in metastatic prostate cancer progression and resistance against chemotherapy.

## 1. Relevance of E2f-regulated nucleotide metabolism *in vivo*

Our group has previously shown that simultaneous depletion of *E2f1* and *E2f2* (DKO) leads to DNA damage induction and the activation of p53-dependent apoptosis, leading to pancreatic atrophy (Iglesias-Ara et al., 2010; Iglesias-Ara et al., 2015). We have now examined whether the observed DNA damage response in DKO samples could be the result of some nucleotide deficiency that would lead to replication stress.

The dNTP supply system is comprised of *de novo* and salvage pathways that are coordinated, such that the total dNTP fluxes that are supplied equal the total demanded by nuclear and mitochondrial DNA replication and repair (Radivoyevitch et al., 2012). Based on our results on gene expression, *de novo* nucleotide synthetic pathway does not seem to be involved in the DNA replication stress of *E2f1/E2f2* DKO cells. The alternative pathway of nucleotide synthesis, known as the *nucleotide salvage pathway*, is used preferentially to *de novo* pathway to synthesize nucleotides by certain cell types, such as brain cells and polymorphonuclear leukocytes (Fasullo & Endres, 2015). Cancer cells have also been reported to depend on the salvage pathway to facilitate survival and growth (Lyssiotis & Cantley, 2013). We found that the expression levels of *Tk1* and *Dck* genes, encoding rate-limiting enzymes of the salvage pathway, were reduced in DKO mice compared to WT. This suggested that E2f1/E2f2 could be controlling cellular nucleotide pools through the salvage pathway, by promoting the expression of *Tk1* and *Dck*. Downregulation of *Tk1* and *Dck* might be causing nucleotide scarcity and DNA damage in DKO pancreas. Indeed, it has been reported that depletion of dCTP pools in $Dck^{-/-}$ mice leads to replication stress, S-phase arrest and DNA damage in hematopoietic progenitor cells (Austin et al., 2012; Toy et al., 2010), and that siRNA knockdown of TK1 targets various types of tumor cells to apoptosis.

We wondered whether increasing nucleotide synthesis in DKO mice could alleviate replication stress and prevent pancreatic atrophy. The murine model for the ATR-Seckel Syndrome presents severely reduced ATR activity resulting in increased RS, stunted growth and premature aging (Murga et al., 2009). However, when these mice are crossed with mice carrying an extra allele of the RRM2 subunit ($Rrm2^{TG}$), the presence of the *Rrm2* transgene significantly reduced the ATR-Seckel associated phenotypes such as reduced body size and craniofacial abnormalities and doubled life span (Lopez-Contreras et al., 2015). These observations suggested that overexpression of the RRM2 subunit leads to increased RNR activity and confers resistance towards replicative damage induced by ATR deficiency. However, contrary to what occurs in the Seckel model, introducing an extra *Rrm2* allele does not rescue the phenotype of *E2f1/E2f2* DKO mice.

One possibility that may account for the failure to revert the aberrant phenotype of DKO pancreas after introducing an extra *Rrm2* allele is that animals lacking *E2f1/E2f2* could have a deficiency of ribonucleotide precursors, that is, the substrates of RNR, such that nucleotide production would be blocked upstream of RNR in our mouse model. Consistent with this possibility, supplementing DKO mice with the complete set of the end products of nucleotide biosynthesis was able to prevent DNA damage and apoptosis. Our findings are in line with those of Kerem and collaborators, who have shown that replication stress elicited by oncogenes, which is a consequence of nucleotide deficiency, can be restored by exogenously supplied nucleosides (Bester et al., 2011).

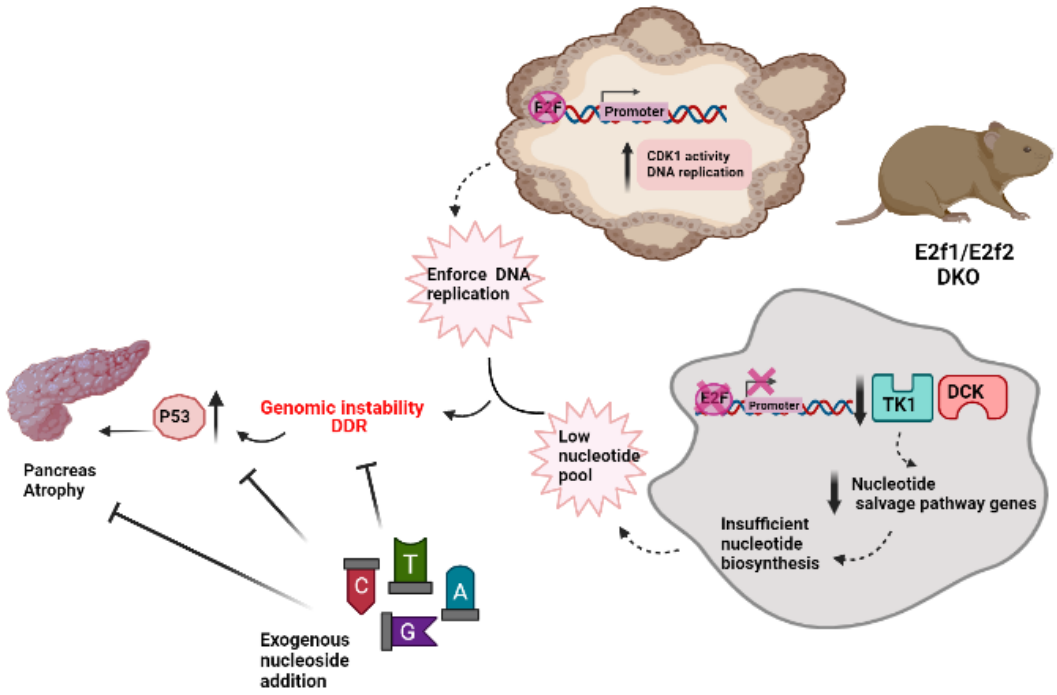


Figure 50. **Model for E2f1/E2f2-mediated regulation of genomic stability and tissue homeostasis in mice.** The cells derived from E2f1$^{-/-}$/E2f2$^{-/-}$ double-knockout (DKO) mice exhibit an aberrant cell cycle regulation, characterized by overexpression of E2f target genes involved in DNA replication or cell cycle progression and repression of cell cycle inhibitors, resulting in unscheduled DNA replication. Furthermore, the expression of E2F targets *Tk1* and *Dck* genes, encoding rate-limiting enzymes of the salvage pathway, were reduced in DKO mice. Thereby loss of E2F1/E2F2 would reduce nucleotide pools in hyper proliferating DKO cells, in which nucleotide scarcity would activate DNA damage response and p53-dependent tissue atrophy, particularly in the pancreas. Exogenously supplied nucleosides ameliorate replication stress and rescue the aberrant phenotype of *E2f1/E2f2* DKO mice.

Taken together, the observed phenotypic rescue triggered by addition of nucleosides suggests that DNA damage response activation and p53-dependent tissue atrophy in mice lacking E2f1 and E2f2 could result from an untimely nucleotide exhaustion, underlying the relevance of E2F in the regulation of cellular nucleoside pools. Moreover, the fact that *Tk1* and *Dck* expression is blunted in DKO pancreas points towards a mechanism guided by an E2F-Tk1/Dck axis to promote nucleotide production in pancreas (figure 50). Future experiments should help clarify the relevance of E2F-Tk1/Dck axis in the pancreatic organ. For instance, we could assess the effect of overexpressing *Tk1* and *Dck* in E2f1/E2f2 DKO mice, following a similar approach to our studies with Rrm2 transgenic mice. Alternatively, we could administer the products of TK1 and DCK enzymatic activities in order to rescue the phenotype of E2f1/E2f2 DKO mice. In this regard, dCMP/dTMP supplementation has been shown to be a very effective pharmacologic treatment in Tk2-deficient mice (Garone et al., 2014; Lopez-Gomez C. et al., 2017).

## 2. Relevance of E2F1/E2F2-regulated nucleotide metabolism in prostate cancer

Based on our observations, E2F-Tk1/Dck axis plays a key role promoting nucleotide production in cells with a low turnover, such as pancreatic cells. Thus, rapidly proliferating cells, such as cancer cells, would be even more dependent on the mechanism governed by E2F to synthesize nucleotides, making the E2F pathway an interesting target for cancer treatment. Keeping this in mind, we aimed to study the relevance of E2F-regulated nucleotide metabolism in cancer.

Before gathering experimental evidences, we focused our attention on available *in silico* data. The increasing availability of *in silico* OMICs data is an important source of information that can be used to analyze the relevance of a particular set of proteins in cancer biology (Simon, 2005). The problems in managing, extracting and analyzing the information that is accessible in the different datasets has encouraged the development of user-friendly tools for basic cancer researchers, such as *cBioportal* (Cerami et al., 2012), *KM plotter* (Nagy et al., 2021) and *Cancertool* (Cortazar et al., 2018). With the help of bioinformatics, research questions can be first studied in *silico*, working with tumor derived data that would be inaccessible otherwise. By using cBioportal and KM plotter analysis we found an inverse correlation between *E2F1* and *E2F2* gene expression and disease free survival, that is, high expression of these genes correlated significantly with a worse prognosis among pancreatic, breast and prostate cancers, which would be the most suitable targets to assess therapies based on E2F inhibition. Interestingly, an equivalent negative correlation between E2F expression and DFS was observed for genes involved in biosynthesis of nucleotides (*TK1*, *DCK* and *TYMS*).

PCa often progresses rapidly and most deaths are caused by metastases that are resistant to conventional therapies. Unfortunately, the optimal therapy for patients with this cancer has yet to be defined. Given this fact, and the availability of prostate-derived cell lines with different degrees of malignancy in our laboratory, we focused on prostate cancer as the paradigm in which to study the relevance of E2F1/2 in the malignant progression of this type of neoplasia, and to explore the usefulness of E2Fs as therapeutic targets. The data that we obtained with *Cancertool* website indicated that the expression of *E2Fs* and its target genes *TK1*, *DCK* and *TYMS* correlates with malignancy in prostate cancer. We confirmed the results by analyzing mRNA expression among prostate cancer cell lines. Expression of *E2F1*, *TK1*, *DCK* and *TYMS* is higher in prostate cancer cells compared to non-tumoral cells. Furthermore, the most malignant PCa cell line, PC3, exhibits the highest differential gene expression levels for most of these genes.

Previous work has already indicated that elevated E2F1 expression might contribute to the progression of PCa (Davis et al., 2006; Libertini et al., 2006). The relevance of E2F in the regulation of nucleotide biosynthesis, however, was not addressed in these studies. Importantly, we performed loss-of-function experiments to show that combined E2F1 and E2F2 activity is necessary in mPCa cells to maintain steady-state levels of the genes involved in nucleotide biosynthesis *TK1*, *DCK* and *TYMS.* It has been shown that accumulation of cells in S phase occurs in contexts of replication stress caused by depletion of nucleotides (Gaillard et al., 2015). Similarly, combined silencing of *E2F1* and *E2F2* led to the accumulation in S phase of cells showing DNA damage and this was accompanied by reduced cellular viability. Interestingly, adding nucleosides or the sole products of TK1 and DCK enzymatic activities improved cellular viability, supporting the notion that E2F/TK1-DCK mechanism is crucial to preserve DNA integrity in mPCa cells. Importantly, combined silencing of TK1 and DCK also resulted in DNA damage, yet the percentage of cells showing DNA damage was lower than in E2F knockdown cells. This indicated that, apart from TK1 and DCK regulation, additional mechanisms may be governed by E2F to restrain DNA damage in S phase.

We studied whether improper activation of CDK1 was concomitant to DNA damage in E2F-depleted cells. Since premature activation of CDK1–cyclin B1 causes DNA damage (Szmyd et al., 2019), restricting CDK1–cyclin B1 activity prior to mitosis is key to maintaining genomic integrity. Galarreta and colleagues have recently shown that widespread activation of CDK1 throughout the cell cycle leads to DNA damage and is toxic for mammalian cells (Galarreta et al., 2021). The restriction of CDK1 activation during S phase is accomplished by the inhibitory phosphorylation of CDK1 in Tyr15, regulated by the E2F targets WEE1 (the main enzyme involved in catalyzing the inhibitory tyrosine phosphorylation of CDK1) and CDC25A (the phosphatase that

eliminates the inhibitory tyrosine phosphorylation of CDK1) (Akopyan et al., 2014; Deng et al., 2019; Lemmens et al., 2018; Elbæk et al., 2020). We showed that combined silencing of E2F1 and E2F2 decreased the relative pCDK1/CDK1 levels, suggesting that E2F1 and E2F2 play a role promoting the inhibitory phosphorylation of CDK1 in order to maintain genomic stability, probably via WEE1 and CDC25A transcriptional regulation (figure 51). Intriguingly, combined silencing of TK1 and DCK did not altered CDK1 phosphorylation status, implying that E2F is preserving DNA integrity by controlling both nucleotide production and CDK1 activity. Previous work has shown that depletion of CDC25A to cells treated with CHK1 inhibitors improves significantly DNA damage and proliferative potential of cells (Beck et al., 2010), and pharmacological inhibition of CDK1 alleviates the genotoxicity imposed by USP7 inhibitors (Galarreta et al., 2021). To address the role of E2Fs on inappropriate CDK1 activation and control of DNA stability it will be interesting to carry out rescue experiments, for example by using commercially available CDK1 inhibitors, or by overexpressing WEE1 or by downregulating CDC25A in E2F1/E2F2 knockdown cells in order to ameliorate DNA damage and improve genomic instability.

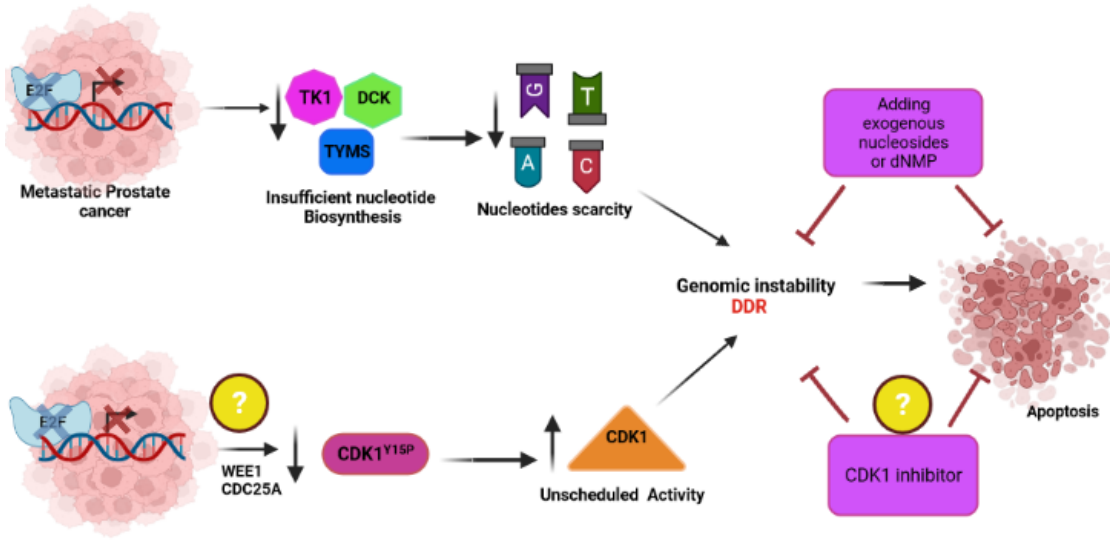


Figure 51. **Model for genomic instability induced upon inhibition of E2F activity**. Lack of E2Fs could potentially induce apoptosis in metastatic prostate cancer through two different pathways. Firstly, the expression of E2f target genes involved in nucleotide biosynthesis *TK1, DCK* and *TYMS*, encoding rate-limiting enzymes of the salvage pathway is reduced. This leads to a shortage of nucleosides and induces DNA damage response activation and apoptosis. The second pathway induced genomic instability via inappropriate CDK1 activation. E2F deprivation may lead to deregulation of its target genes WEE1 and CDC25A and promote aberrant activation of CDK1 via dephosphorylation of an inhibitory tyrosine, leading to cell death.

The dependency of prostate cancer cells on E2F activity for their correct progression in the cell cycle that we have uncovered represents a vulnerability that could be exploited therapeutically.

## 3. Reversion of resistance to 5-FU in PC3 cells by targeting E2F

The dependency of cancer cells on cell cycle control functions to endure high levels of stress associated with their aberrant proliferation raises new therapeutic opportunities for cancer treatment (Matthews et al., 2022). We have shown that E2F activity is essential for the correct progression in the cell cycle of mPCa cells. This makes E2F an attractive target to consider for the treatment of this type of cancer. As indicated above, one of the branches that is regulated by E2F for the correct progression through the cell cycle is the production of the adequate level of nucleotides, by the transcriptional regulation of *de novo* and salvage pathway genes *TYMS*, *TK1* and *DCK*. Nucleotide production has been already targeted to treat cancer. Indeed, nucleotide analogs such as 5-FU nowadays are used to treat several cancer types, including prostate cancer (Longley et al., 2003). 5-FU induces cytotoxicity primarily by interfering with *de novo* synthesis of nucleosides, through its interaction with *TYMS* encoding enzyme TS (Longley et al., 2003). In fact, TS and other enzymes involved in the metabolic process of 5-FU have been shown to predict sensitivity to 5-FU and/or prognosis (Etienne et al., 1995; Johnston et al., 1995).

However, various clinical trials on the role of 5-FU in advanced prostate cancer have reported a low response rate (Yagoda & Petrylak, 1993). Mechanisms of 5-FU resistance have been intensively investigated but many details are still largely unknown (Longley et al., 2003). In this sense, a recent single-cell RNA-seq analysis of colon cancer has uncovered three distinct transcriptome phenotypes upon 5-FU treatment related to apoptosis, cell-cycle checkpoint and stress resistance, which are providing a resource for understanding chemoresistance to 5-FU (Park et al., 2020). Although it has been widely thought that TS is a main molecular mechanism governing 5-FU sensitivity, and targeting TS is a key strategy to reverse 5-FU resistance (Copur et al., 1995), the contribution of the salvage pathway enzymes in the resistance to 5-FU awaited to be deeply investigated.

Based on our data on mPCa cell lines, whereby depletion of E2F1/E2F2 downregulates the expression of salvage pathway genes TK1 and DCK, we speculated that therapies based on the combination of 5-FU and E2F inhibition could fully prevent nucleoside biosynthesis, and thereby, induce apoptosis in tumor cells. Analysis of cellular viability after 5FU titration (dose-response) in LNCaP, DU145 and PC3 cell lines demonstrated the cell line with the highest metastatic potential, PC3, showed the highest resistance to 5-FU induced apoptosis. This result implies that malignancy in PCa cell lines correlates with resistance to 5-FU. The fact that PC3 cells express high levels of E2F1

and E2F2, and are resistant to 5-FU lead us to speculate that PC3 cells could overcome the reduction of nucleotide pools imposed by 5-FU by activating the expression of E2F target genes coding for enzymes responsible for the synthesis of nucleosides. Consistently with published data (Sulzyc-Bielicka et al., 2016), we found that expression of E2F target *TYMS* is induced by 5-FU.

Importantly, we also detected upregulation of *TK1* and *DCK* salvage pathway genes. Moreover, we showed that E2F1/2 combined activity is essential for the induction of *TK1*, *DCK* and *TYMS* by 5-FU. We next asked whether E2F1 and E2F2 are necessary for the resistance of mPCa cells to 5-FU. Interestingly, E2F silencing reversed the resistance of mPCa cell to 5-FU, that is, it sensitized mPCa cells to death after treatment with 5FU (Figure 52). Reversion of resistance to 5-FU has also been observed upon knockdown of Bcl-XL protein expression by Bcl-XL-specific small interfering RNA in 5-FU-resistant colon cancer, although the effect was only moderate (Zhu et al., 2005). A better sensitization was observed in cholangiocarcinoma and colon cancer cells after silencing of FOXM1, a transcription factor that promotes TYMS expression (Intuyod et al., 2018; B. Varghese et al., 2019), and more recently in various cancer cell lines with the use of a small molecule thought to inhibit E2F1, in line with our findings (Rather et al., 2021).

Determining how tumor progression can be inhibited by interfering with nucleotide metabolism has received increasing attention (Abt et al., 2022; Ma et al., 2021; Ogrodzinski et al., 2021). Our results in mPCa cancer are in agreement with those recently published by Lunt´s group in breast cancer, showing that distinct histologic subtypes exhibit different metabolic vulnerabilities in terms of their preferred nucleotide biosynthesis pathways, and that inhibiting the preferred pathway greatly impacts metabolism as well as *in vivo* tumor growth (Ogrodzinski et al., 2021). Crucially, they also show that targeting the non-preferred pathway is not only less effective in controlling tumor growth but may have the opposite effect of increasing tumor growth. Similarly, our results underscore a critical need to elucidate the distinct metabolic preferences of different cancer in order to design effective targeted therapies for each of them.

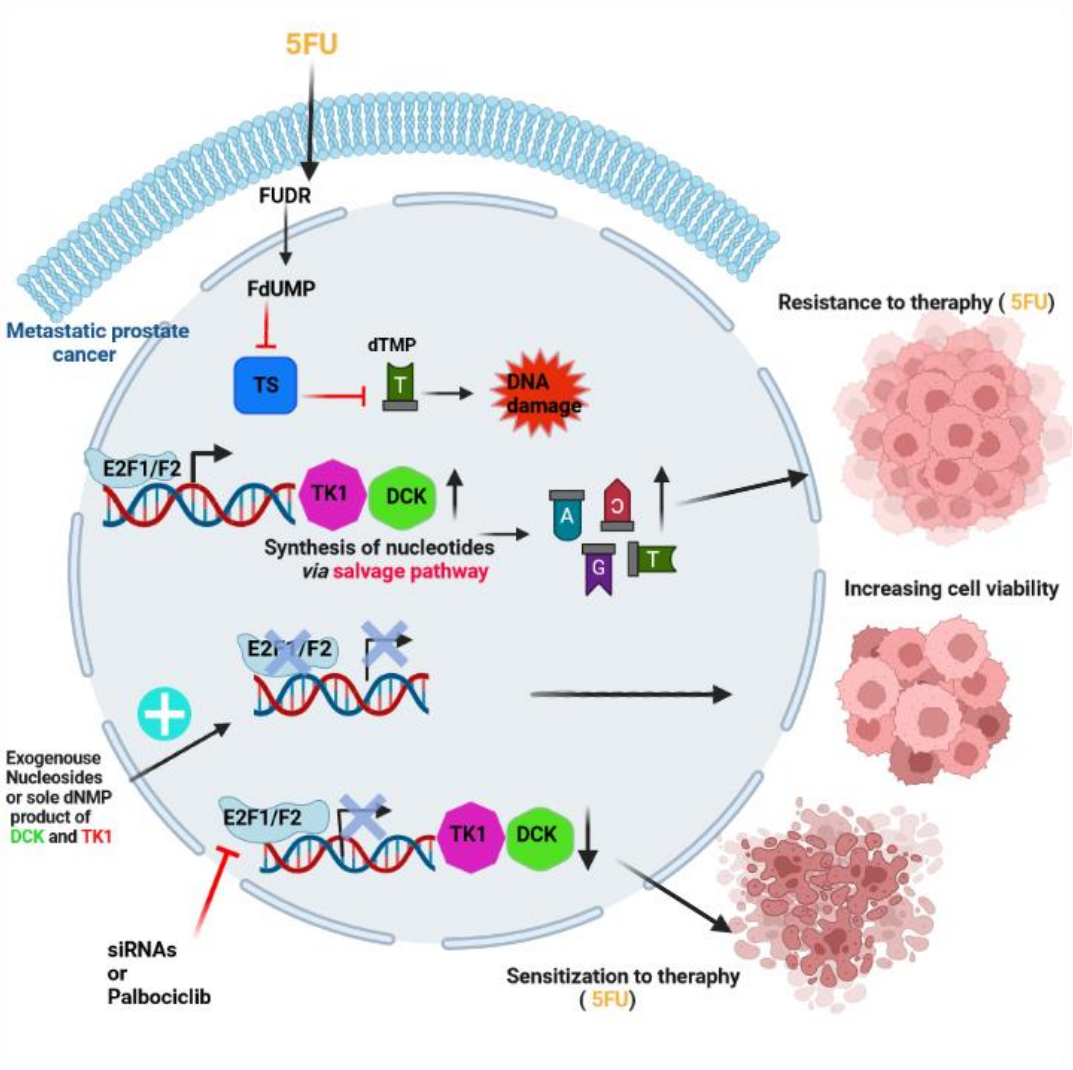


Figure 52. **E2F-dependent mechanisms of resistance and sensitivity to 5-FU in prostate cancer cells.** 5-FU enters into cells by facilitated transport using the same mechanism as that of uracil. After entering into the cells, 5-FU is converted into fluorodeoxyuridine monophosphate (FdUMP). Thymidine synthase (TS) helps in the biosynthesis of thymidylate by catalyzing the methylation of deoxyuridine monophosphate (dUMP) to dTMP. Binding of FdUMP to TS blocks the access of dUMP by inhibiting the synthesis of dTMP. A decrease in the level of dTMP subsequently perturbs the level of other deoxynucleotides resulting in severe disruption of DNA synthesis and repair. PC3 cells with the highest metastatic potential are resistant to 5-FU induced apoptosis, through the activation of E2F target genes *TK1*, *DCK* and *TYMS* coding for enzymes responsible for the synthesis of nucleosides involved in *de novo* and salvage pathway. Their increased expression would overcome the reduction of nucleotide pools imposed by 5FU. Adding nucleosides or the sole products of TK1 and DCK enzymatic activities increased the viability E2F1/2 knockdown cells treated to 5-FU. E2F silencing or E2F pathway inhibitor palbociclib could prevent nucleotide biosynthesis and sensitize tumor cells to cell death after treatment with 5-FU.

Based on our data on metastatic prostate cancer cells, inhibition of E2F1/E2F2 could be a promising strategy to fully prevent nucleotide biosynthesis and sensitize tumor cells to cell death after treatment with 5-FU. E2F proteins, similarly to most transcription factors, are not easily "druggable", and there are no E2F inhibitors in clinical use yet. We considered that an alternative possibility to inhibit E2F activity would be to use cyclin-dependent kinase 4/6 inhibitors (CDK4/6), which have entered the clinical setting for patients with metastatic breast cancer (palbociclib, ribociclib, and abemaciclib). They inhibit E2F activity by preventing pRB phosphorylation and subsequent E2F release (Roberts et al., 2020) and by reprogramming metabolism through a pathway involving MTOR activation (Paakinaho et al., 2019). These inhibitors are currently being tested in multiple tumor types, including prostate cancer cells (Comstock et al., 2013), in most cases in combination with available drugs targeting other cellular pathways (Asghar et al., 2015; Salvador-Barbero et al., 2020).

Interestingly, we detected an additive effect of a combination of palbociclib and 5-FU in the colony forming capacity of PC3 cells, nicely observed with the lowest concentration of palbociclib tested. Indeed, independent treatment with 5-FU or a low dose of palbociclib has a minor effect in colony formation, whereas the combination of both inhibitors potently reduced the viability of PC3 cells. Based on our data and considering that almost 50% of prostate cancers overexpress CDK6 (Lim et al., 2005), it would be appropriate to assess the usefulness of CDK4/6 inhibitors alone or in combination with 5-FU in clinical trials enrolling patients with highly malignant prostate cancer (Figure 52).

In line with our results, a number of preclinical studies suggest that the combination of chemotherapy and CDK4/6 inhibition can have cooperative anti-tumor effects; similar observations are beginning to emerge from clinical studies. Palbociclib, ribociclib, and abemaciclib have been shown to enhance, chemotherapy cytotoxicity when combined with camptothecin, carboplatin, cisplatin, docetaxel, doxorubicin, 5FU, gemcitabine, irinotecan, paclitaxel, and temozolomide (Cao et al., 2019; Franco et al., 2014; Salvador-Barbero et al., 2020). These effects were shown in RB-proficient *in vitro* and *in vivo* models of non-small cell lung carcinoma (NSCLC), ovarian cancer, gastric cancer, TNBC, atypical teratoid rhabdoid tumors, Ewing sarcoma, pancreatic cancer and glioblastoma using both sequential and concurrent dosing schedules (Huang et al., 2012; Iyengar et al., 2018; O'Brien et al., 2018; Raub et al., 2015). One explanation has been the reduced expression of TS. These effects on gene expression could potentially enhance the response to selected chemotherapies by limiting the threshold needed for efficacy of chemotherapy (Dean et al., 2012; Hamilton et al., 2014). Multiple studies have demonstrated that CDK4/6 inhibition can enhance chemotherapy-induced apoptosis (Huang et al., 2012), and that CDK4/6 are upstream regulators of

transcription factors that control global gene expression leading to changes in metabolism, DNA repair and cell plasticity, all of which can render a cancer cell more susceptible to chemotherapy cytotoxicity (Klein et al., 2018).

According to our data, the use of CDK4/6 inhibitors should be considered in prostate cancer treatment. It would be important to select the target patient population based on the mechanism of action that we underscored in order to obtain the benefit from the treatment. Combinatorial therapy with CDK4/6 inhibitors in order to delay resistance or provide synergistic anti-proliferative effects highlights the potential clinical utility of these inhibitors in prostate cancer and underscores the need for near-term clinical studies of these agents in patients with advanced prostate cancer.

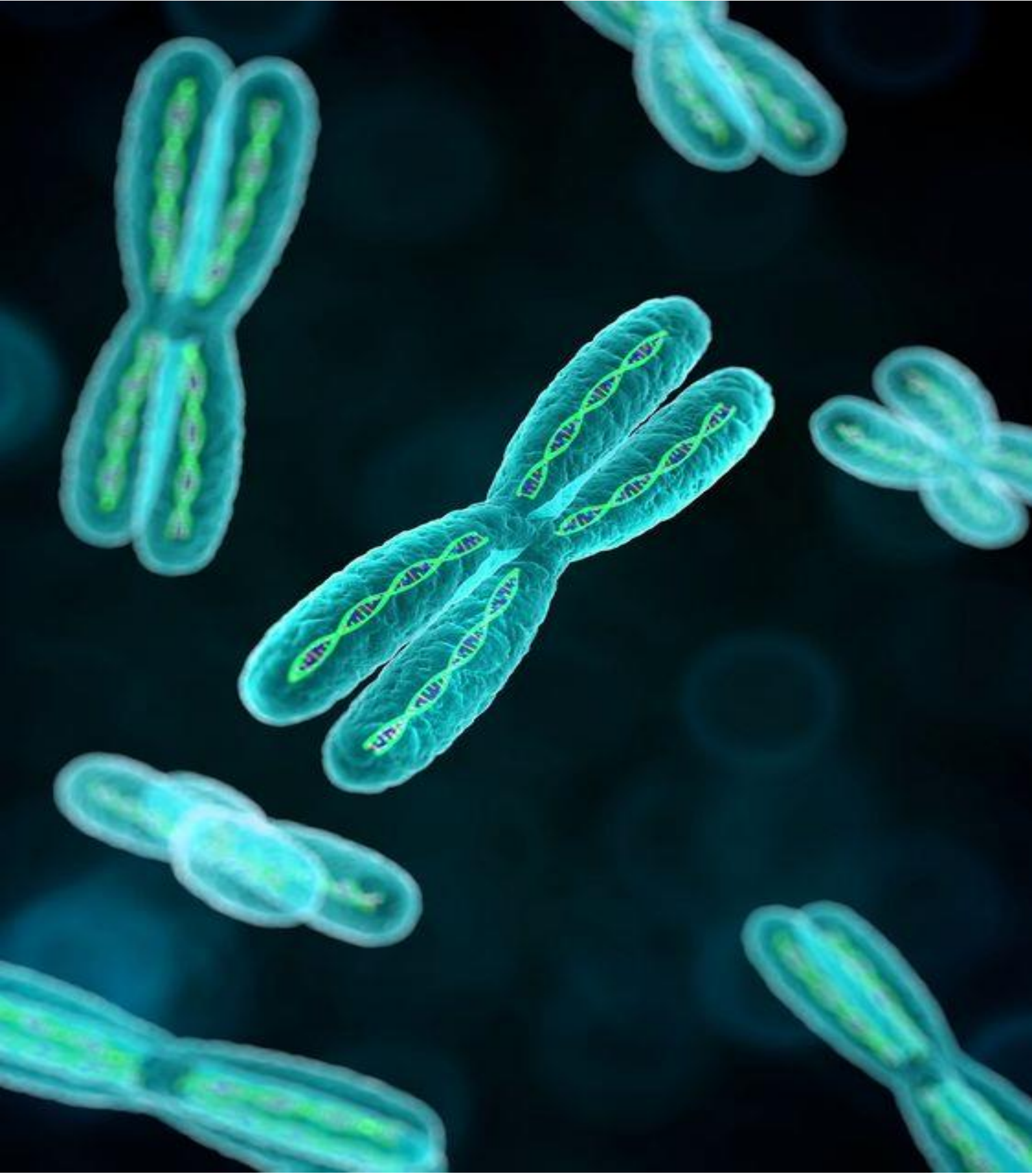

# Conclusions

1 **E2F1 and E2F2 play a critical role in preserving genomic stability through the transcriptional regulation of genes encoding rate-limiting enzymes of the salvage pathway for nucleotide production (*TK1* and *DCK*).** Loss of E2f1/E2f2 in mice reduces *Tk1* and *Dck* gene expression, resulting in nucleotide scarcity that induces DNA damage, whereas exogenously supplied nucleosides ameliorate signs of replication stress and DNA damage response in *E2f1/E2f2* DKO mice.

2 **The mechanism governed by E2F1 and E2F2 to sustain DNA integrity is a potential therapeutic target for cancer treatment.** The expression of E2F1/E2F2 correlates with malignancy in prostate cancer. This expression is necessary to maintain steady-state levels of *TK1*, *DCK* and *TYMS* and to prevent genomic instability during S phase in metastatic prostate cancer cells. Exogenous supply of nucleosides or the sole products of TK1 and DCK enzymatic activities improves replication stress and cellular viability of E2F1/E2F2-depleted prostate cancer cells.

3 **E2F1 and E2F2 control the activity of the kinase CDK1**. Depletion of E2F1/E2F2 reduces dramatically the levels of the inhibitory Tyr-15 phosphorylation of CDK1, suggesting that E2F preserves DNA integrity by controlling both nucleotide production and CDK1 activity.

4 **Prostate cancer cells with the highest metastatic potential are resistant to 5-FU induced apoptosis, through the activation of E2F target genes *TK1*, *DCK* and *TYMS*.** Their increased expression overcomes the reduction of nucleotide pools imposed by 5-FU. Adding nucleosides or the sole products of TK1 and DCK enzymatic activities increases the viability of E2F1/2 knockdown cells treated to 5-FU.

5 **Inhibition of E2F1/E2F2 activity by CDK inhibitor palbociclib sensitizes prostate tumor cells to cell death after treatment with 5-FU.** Thus, the combination of palbociclib and 5-FU could be a promising strategy for prostate cancer treatment.

# References

Abt, E. R., Le, T. M., Dann, A. M., Capri, J. R., Poddar, S., Lok, V., Li, L., Liang, K., Creech, A. L., Rashid, K., Kim, W., Wu, N., Cui, J., Cho, A., Lee, H. R., Rosser, E. W., Link, J. M., Czernin, J., Wu, T.-T., & Radu, C. G. (2022). Reprogramming of nucleotide metabolism by interferon confers dependence on the replication stress response pathway in pancreatic cancer cells. *Cell Reports*, *38*(2). https://doi.org/10.1016/j.celrep.2021.110236

Adams, M. R., Sears, R., Nuckolls, F., Leone, G., & Nevins, J. R. (2000). Complex Transcriptional Regulatory Mechanisms Control Expression of the E2F3 Locus. *Molecular and Cellular Biology*, *20*(10). https://doi.org/10.1128/mcb.20.10.3633-3639.2000

Aguilera, A., & García-Muse, T. (2013). Causes of Genome Instability. *Annual Review of Genetics*, *47*(1). https://doi.org/10.1146/annurev-genet-111212-133232

Anglana, M., Apiou, F., Bensimon, A., and Debastisse, M. (2003). Dynamics of DNA replication in mammalian somatic cells: nucleotide pool modulates origin choice and interorigin spacing. *Cell, 114*(3). https://doi.org/10.1016/s0092-8674(03)00569-5.

Antoni, L., Sodha, N., Collins, I., & Garrett, M. D. (2007). CHK2 kinase: cancer susceptibility and cancer therapy - two sides of the same coin?. *Nature Reviews Cancer*, *7*(12). https://doi.org/10.1038/nrc2251

Arnér, E. S. J., & Eriksson, S. (1995). Mammalian deoxyribonucleoside kinases. *Pharmacology and Therapeutics*, *67*(2). https://doi.org/10.1016/0163-7258(95)00015-9

Asghar, U., Witkiewicz, A. K., Turner, N. C., & Knudsen, E. S. (2015). The history and future of targeting cyclin-dependent kinases in cancer therapy. *Nature Reviews Drug Discovery*, *14*(2). https://doi.org/10.1038/nrd4504

Attwooll, C., Lazzerini Denchi, E., & Helin, K. (2004). The E2F family: specific functions and overlapping interests. *The EMBO Journal*, *23*(24). https://doi.org/10.1038/sj.emboj.7600481

Austin, W. R., Armijo, A. L., Campbell, D. O., Singh, A. S., Hsieh, T., Nathanson, D., Herschman, H. R., Phelps, M. E., Witte, O. N., Czernin, J., & Radu, C. G. (2012). Nucleoside salvage pathway kinases regulate hematopoiesis by linking nucleotide metabolism with replication stress. *Journal of Experimental Medicine*, *209*(12). https://doi.org/10.1084/jem.20121061

Aye, Y., Li, M., Long, M. J. C., & Weiss, R. S. (2015). Ribonucleotide reductase and cancer: biological mechanisms and targeted therapies. *Oncogene*, *34*(16). https://doi.org/10.1038/onc.2014.155

Beck, H., Nähse, V., Larsen, M. S., Groth, P., Clancy, T., Lees, M., Jørgensen, M., Helleday, T., Syljuåsen, R. G., & Sørensen, C. S. Regulators of cyclin-dependent kinases are crucial for maintaining genome integrity in S phase. (2010).*The Journal of Cell Biology, 188*(5). https://doi.org/ 10.1083/jcb.200905059

Beck, H., Nähse, V., Larsen, M. S., O'Hanlon, K. A., Patzke, S., Holmberg, C., Mejlvang, J., Groth, A., Nielsen, O., Syljuåsen, R. G., Sørensen, C. S,. Cyclin-dependent kinase suppression by WEE1 kinase protects the genome through control of replication initiation and nucleotide consumption. (2012). *Molecular and Cell Biology, 32*(20). https://doi.org/ 10.1128/MCB.00412-12.

Bertoli, C., Skotheim, J. M., & de Bruin, R. A. M. (2013). Control of cell cycle transcription during G1 and S phases. *Nature Reviews Molecular Cell Biology*, *14*(8). https://doi.org/10.1038/nrm3629

Bester, A. C., Roniger, M., Oren, Y. S., Im, M. M., Sarni, D., Chaoat, M., Bensimon, A., Zamir, G., Shewach, D. S., & Kerem, B. (2011). Nucleotide deficiency promotes genomic instability in early stages of cancer development. *Cell*, *145*(3). https://doi.org/10.1016/j.cell.2011.03.044

Bjorklund, D. F., & Harnishfeger, K. K. (1990). The resources construct in cognitive development: Diverse sources of evidence and a theory of inefficient inhibition. *Developmental Review*, *10*(1). https://doi.org/10.1016/0273-2297(90)90004-N

Blakley, R. L., & Vitols, E. (1968). The Control of Nucleotide Biosynthesis. *Annual Review of Biochemistry*, *37*(1). https://doi.org/10.1146/annurev.bi.37.070168.001221

Blesa, J. M. G., Marco, V. G., Giner-Bosch, V., Cerezuela Fuentes, P., & Candel, V. A. (2011a). Phase II Trial of Oxaliplatin and Capecitabine After Progression to First-Line Chemotherapy in Androgen-Independent Prostate Cancer Patients. *American Journal of Clinical Oncology*, *34*(2). https://doi.org/10.1097/COC.0b013e3181d6b453

Bonate, P. L., Arthaud, L., Cantrell, W. R., Stephenson, K., Secrist, J. A., & Weitman, S. (2006). Discovery and development of clofarabine: a nucleoside analogue for treating cancer. *Nature Reviews Drug Discovery*, *5*(10). https://doi.org/10.1038/nrd2055

Bubendorf, L., Schöpfer, A., Wagner, U., Sauter, G., Moch, H., Willi, N., Gasser, T. C., & Mihatsch, M. J. (2000). Metastatic patterns of prostate cancer: An autopsy study of 1,589 patients. *Human Pathology*, *31*(5). https://doi.org/10.1053/hp.2000.6698

Buj, R., & Aird, Katherine. M. (2018). Deoxyribonucleotide triphosphate metabolism in cancer and metabolic disease. *Frontiers in Endocrinology, 9*. https://doi.org/10.3389/fendo.2018.00177

Bunz, F., Hwang, P. M., Torrance, C., Waldman, T., Zhang, Y., Dillehay, L., Williams, J., Lengauer, C., Kinzler, K. W., & Vogelstein, B. (1999). Disruption of p53 in human cancer cells alters the responses to therapeutic agents. *The Journal of Clinical Investigation*, *104*(3). https://doi.org/10.1172/JCI6863

Burrell, R. A., McClelland, S. E., Endesfelder, D., Groth, P., Weller, M.-C., Shaikh, N., Domingo, E., Kanu, N., Dewhurst, S. M., Gronroos, E., Chew, S. K., Rowan, A. J., Schenk, A., Sheffer, M., Howell, M., Kschischo, M., Behrens, A., Helleday, T., Bartek, J., … Swanton, C. (2013).

Replication stress links structural and numerical cancer chromosomal instability. *Nature*, *494*(7438). https://doi.org/10.1038/nature11935

Caillot, M., Bourgeais, J., Dakik, H., Costé, É., Mazure, N. M., Lelièvre, É., Coqueret, O., Hérault, O., Mazurier, F., & Sola, B. (2020). Cyclin D1 targets hexokinase 2 to control aerobic glycolysis in myeloma cells. *Oncogenesis*, *9*(7). https://doi.org/10.1038/s41389-020-00253-3

Cao, J., Zhu, Z., Wang, H., Nichols, T. C., Lui, G. Y. L., Deng, S., Rejto, P. A., VanArsdale, T., Hardwick, J. S., Weinrich, S. L., & Wei, P. (2019). Combining CDK4/6 inhibition with taxanes enhances anti-tumor efficacy by sustained impairment of pRB-E2F pathways in squamous cell lung cancer. *Oncogene*, *38*(21). https://doi.org/10.1038/s41388-019-0708-7

Carr, S. M., Poppy Roworth, A., Chan, C., & la Thangue, N. B. (2015). Post-translational control of transcription factors: Methylation ranks highly. *FEBS Journal, 282*(23). https://doi.org/10.1111/febs.13524

Cerami, E., Gao, J., Dogrusoz, U., Gross, B. E., Sumer, S. O., Aksoy, B. A., Jacobsen, A., Byrne, C. J., Heuer, M. L., Larsson, E., Antipin, Y., Reva, B., Goldberg, A. P., Sander, C., & Schultz, N. (2012a). The cBio Cancer Genomics Portal: An Open Platform for Exploring Multidimensional Cancer Genomics Data. *Cancer Discovery*, *2*(5). https://doi.org/10.1158/2159-8290.CD-12-0095

Chabes, A. L., Björklund, S., & Thelander, L. (2004). S Phase-specific Transcription of the Mouse Ribonucleotide Reductase R2 Gene Requires Both a Proximal Repressive E2F-binding Site and an Upstream Promoter Activating Region. *Journal of Biological Chemistry*, *279*(11). https://doi.org/10.1074/jbc.M312482200

Chaudhuri, L., Vincelette, N. D., Koh, B. D., Naylor, R. M., Flatten, K. S., Peterson, K. L., McNally, A., Gojo, I., Karp, J. E., Mesa, R. A., Sproat, L. O., Bogenberger, J. M., Kaufmann, S. H., & Tibes, R. (2014). CHK1 and WEE1 inhibition combine synergistically to enhance therapeutic efficacy in acute myeloid leukemia ex vivo. *Haematologica*, *99*(4). https://doi.org/10.3324/haematol.2013.093187

Chen, H. Z., Tsai, S.Y., & Leone, G. (2009). Emerging roles of E2Fs in cancer: an exit from cell cycle control. *Nature Reviews. Cancer*, *9*(11). https://doi.org/10.1038/nrc2696

Copur, S., Aiba, K., Drake, J. C., Allegra, C. J., & Chu, E. (1995). Thymidylate synthase gene amplification in human colon cancer cell lines resistant to 5-fluorouracil. *Biochemical Pharmacology*, *49*(10). https://doi.org/10.1016/0006-2952(95)00067-A

Comstock C. E., Augello, M. A., Goodwin, J. F., de Leeuw, R., Schiewer, M. J., Ostrander WF, J. r., Burkhart, R. A., McClendon, A. K., McCue, P.A., Trabulsi, E. J., Lallas, C. D., Gomella, L. G., Centenera, M. M., Brody, J. R., Butler, L. M., Tilley, W. D. & Knudsen, K. E. (2013). *Oncogene, 32*(48). https://doi.org/10.1038/onc.2013.83

Cortazar, A. R., Torrano, V., Martín-Martín, N., Caro-Maldonado, A., Camacho, L., Hermanova, I., Guruceaga, E., Lorenzo-Martín, L. F., Caloto, R., Gomis, R. R., Apaolaza, I., Quesada, V., Trka, J., Gomez-Muñoz, A., Vincent, S., Bustelo, X. R., Planes, F. J., Aransay, A. M., & Carracedo, A. (2018). CANCERTOOL: A Visualization and Representation Interface to Exploit Cancer Datasets. *Cancer Research*, *78*(21). https://doi.org/10.1158/0008-5472.CAN-18-1669

Courbet, S., Gay, S., Arnoult, N., Wronka, G., Anglana, M., Brison, O., & Debatisse, M. (2008). Replication fork movement sets chromatin loop size and origin choice in mammalian cells. *Nature*, *455(7212)*. https://doi.org/10.1038/nature07233

Cretella, D., Fumarola, C., Bonelli, M., Alfieri, R., la Monica, S., Digiacomo, G., Cavazzoni, A., Galetti, M., Generali, D., & Petronini, P. G. (2019). Pre-treatment with the CDK4/6 inhibitor palbociclib improves the efficacy of paclitaxel in TNBC cells. *Scientific Reports*, *9*(1). https://doi.org/10.1038/s41598-019-49484-4

Crosio, C., Fimia, G. M., Loury, R., Kimura, M., Okano, Y., Zhou, H., Sen, S., Allis, C. D., & Sassone-Corsi, P. (2002). Mitotic Phosphorylation of Histone H3: Spatio-Temporal Regulation by Mammalian Aurora Kinases. *Molecular and Cellular Biology*, *22*(3). https://doi.org/10.1128/MCB.22.3.874-885.2002

Danenberg, P. (1997). Thymidylate synthetase - a target enzyme in cancer chemotherapy. *Biochimica et Biophysica Acta (BBA) - Reviews on Cancer, 473*(2) https://doi.org/10.1016/0304-419X(77)90001-4.

Davis, J. N., Wojno, K. J., Daignault, S., Hofer, M. D., Kuefer, R., Rubin, M. A., & Day, M. L. (2006). Elevated E2F1 Inhibits Transcription of the Androgen Receptor in Metastatic Hormone-Resistant Prostate Cancer. *Cancer Research*, *66*(24). https://doi.org/10.1158/0008-5472.CAN-06-2497

de Angelis, P. M., Svendsrud, D. H., Kravik, K. L., & Stokke, T. (2006). Cellular response to 5-fluorouracil (5-FU) in 5-FU-resistant colon cancer cell lines during treatment and recovery. *Molecular Cancer*, *5*(1). https://doi.org/10.1186/1476-4598-5-20

Dean, J. L., McClendon, A. K., & Knudsen, E. S. (2012). Modification of the DNA Damage Response by Therapeutic CDK4/6 Inhibition. *Journal of Biological Chemistry*, *287*(34). https://doi.org/10.1074/jbc.M112.365494

DeGregori, J., Kowalik, T., & Nevins, J. R. (1995). Cellular targets for activation by the E2F1 transcription factor include DNA synthesis- and G1/S-regulatory genes. *Molecular and Cellular Biology*, *15*(8). https://doi.org/10.1128/MCB.15.8.4215

Denis, L., & Murphy, G. P. (1993). Overview of phase III trials on combined androgen treatment in patients with metastatic prostate cancer. *Cancer*, *72*(12). https://doi.org/10.1002/1097-0142(19931215)72:12+<3888::aid-cncr2820721726>3.0.co;2-b

Dimova, D. K., & Dyson, N. J. (2005). The E2F transcriptional network: old acquaintances with new faces. *Oncogene*, *24*(17). https://doi.org/10.1038/sj.onc.1208612

Dobbelstein, M., & Sørensen, C. S. (2015). Exploiting replicative stress to treat cancer. *Nature Reviews Drug Discovery*, *14*(6). https://doi.org/10.1038/nrd4553

Donati, G., Peddigari, S., Mercer, C. A., & Thomas, G. (2013). 5S Ribosomal RNA Is an Essential Component of a Nascent Ribosomal Precursor Complex that Regulates the Hdm2-p53 Checkpoint. *Cell Reports*, *4*(1). https://doi.org/10.1016/j.celrep.2013.05.045

Dyson, N. (1998). The regulation of E2F by pRB-family proteins. *Genes & Development*, *12*(15). https://doi.org/10.1101/gad.12.15.2245

Eaton, J. S., Lin, Z. P., Sartorelli, A. C., Bonawitz, N. D., & Shadel, G. S. (2007). Ataxia-telangiectasia mutated kinase regulates ribonucleotide reductase and mitochondrial homeostasis. *Journal of Clinical Investigation*, *117*(9). https://doi.org/10.1172/JCI31604

Eisenberger, M. A., Blumenstein, B. A., Crawford, E. D., Miller, G., McLeod, D. G., Loehrer, P. J., Wilding, G., Sears, K., Culkin, D. J., Thompson, I. M., Bueschen, A. J., & Lowe, B. A. (1998). Bilateral Orchiectomy with or without Flutamide for Metastatic Prostate Cancer. *New England Journal of Medicine*, *339*(15). https://doi.org/10.1056/NEJM199810083391504

Elbæk, C. R., Petrosius, V., & Sørensen, C. S. (2020). WEE1 kinase limits CDK activities to safeguard DNA replication and mitotic entry. *Mutation Research/Fundamental and Molecular Mechanisms of Mutagenesis*, *819*. https://doi.org/10.1016/j.mrfmmm.2020.111694

Etienne, M. C., Chéradame, S., Fischel, J. L., Formento, P., Dassonville, O., Renée, N., Schneider, M., Thyss, A., Demard, F., & Milano, G. (1995). Response to fluorouracil therapy in cancer patients: the role of tumoral dihydropyrimidine dehydrogenase activity. *Journal of Clinical Oncology*, *13*(7). https://doi.org/10.1200/JCO.1995.13.7.1663

Ewald, B., Sampath, D., & Plunkett, W. (2007). H2AX phosphorylation marks gemcitabine-induced stalled replication forks and their collapse upon S-phase checkpoint abrogation. *Molecular Cancer Therapeutics*, *6*(4). https://doi.org/10.1158/1535-7163.MCT-06-0633

Fairman, J. W., Wijerathna, S. R., Ahmad, M. F., Xu, H., Nakano, R., Jha, S., Prendergast, J., Welin, R. M., Flodin, S., Roos, A., Nordlund, P., Li, Z., Walz, T., & Dealwis, C. G. (2011). Structural basis for allosteric regulation of human ribonucleotide reductase by nucleotide-induced oligomerization. *Nature Structural & Molecular Biology*, *18*(3). https://doi.org/10.1038/nsmb.2007

Fang, F., Hoskins, J., & Butler, J. S. (2004). 5-Fluorouracil Enhances Exosome-Dependent Accumulation of Polyadenylated rRNAs. *Molecular and Cellular Biology*, *24*(24). https://doi.org/10.1128/MCB.24.24.10766-10776.2004

Fasullo, M., & Endres, L. (2015). Nucleotide Salvage Deficiencies, DNA Damage and Neurodegeneration. *International Journal of Molecular Sciences*, *16*(12). https://doi.org/10.3390/ijms16059431

Field, S. J., Tsai, F. Y., Kuo, F., Zubiaga, A. M., Kaelin, W. G., Livingston, D. M., Orkin, S. H., & Greenberg, M. E. (1996a). E2F-1 Functions in Mice to Promote Apoptosis and Suppress Proliferation. *Cell*, *85*(4). https://doi.org/10.1016/S0092-8674 (00)81255-6

Fisher, R. P. (2012). The CDK Network: Linking Cycles of Cell Division and Gene Expression. *Genes & Cancer*, *3*(11–12). https://doi.org/10.1177/1947601912473308

Franco, J., Witkiewicz, A. K., & Knudsen, E. S. (2014). CDK4/6 inhibitors have potent activity in combination with pathway selective therapeutic agents in models of pancreatic cancer. *Oncotarget*, *5*(15). https://doi.org/10.18632/oncotarget.2270

Fustin, J. M., Doi, M., Yamada, H., Komatsu, R., Shimba, S., & Okamura, H. (2012). Rhythmic Nucleotide Synthesis in the Liver: Temporal Segregation of Metabolites. *Cell Reports*, *1*(4). https://doi.org/10.1016/j.celrep.2012.03.001

Fu, Y., Long, M. J. C., Rigney, M., Parvez, S., Blessing, W. A., & Aye, Y. (2013). Uncoupling of Allosteric and Oligomeric Regulation in a Functional Hybrid Enzyme Constructed from Escherichia coli and Human Ribonucleotide Reductase. *Biochemistry*, *52*(40). https://doi.org/10.1021/bi400781z

Gaillard, H., García-Muse, T., & Aguilera, A. (2015). Replication stress and cancer. *Nature Reviews Cancer*, *15*(5). https://doi.org/10.1038/nrc3916

Galarreta, A., Valledor, P., Ubieto-Capella, P., Lafarga, V., Zarzuela, E., Muñoz, J., Malumbres, M., Lecona, E., & Fernandez-Capetillo, O. (2021). USP7 limits CDK1 activity throughout the cell cycle. *The EMBO Journal*, *40*(11). https://doi.org/10.15252/embj.201899692

Gao, J., Aksoy, B. A., Dogrusoz, U., Dresdner, G., Gross, B., Sumer, S. O., Sun, Y., Jacobsen, A., Sinha, R., Larsson, E., Cerami, E., Sander, C., & Schultz, N. (2013). Integrative Analysis of Complex Cancer Genomics and Clinical Profiles Using the cBioPortal. *Science Signaling*, *6*(269). https://doi.org/10.1126/scisignal.2004088

García, I., Murga, M., Vicario, A., Field, S. J., & Zubiaga, A. M. (2000). A role for E2F1 in the induction of apoptosis during thymic negative selection. *Cell Growth & Differentiation 11(2):91-8. PMID: 10714765*

Garone, C., Garcia-Diaz, B., Emmanuele, V., Lopez, L. C., Tadesse, S., Akman, H. O., Tanji, K., Quinzii, C. M., & Hirano, M. (2014). Deoxypyrimidine monophosphate bypass therapy for thymidine kinase 2 deficiency. *EMBO Molecular Medicine*, *6*(8). https://doi.org/10.15252/emmm.201404092

Ge, X. Q., Jackson, D. A., & Blow, J. J. (2007). Dormant origins licensed by excess Mcm2-7 are required for human cells to survive replicative stress. *Genes & development, 21*(24). https://doi.org/10.1101/gad.457807

Gong, C., Liu, H., Song, R., Zhong, T., Lou, M., Wang, T., Qi, H., Shen, J., Zhu, L., & Shao, J. (2016). ATR–CHK1–E2F3 signaling transactivates human ribonucleotide reductase small subunit M2 for DNA repair induced by the chemical carcinogen MNNG. *Biochimica et Biophysica Acta (BBA) - Gene Regulatory Mechanisms*, *1859*(4). https://doi.org/10.1016/j.bbagrm.2016.02.012

Hagenkort, A., Paulin, C. B. J., Desroses, M., Sarno, A., Wiita, E., Mortusewicz, O., Koolmeister, T., Loseva, O., Jemth, A.-S., Almlöf, I., Homan, E., Lundbäck, T., Gustavsson, A.-L., Scobie, M., & Helleday, T. (2017). dUTPase inhibition augments replication defects of 5-Fluorouracil. *Oncotarget*, *8*(14). https://doi.org/10.18632/oncotarget.15785

Hamilton, G., Klameth, L., Rath, B., & Thalhammer, T. (2014). Synergism of Cyclin-Dependent Kinase Inhibitors with Camptothecin Derivatives in Small Cell Lung Cancer Cell Lines. *Molecules*, *19*(2). https://doi.org/10.3390/molecules19022077

Helin, K., Lees, J. A., Vidal, M., Dyson, N., Harlow, E., & Fattaey, A. (1992). A cDNA encoding a pRB-binding protein with properties of the transcription factor E2F. *Cell*, *70*(2). https://doi.org/10.1016/0092-8674(92)90107-n

Heller, R. S., Stoffers, D. A., Bock, T., Svenstrup, K., Jensen, J., Horn, T., Miller, C. P., Habener, J. F., Madsen, O. D., & Serup, P. (2001). *Improved Glucose Tolerance and Acinar Dysmorphogenesis by Targeted Expression of Transcription Factor PDX-1 to the Exocrine Pancreas*. https://doi.org/10.2337/diabetes.50.7.1553.

Hellerstedt, B., Pienta, K. J., Redman, B. G., Esper, P., Dunn, R., Fardig, J., Olson, K., & Smith, D. C. (2003). Phase II trial of oral cyclophosphamide, prednisone, and diethylstilbestrol for androgen-independent prostate carcinoma. *Cancer*, *98*(8). https://doi.org/10.1002/cncr.11686

Helmrich, A., Ballarino, M., Nudler, E., & Tora, L. (2013). Transcription-replication encounters, consequences and genomic instability. *Nature Structural & Molecular Biology*, *20*(4). https://doi.org/10.1038/nsmb.2543

Herlihy, A., & de Bruin, R. (2017). The Role of the Transcriptional Response to DNA Replication Stress. *Genes*, *8*(3). https://doi.org/10.3390/genes8030092

Hill, R., Song, Y., Cardiff, R. D., & van Dyke, T. (2005). Heterogeneous tumor evolution initiated by loss of pRb function in a preclinical prostate cancer model. *Cancer Research*, *65*(22), 10243–10254. https://doi.org/10.1158/0008-5472.CAN-05-1579

Hirschey, M. D., DeBerardinis, R. J., Diehl, A. M. E., Drew, J. E., Frezza, C., Green, M. F., Jones, L. W., Ko, Y. H., Le, A., Lea, M. A., Locasale, J. W., Longo, V. D., Lyssiotis, C. A., McDonnell, E., Mehrmohamadi, M., Michelotti, G., Muralidhar, V., Murphy, M. P., Pedersen, P. L., &

Wellen, K. E. (2015). Dysregulated metabolism contributes to oncogenesis. *Seminars in Cancer Biology*, *35*. Suppl:S129-S150. https://doi.org/10.1016/j.semcancer.2015.10.002

Huang, P., & Plunkett, W. (1991). Action of 9-beta-D-arabinofuranosyl-2-fluoroadenine on RNA metabolism. *Molecular Pharmacology*, *39(4):449-55* PMID: 1708088

Huang, X., & Darzynkiewicz, Z. (2006). Cytometric Assessment of Histone H2AX Phosphorylation. In DNA Repair Protocols. *Methods in Molecular Biology, 314*(73). https://doi.org/10.1385/1-59259-973-7:073

Huang, X., di Liberto, M., Jayabalan, D., Liang, J., Ely, S., Bretz, J., Shaffer, A. L., Louie, T., Chen, I., Randolph, S., Hahn, W. C., Staudt, L. M., Niesvizky, R., Moore, M. A. S., & Chen-Kiang, S. (2012). Prolonged early G1 arrest by selective CDK4/CDK6 inhibition sensitizes myeloma cells to cytotoxic killing through cell cycle–coupled loss of IRF4. *Blood*, *120*(5). https://doi.org/10.1182/blood-2012-03-415984

Iglesias, A., Murga, M., Laresgoiti, U., Skoudy, A., Bernales, I., Fullaondo, A., Moreno, B., Lloreta, J., Field, S. J., Real, F. X., & Zubiaga, A. M. (2004). Diabetes and exocrine pancreatic insufficiency in E2F1/E2F2 double-mutant mice. *Journal of Clinical Investigation*, *113*(10), 1398–1407. https://doi.org/10.1172/JCI200418879

Iglesias-Ara, A., Zenarruzabeitia, O., Buelta, L., Merino, J., & Zubiaga, A. M. (2015). E2F1 and E2F2 prevent replicative stress and subsequent p53-dependent organ involution. *Cell Death and Differentiation*, *22*(10). https://doi.org/10.1038/cdd.2015.4

Iglesias-Ara,A., Zenarruzabeitia,O., Fernandez-Rueda,J., Sanchez-Tillo,E., Field,S.J., Celada,A., & Zubiaga,A. M. (2010). Accelerated DNA replication in E2F1- and E2F2-deficient macrophages leads to induction of the DNA damage response and p21CIP1-dependent senescence. *Oncogens, 29*(41). https://doi.org/10.1038/onc.2010.296

Infante, A., Laresgoiti, U., Fernández-Rueda, J., Fullaondo, A., Galán, J., Díaz-Uriarte, R., Malumbres, M., Field, S. J., & M. Zubiaga, A. (2008). E2F2 represses cell cycle regulators to maintain quiescence. *Cell Cycle*, *7*(24). https://doi.org/10.4161/cc.7.24.7379

Intuyod, K., Saavedra-García, P., Zona, S., Lai, C.F., Jiramongkol, Y., Vaeteewoottacharn, K., Pairojkul, C., Yao, S., Yong, J.-S., Trakansuebkul, S., Waraasawapati, S., Luvira, V., Wongkham, S., Pinlaor, S., & Lam, E. W.F. (2018). FOXM1 modulates 5-fluorouracil sensitivity in cholangiocarcinoma through thymidylate synthase (TYMS): implications of FOXM1–TYMS axis uncoupling in 5-FU resistance. *Cell Death & Disease*, *9*(12). https://doi.org/10.1038/s41419-018-1235-0

Ishida, S., Huang, E., Zuzan, H., Spang, R., Leone, G., West, M., & Nevins, J. R. (2001). Role for E2F in Control of Both DNA Replication and Mitotic Functions as Revealed from DNA Microarray Analysis. *Molecular and Cellular Biology*, *21*(14). https://doi.org/10.1128/mcb.21.14.4684-4699.2001

Iyengar, M., O'Hayer, P., Cole, A., Sebastian, T., Yang, K., Coffman, L., & Buckanovich, R. J. (2018). CDK4/6 inhibition as maintenance and combination therapy for high grade serous ovarian cancer. *Oncotarget*, *9*(21). https://doi.org/10.18632/oncotarget.24585

Jakob, C., Liersch, T., Meyer, W., Baretton, G. B., Häusler, P., Schwabe, W., Becker, H., & Aust, D. E. (2005). Immunohistochemical analysis of thymidylate synthase, thymidine phosphorylase, and dihydropyrimidine dehydrogenase in rectal cancer (cUICC II/III): correlation with histopathologic tumor regression after 5-fluorouracil-based long-term neoadjuvant chemoradiotherapy. *The American Journal of Surgical Pathology*, *29*(10). https://doi.org/10.1097/01.pas.0000170346.55304.88

Jarrard, D. F., Modder, J., Fadden, P., Fu, V., Sebree, L., Heisey, D., Schwarze, S. R., & Friedl, A. (2002). Alterations in the p16/pRb cell cycle checkpoint occur commonly in primary and metastatic human prostate cancer. *Cancer Letters*, *185*(2). https://doi.org/10.1016/S0304-3835(02)00282-3

Johansson, M., & Norda, A. (2000). Conserved gene structure and transcription factor sites in the human and mouse deoxycytidine kinase genes1. *FEBS Lett, 487*(2). https://doi.org/ 10.1016/s0014-5793(00)02347-4

Johnson, D. G., Schwarz, J. K., Cress, W. D., & Nevins, J. R. (1993). Expression of transcription factor E2F1 induces quiescent cells to enter S phase. *Nature*, *365*(6444). https://doi.org/10.1038/365349a0

Johnston, P. G., Lenz, H. J., Leichman, C. G., Danenberg, K. D., Allegra, C. J., Danenberg, P. v, & Leichman, L. (1995). Thymidylate synthase gene and protein expression correlate and are associated with response to 5-fluorouracil in human colorectal and gastric tumors. *Cancer Research*, *55(7):1407-12. PMID: 7882343*

Kent, L. N., Bae, S., Tsai, S.-Y., Tang, X., Srivastava, A., Koivisto, C., Martin, C. K., Ridolfi, E., Miller, G. C., Zorko, S. M., Plevris, E., Hadjiyannis, Y., Perez, M., Nolan, E., Kladney, R., Westendorp, B., de Bruin, A., Fernandez, S., Rosol, T. J., & Leone, G. (2017). Dosage-dependent copy number gains in E2f1 and E2f3 drive hepatocellular carcinoma. *Journal of Clinical Investigation*, *127*(3). https://doi.org/10.1172/JCI87583

Kent, L. N., & Leone, G. (2019). The broken cycle: E2F dysfunction in cancer. *Nature Reviews Cancer, 19*(6). *Nature Reviews Cancer 19*(6). https://doi.org/10.1038/s41568-019-0143-7

Kent, L. N., Rakijas, J. B., Pandit, S. K., Westendorp, B., Chen, H.-Z., Huntington, J. T., Tang, X., Bae, S., Srivastava, A., Senapati, S., Koivisto, C., Martin, C. K., Cuitino, M. C., Perez, M., Clouse, J. M., Chokshi, V., Shinde, N., Kladney, R., Sun, D., … Leone, G. (2016). E2f8 mediates tumor suppression in postnatal liver development. *Journal of Clinical Investigation*, *126*(8). https://doi.org/10.1172/JCI85506

Klein, M. E., Kovatcheva, M., Davis, L. E., Tap, W. D., & Koff, A. (2018). CDK4/6 Inhibitors: The Mechanism of Action May Not Be as Simple as Once Thought. *Cancer Cell*, *34*(1). https://doi.org/10.1016/j.ccell.2018.03.023

Koç, A., Wheeler, L. J., Mathews, C. K., & Merrill, G. F. (2004). Hydroxyurea Arrests DNA Replication by a Mechanism that Preserves Basal dNTP Pools. *Journal of Biological Chemistry*, *279*(1). https://doi.org/10.1074/jbc.M303952200

Kolch, W., Kotwaliwale, A., Vass, K., & Janosch, P. (2002). The role of Raf kinases in malignant transformation. *Expert Reviews in Molecular Medicine*, *4*(8). https://doi.org/10.1017/S1462399402004386

Kovacs, L. A. S., Orlando, D. A., & Haase, S. B. (2008). Transcription network and cyclin/CDKs: The yin and yang of cell cycle oscillators. *Cell Cycle*, *7*(17). https://doi.org/10.4161/cc.7.17.6515

Kovesdi, I., Reichel, R., & Nevins, J. R. (1986). Identification of a cellular transcription factor involved in E1A trans-activation. *Cell*, *45*(2). https://doi.org/10.1016/0092-8674(86)90386-7

Krek, W., Livingston, D. M., & Shirodkar, S. (1993). Binding to DNA and the Retinoblastoma Gene Product Promoted by Complex Formation of Different E2F Family Members. *Science*, *262*(5139). https://doi.org/10.1126/science.8248803

Kunz, B. A., Kohalmi, S. E., Kunkel, T. A., Mathews, C. K., McIntosh, E. M., & Reidy, J. A. (1994). Deoxyribonucleoside triphosphate levels: A critical factor in the maintenance of genetic stability. *Mutation Research/Reviews in Genetic Toxicology*, *318*(1). https://doi.org/10.1016/0165-1110(94)90006-X

Kwon, J. S., Everetts, N. J., Wang, X., Wang, W., della Croce, K., Xing, J., & Yao, G. (2017). Controlling Depth of Cellular Quiescence by an Rb-E2F Network Switch. *Cell Reports*, *20*(13), 3223–3235. https://doi.org/10.1016/j.celrep.2017.09.007

Lambert, S., & Carr, A. M. (2013). Impediments to replication fork movement: stabilisation, reactivation and genome instability. *Chromosoma*, *122*(1–2). https://doi.org/10.1007/s00412-013-0398-9

Lane, A. N., & Fan, T. W. M. (2015). Regulation of mammalian nucleotide metabolism and biosynthesis. *Nucleic Acids Research*, *43*(4). https://doi.org/10.1093/nar/gkv047

Lan, W., Bian, B., Xia, Y., Dou, S., Gayet, O., Bigonnet, M., Santofimia-Castaño, P., Cong, M., Peng, L., Dusetti, N., & Iovanna, J. (2018). E2F signature is predictive for the pancreatic adenocarcinoma clinical outcome and sensitivity to E2F inhibitors, but not for the response to cytotoxic-based treatments. *Scientific Reports*, *8*(1). https://doi.org/10.1038/s41598-018-26613-z

Lapointe, J., Li, C., Higgins, J. P., van de Rijn, M., Bair, E., Montgomery, K., Ferrari, M., Egevad, L., Rayford, W., Bergerheim, U., Ekman, P., DeMarzo, A. M., Tibshirani, R., Botstein, D., Brown, P. O., Brooks, J. D., & Pollack, J. R. (2004). Gene expression profiling identifies clinically relevant subtypes of prostate cancer. *Proceedings of the National Academy of Sciences*, *101*(3). https://doi.org/10.1073/pnas.0304146101

Laresgoiti, U., Apraiz, A., Olea, M., Mitxelena, J., Osinalde, N., Rodriguez, J. A., Fullaondo, A., & Zubiaga, A. M. (2013). E2F2 and CREB cooperatively regulate transcriptional activity of cell cycle genes. *Nucleic Acids Research*, *41*(22). https://doi.org/10.1093/nar/gkt821

Lea, N. C., Orr, S. J., Stoeber, K., Williams, G. H., Lam, E. W.-F., Ibrahim, M. A. A., Mufti, G. J., & Thomas, N. S. B. (2003). Commitment Point during $G_0 \rightarrow G_1$ That Controls Entry into the Cell Cycle. *Molecular and Cellular Biology*, *23*(7). https://doi.org/10.1128/MCB.23.7.2351-2361.2003

Liang, J. T., Huang, K. C., Cheng, Y. M., Hsu, H. C., Cheng, A. L., Hsu, C. H., Yeh, K. H., Wang, S. M., & Chang, K. J. (2002). P53 overexpression predicts poor chemosensitivity to high-dose 5-fluorouracil plus leucovorin chemotherapy for stage IV colorectal cancers after palliative bowel resection. *International Journal of Cancer*, *97*(4). https://doi.org/10.1002/ijc.1637

Libertini, S. J., Tepper, C. G., Guadalupe, M., Lu, Y., Asmuth, D. M., & Mudryj, M. (2006). E2F1 expression in LNCaP prostate cancer cells deregulates androgen dependent growth, suppresses differentiation, and enhances apoptosis. *The Prostate*, *66*(1). https://doi.org/10.1002/pros.20314

Li, F. X., Zhu, J. W., Tessem, J. S., Beilke, J., Varella-Garcia, M., Jensen, J., Hogan, C. J., & Degregori, J. (2003). *The development of diabetes in E2f1E2f2 mutant mice reveals important roles for bone marrow-derived cells in preventing islet cell loss*. *Proceedings of the National Academy of Sciences of the United States of America, 100*(22). https://doi.org/10.1073/pnas.2231861100

Ligabue, A., Marverti, G., Liebl, U., & Myllykallio, H. (2012). Transcriptional Activation and Cell Cycle Block Are the Keys for 5-Fluorouracil Induced Up-Regulation of Human Thymidylate Synthase Expression. *Plos One*, *7*(10). https://doi.org/10.1371/journal.pone.0047318

Lim, C. B., Zhang, D., & Lee, C. G. (2006). FAT 10, a gene up-regulated in various cancers, is cell-cycle regulated. *Cell Division*, *1*(1). https://doi.org/10.1186/1747-1028-1-20

Lim, J. T. E., Mansukhani, M., & Weinstein, I. B. (2005). Cyclin-dependent kinase 6 associates with the androgen receptor and enhances its transcriptional activity in prostate cancer cells. *Proceedings of the National Academy of Sciences*, *102*(14). https://doi.org/10.1073/pnas.0501203102

Lin, Y. L., & Pasero, P. (2021). Replication stress: from chromatin to immunity and beyond. *Current Opinion in Genetics & Development*, *71*. https://doi.org/10.1016/j.gde.2021.08.004

Liontos, M., Koutsami, M., Sideridou, M., Evangelou, K., Kletsas, D., Levy, B., Kotsinas, A., Nahum, O., Zoumpourlis, V., Kouloukoussa, M., Lygerou, Z., Taraviras, S., Kittas, C., Bartkova, J., Papavassiliou, A. G., Bartek, J., Halazonetis, T. D., & Gorgoulis, V. G. (2007). Deregulated overexpression of hCdt1 and hCdc6 promotes malignant behavior. *Cancer Research*, *67*(22). https://doi.org/10.1158/0008-5472.CAN-07-2837

Liu, X., Lai, L., Wang, X., Xue, L., Leora, S., Wu, J., Hu, S., Zhang, K., Kuo, M. L., Zhou, L., Zhang, H., Wang, Y., Wang, Y., Zhou, B., Nelson, R. A., Zheng, S., Zhang, S., Chu, P., & Yen, Y. (2011). Ribonucleotide Reductase Small Subunit M2B Prognoses Better Survival in Colorectal Cancer. *Cancer Research*, *71*(9). https://doi.org/10.1158/0008-5472.CAN-11-0054

Longley, D. B., Harkin, D. P., & Johnston, P. G. (2003). 5-Fluorouracil: mechanisms of action and clinical strategies. *Nature Reviews Cancer*, *3*(5). https://doi.org/10.1038/nrc1074

Lopez-Contreras, A. J., Specks, J., Barlow, J. H., Ambrogio, C., Desler, C., Vikingsson, S., Rodrigo-Perez, S., Green, H., Rasmussen, L. J., Murga, M., Nussenzweig, A., & Fernandez-Capetillo, O. (2015). Increased Rrm2 gene dosage reduces fragile site breakage and prolongs survival of ATR mutant mice. *Genes & Development*. 29(7). https://doi.org/10.1101/gad.256958

Luengo, A., Gui, D. Y., & vander Heiden, M. G. (2017). Targeting Metabolism for Cancer Therapy. *Cell Chemical Biology*, *24*(9). https://doi.org/10.1016/j.chembiol.2017.08.028

Lv, Y., Xiao, J., Liu, J., & Xing, F. (2017). E2F8 is a Potential Therapeutic Target for Hepatocellular Carcinoma. *Journal of Cancer*, *8*(7). https://doi.org/10.7150/jca.18255

Lyssiotis, C. A., & Cantley, L. C. (2013). Metabolic syndrome: F stands for fructose and fat. *Nature*, *502*(7470). https://doi.org/10.1038/502181a

MacDougall, C. A., Byun, T. S., Van, C., Yee, M., & Cimprich, K. A. (2007). The structural determinants of checkpoint activation. *Genes & Development*, *21*(8). https://doi.org/10.1101/gad.1522607

Ma, J., Zhong, M., Xiong, Y., Gao, Z., Wu, Z., Liu, Y., & Hong, X. (2021). Emerging roles of nucleotide metabolism in cancer development: progress and prospect. *Aging*, *13*(9). https://doi.org/10.18632/aging.202962

Malumbres, M. (2014). Cyclin-dependent kinases. *Genome Biology*, *15*(6). https://doi.org/10.1186/gb4184

Mannava, S., Moparthy, K. C., Wheeler, L. J., Leonova, K. I., Wawrzyniak, J. A., Bianchi-Smiraglia, A., Berman, A. E., Flanagan, S., Shewach, D. S., Zeitouni, N. C., Gudkov, A. v., Mathews, C. K., & Nikiforov, M. A. (2012). Ribonucleotide reductase and thymidylate synthase or exogenous deoxyribonucleosides reduce DNA damage and senescence caused by C-MYC depletion. *Aging*, *4*(12). https://doi.org/10.18632/aging.100512

Mannava, S., Moparthy, K. C., Wheeler, L. J., Natarajan, V., Zucker, S. N., Fink, E. E., Im, M., Flanagan, S., Burhans, W. C., Zeitouni, N. C., Shewach, D. S., Mathews, C. K., & Nikiforov,

M. A. (2013). Depletion of Deoxyribonucleotide Pools Is an Endogenous Source of DNA Damage in Cells Undergoing Oncogene-Induced Senescence. *The American Journal of Pathology*, *182*(1). https://doi.org/10.1016/j.ajpath.2012.09.011

Manning, A. L., & Dyson, N. J. (2012). RB: Mitotic implications of a tumour suppressor. *Nature Reviews Cancer, 12*(3). https://doi.org/10.1038/nrc3216

Manogue, C., Ledet, E., Guddati, A. K., Lewis, B., & Sartor, O. (2018). Extreme Prostate-Specific Antigen Response to Infusional 5-Flourouracil in Castrate-Resistant Prostate Cancer. *The Oncologist*, *23*(3). https://doi.org/10.1634/theoncologist.2017-0450

Mathews, C. K. (2006). DNA precursor metabolism and genomic stability. *The FASEB Journal*, *20*(9). https://doi.org/10.1096/fj.06-5730rev

Matsuoka, S., Ballif, B. A., Smogorzewska, A., McDonald, E. R., Hurov, K. E., Luo, J., Bakalarski, C. E., Zhao, Z., Solimini, N., Lerenthal, Y., Shiloh, Y., Gygi, S. P., & Elledge, S. J. (2007). ATM and ATR Substrate Analysis Reveals Extensive Protein Networks Responsive to DNA Damage. *Science*, *316*(5828). https://doi.org/10.1126/science.1140321

Matthews, H. K., Bertoli, C., & de Bruin, R. A. M. (2022). Cell cycle control in cancer. *Nature Reviews Molecular Cell Biology*, *23*(1). https://doi.org/10.1038/s41580-021-00404-3

McMurray, C. T. (2010). Mechanisms of trinucleotide repeat instability during human development. *Nature Reviews. Genetics*, *11*(11). https://doi.org/10.1038/nrg2828

Melamed, J., Einhorn, J. M., & Ittmann, M. M. (1997). Allelic loss on chromosome 13q in human prostate carcinoma. *Clinical Cancer Research. 3(10):1867-72*. PMID: 9815575

Mitxelena, J., Apraiz, A., Vallejo-Rodríguez, J., Malumbres, M., & Zubiaga, A. M. (2016). E2F7 regulates transcription and maturation of multiple microRNAs to restrain cell proliferation. *Nucleic Acids Research*, *44*(12). https://doi.org/10.1093/nar/gkw146

Moffatt, B. A., & Ashihara, H. (2002). Purine and Pyrimidine Nucleotide Synthesis and Metabolism. *The Arabidopsis Book*, *1*. https://doi.org/10.1199/tab.0018

Morikawa, T., Maeda, D., Kume, H., Homma, Y., & Fukayama, M. (2010). Ribonucleotide reductase M2 subunit is a novel diagnostic marker and a potential therapeutic target in bladder cancer. *Histopathology*, *57*(6). https://doi.org/10.1111/j.1365-2559.2010.03725.x

Morrissey, C., & Vessella, R. L. (2007). The role of tumor microenvironment in prostate cancer bone metastasis. *Journal of Cellular Biochemistry*, *101*(4). https://doi.org/10.1002/jcb.21214

Müller, H., & Helin, K. (2000). The E2F transcription factors: key regulators of cell proliferation. *Biochimica et Biophysica Acta (BBA) - Reviews on Cancer*, *1470*(1). https://doi.org/10.1016/S0304-419X(99)00030-X

Murga, M., Fernández-Capetillo, O., Field, S. J., Moreno, B., R.-Borlado, L., Fujiwara, Y., Balomenos, D., Vicario, A., Carrera, A. C., Orkin, S. H., Greenberg, M. E., & Zubiaga, A. M. (2001a). Mutation of E2F2 in Mice Causes Enhanced T Lymphocyte Proliferation, Leading to the Development of Autoimmunity. *Immunity*, *15*(6). https://doi.org/10.1016/S1074-7613(01)00254-0

Murga, M., Bunting, S., Montaña, M. F., Soria, R., Mulero, F., Cañamero, M., Lee, Y., McKinnon, P. J., Nussenzweig, A., & Fernandez-Capetillo, O. (2009) A mouse model of ATR-Seckel shows embryonic replicative stress and accelerated aging. *Nature Genetics, 41*(8). https://doi.org/ 10.1038/ng.420.

Nagy, Á., Munkácsy, G., & Győrffy, B. (2021). Pancancer survival analysis of cancer hallmark genes. *Scientific Reports*, *11*(1). https://doi.org/10.1038/s41598-021-84787-5

Narasimha, A. M., Kaulich, M., Shapiro, G. S., Choi, Y. J., Sicinski, P., & Dowdy, S. F. (2014). Cyclin D activates the Rb tumor suppressor by mono-phosphorylation. *eLife*, *3*. https://doi.org/10.7554/eLife.02872

Nathanson, D. A., Armijo, A. L., Tom, M., Li, Z., Dimitrova, E., Austin, W. R., Nomme, J., Campbell, D. O., Ta, L., Le, T. M., Lee, J. T., Darvish, R., Gordin, A., Wei, L., Liao, H.-I., Wilks, M., Martin, C., Sadeghi, S., Murphy, J. M., … Radu, C. G. (2014). Co-targeting of convergent nucleotide biosynthetic pathways for leukemia eradication. *Journal of Experimental Medicine*, *211*(3). https://doi.org/10.1084/jem.20131738

Nevins, J. R. (2001). The Rb/E2F pathway and cancer. *Human Molecular Genetics*, *10*(7). https://doi.org/10.1093/hmg/10.7.699

O'Brien, N., Conklin, D., Beckmann, R., Luo, T., Chau, K., Thomas, J., Mc Nulty, A., Marchal, C., Kalous, O., von Euw, E., Hurvitz, S., Mockbee, C., & Slamon, D. J. (2018). Preclinical Activity of Abemaciclib Alone or in Combination with Antimitotic and Targeted Therapies in Breast Cancer. *Molecular Cancer Therapeutics*, *17*(5). https://doi.org/10.1158/1535-7163.MCT-17-0290

Ogris, E., Rotheneder, H., Mudrak, I., Pichler, A., & Wintersberger, E. (1993). A binding site for transcription factor E2F is a target for trans activation of murine thymidine kinase by polyomavirus large T antigen and plays an important role in growth regulation of the gene. *Journal of Virology*, *67*(4). https://doi.org/10.1128/jvi.67.4.1765-1771.1993

Ogrodzinski, M. P., Teoh, S. T., & Lunt, S. Y. (2021). Targeting Subtype-Specific Metabolic Preferences in Nucleotide Biosynthesis Inhibits Tumor Growth in a Breast Cancer Model. *Cancer Research*, *81*(2). https://doi.org/10.1158/0008-5472.CAN-20-1666

Paakinaho, V., Swinstead, E. E., Presman, D. M., Grøntved, L., & Hager, G. L. (2019). Meta-analysis of Chromatin Programming by Steroid Receptors. *Cell Reports*, *28*(13). https://doi.org/10.1016/j.celrep.2019.08.039

Paeschke, K., Bochman, M. L., Garcia, P. D., Cejka, P., Friedman, K. L., Kowalczykowski, S. C., & Zakian, V. A. (2013). Pif1 family helicases suppress genome instability at G-quadruplex motifs. *Nature*, *497*(7450). https://doi.org/10.1038/nature12149

Park, S. R., Namkoong, S., Friesen, L., Cho, C.-S., Zhang, Z. Z., Chen, Y.-C., Yoon, E., Kim, C. H., Kwak, H., Kang, H. M., & Lee, J. H. (2020). Single-Cell Transcriptome Analysis of Colon Cancer Cell Response to 5-Fluorouracil-Induced DNA Damage. *Cell Reports*, *32*(8). https://doi.org/10.1016/j.celrep.2020.108077

Pennycook, B. R., & Barr, A. R. (2020). Restriction point regulation at the crossroads between quiescence and cell proliferation. *FEBS Letters*, *594*(13). https://doi.org/10.1002/1873-3468.13867

Phillips, S., Barton, C., Lee, S., Morton, D., Wallace, D., Lemoine, N., & Neoptolemos, J. (1994). Loss of the retinoblastoma susceptibility gene (RB1) is a frequent and early event in prostatic tumorigenesis. *British Journal of Cancer*, *70*(6). https://doi.org/10.1038/bjc.1994.482

Plentz, R. R., Manns, M. P., & Greten, T. F. (2010). Molecular therapy of pancreatic cancer. *Minerva Endocrinologica*, *35(1):27-33.* PMID: 20386525

Polager, S., Kalma, Y., Berkovich, E., & Ginsberg, D. (2002). E2Fs up-regulate expression of genes involved in DNA replication, DNA repair and mitosis. *Oncogene*, *21*(3). https://doi.org/10.1038/sj.onc.1205102

Poppy Roworth, A., Ghari, F., & la Thangue, N. B. (2015). To live or let die–complexity within the E2F1 pathway. *Molecular and Cellular Oncology,* *2*(1). https://doi.org/10.4161/23723548.2014.970480

Pusapati, R. v, Weaks, R. L., Rounbehler, R. J., McArthur, M. J., & Johnson, D. G. (2010). E2F2 suppresses Myc-induced proliferation and tumorigenesis. *Molecular Carcinogenesis*, *49*(2). https://doi.org/10.1002/mc.20584

Radivoyevitch, T., Saunthararajah, Y., Pink, J., Ferris, G., Lent, I., Jackson, M., Junk, D., & Kunos, C. (2012a). dNTP Supply Gene Expression Patterns after P53 Loss. *Cancers*, *4*(4). https://doi.org/10.3390/cancers4041212

Rajeshkumar, N. V., de Oliveira, E., Ottenhof, N., Watters, J., Brooks, D., Demuth, T., Shumway, S. D., Mizuarai, S., Hirai, H., Maitra, A., & Hidalgo, M. (2011). MK-1775, a Potent Wee1 Inhibitor, Synergizes with Gemcitabine to Achieve Tumor Regressions, Selectively in p53-Deficient Pancreatic Cancer Xenografts. *Clinical Cancer Research*, *17*(9). https://doi.org/10.1158/1078-0432.CCR-10-2580

Rather, G. M., Anyanwu, M., Minko, T., Garbuzenko, O., Szekely, Z., & Bertino, J. R. (2021). Anti-Tumor Effects of a Penetratin Peptide Targeting Transcription of E2F-1, 2 and 3a is enhanced When Used in Combination with Pemetrexed or Cisplatin. *Cancers*, *13*(5). https://doi.org/10.3390/cancers13050972

Raub, T. J., Wishart, G. N., Kulanthaivel, P., Staton, B. A., Ajamie, R. T., Sawada, G. A., Gelbert, L. M., Shannon, H. E., Sanchez-Martinez, C., & de Dios, A. (2015). Brain Exposure of Two Selective Dual CDK4 and CDK6 Inhibitors and the Antitumor Activity of CDK4 and CDK6 Inhibition in Combination with Temozolomide in an Intracranial Glioblastoma Xenograft. *Drug Metabolism and Disposition*, *43*(9). https://doi.org/10.1124/dmd.114.062745

Reichard, P. (1988). INTERACTIONS BETWEEN DEOXYRIBONUCLEOTIDE AND DNA SYNTHESIS. *Annual Review of Biochemistry*, *57*(1). https://doi.org/10.1146/annurev.bi.57.070188.002025

Ren, B., Cam, H., Takahashi, Y., Volkert, T., Terragni, J., Young, R. A., & Dynlacht, B. D. (2002). E2F integrates cell cycle progression with DNA repair, replication, and G $_2$ /M checkpoints. *Genes & Development*, *16*(2). https://doi.org/10.1101/gad.949802

Ren, Z., Kang, W., Wang, L., Sun, B., Ma, J., Zheng, C., Sun, J., Tian, Z., Yang, X., & Xiao, W. (2014). E2F1 renders prostate cancer cell resistant to ICAM-1 mediated antitumor immunity by NF-κB modulation. *Molecular Cancer*, *13*(1). https://doi.org/10.1186/1476-4598-13-84

Roberts, P. J., Kumarasamy, V., Witkiewicz, A. K., & Knudsen, E. S. (2020). Chemotherapy and CDK4/6 Inhibitors: Unexpected Bedfellows. *Molecular Cancer Therapeutics*, *19*(8). https://doi.org/10.1158/1535-7163.MCT-18-1161

Roberts, S. G., Blute, M. L., Bergstralh, E. J., Slezak, J. M., & Zincke, H. (2001). PSA Doubling Time as a Predictor of Clinical Progression After Biochemical Failure Following Radical Prostatectomy for Prostate Cancer. *Mayo Clinic Proceedings*, *76*(6). https://doi.org/10.4065/76.6.576

Rubin, S. M., Sage, J., & Skotheim, J. M. (2020). Integrating Old and New Paradigms of G1/S Control. *Molecular Cell*, *80*(2). https://doi.org/10.1016/j.molcel.2020.08.020

Sabatinos, S. A. (2010). Recovering a Stalled Replication Fork. *Nature Education, 3(9):31*

Sabini, E., Hazra, S., Ort, S., Konrad, M., & Lavie, A. (2008). Structural Basis for Substrate Promiscuity of dCK. *Journal of Molecular Biology*, *378*(3). https://doi.org/10.1016/j.jmb.2008.02.061

Sabini, J., Siepmann, M., & Stein, J. (2001). Target Article: "The Really Fundamental Attribution Error in Social Psychological Research." *Psychological Inquiry*, *12*(1). https://doi.org/10.1207/S15327965PLI1201_01

Salvador-Barbero, B., Álvarez-Fernández, M., Zapatero-Solana, E., el Bakkali, A., Menéndez, M. del C., López-Casas, P. P., di Domenico, T., Xie, T., VanArsdale, T., Shields, D. J., Hidalgo, M., & Malumbres, M. (2020). CDK4/6 Inhibitors Impair Recovery from Cytotoxic Chemotherapy in Pancreatic Adenocarcinoma. *Cancer Cell*, *37*(3). https://doi.org/10.1016/j.ccell.2020.01.007

Sandelin, A., Wasserman, W. W., & Lenhard, B. (2004). ConSite: web-based prediction of regulatory elements using cross-species comparison. *Nucleic Acids Research*, *32* (Web Server issue):W249-52. https://doi.org/10.1093/nar/gkh372

Sausville, E., Lorusso, P., Carducci, M., Carter, J., Quinn, M. F., Malburg, L., Azad, N., Cosgrove, D., Knight, R., Barker, P., Zabludoff, S., Agbo, F., Oakes, P., & Senderowicz, A. (2014). Phase I dose-escalation study of AZD7762, a checkpoint kinase inhibitor, in combination with gemcitabine in US patients with advanced solid tumors. *Cancer Chemotherapy and Pharmacology*, *73*(3). https://doi.org/10.1007/s00280-014-2380-5

Scheijen, B., Bronk, M., van der Meer, T., de Jong, D., & Bernards, R. (2004). High incidence of thymic epithelial tumors in E2F2 transgenic mice. *The Journal of Biological Chemistry*, *279*(11). https://doi.org/10.1074/jbc.M313682200

Schvartzman, J. M., Duijf, P. H. G., Sotillo, R., Coker, C., & Benezra, R. (2011). Mad2 is a critical mediator of the chromosome instability observed upon Rb and p53 pathway inhibition. *Cancer Cell*, *19*(6), 701–714. https://doi.org/10.1016/j.ccr.2011.04.017

Sethy, C., & Kundu, C. N. (2021). 5-Fluorouracil (5-FU) resistance and the new strategy to enhance the sensitivity against cancer: Implication of DNA repair inhibition. *Biomedicine & Pharmacotherapy*, *137*. https://doi.org/10.1016/j.biopha.2021.111285

Shimizu, I., Yoshida, Y., Suda, M., & Minamino, T. (2014). DNA damage response and metabolic disease. *Cell Metabolism, 20*(6). https://doi.org/10.1016/j.cmet.2014.10.008

Simon, R. (2005). Bioinformatics in cancer therapeutics—hype or hope? *Nature Clinical Practice Oncology*, *2*(5). https://doi.org/10.1038/ncponc0176

Sørensen, C. S., Hansen, L. T., Dziegielewski, J., Syljuåsen, R. G., Lundin, C., Bartek, J., & Helleday, T. (2005). The cell-cycle checkpoint kinase Chk1 is required for mammalian homologous recombination repair. *Nature Cell Biology*, *7*(2). https://doi.org/10.1038/ncb1212

Sørensen, C. S., & Syljuåsen, R. G. (2012). Safeguarding genome integrity: the checkpoint kinases ATR, CHK1 and WEE1 restrain CDK activity during normal DNA replication. *Nucleic Acids Research*, *40*(2). https://doi.org/10.1093/nar/gkr697

Sotillo, R., Schvartzman, J.-M., Socci, N. D., & Benezra, R. (2010). Mad2-induced chromosome instability leads to lung tumour relapse after oncogene withdrawal. *Nature*, *464*(7287). https://doi.org/10.1038/nature08803

Srinivasan, S. v, Dominguez-Sola, D., Wang, L. C., Hyrien, O., & Gautier, J. (2013). Cdc45 is a critical effector of myc-dependent DNA replication stress. *Cell Reports*, *3*(5). https://doi.org/10.1016/j.celrep.2013.04.002

Stice, J. P., Wardell, S. E., Norris, J. D., Yllanes, A. P., Alley, H. M., Haney, V. O., White, H. S., Safi, R., Winter, P. S., Cocce, K. J., Kishton, R. J., Lawrence, S. A., Strum, J. C., & McDonnell, D.

P. (2017). CDK4/6 Therapeutic Intervention and Viable Alternative to Taxanes in CRPC. *Molecular Cancer Research*, *15*(6). https://doi.org/10.1158/1541-7786.MCR-17-0028

Stope, M. (2021). Phosphorylation of histone H2A.X as a DNA-associated biomarker (Review). *World Academy of Sciences Journal*, *3*(3). https://doi.org/10.3892/wasj.2021.102

Sulzyc-Bielicka, V., Domagala, P., Bielicki, D., Safranow, K., & Domagala, W. (2014). Thymidylate synthase expression and p21WAF1/p53 phenotype of colon cancers identify patients who may benefit from 5-fluorouracil based therapy. *Cellular Oncology*, *37*(1). https://doi.org/10.1007/s13402-013-0159-z

Sulzyc-Bielicka, V., Domagala, P., Bielicki, D., Safranow, K., Rogowski, W., & Domagala, W. (2016a). E2F1/TS Immunophenotype and Survival of Patients with Colorectal Cancer Treated with 5FU-Based Adjuvant Therapy. *Pathology & Oncology Research*, *22*(3). https://doi.org/10.1007/s12253-016-0043-z

Szmyd, R., Niska-Blakie, J., Diril, M. K., Renck Nunes, P., Tzelepis, K., Lacroix, A., van Hul, N., Deng, L.-W., Matos, J., Dreesen, O., Bisteau, X., & Kaldis, P. (2019). Premature activation of Cdk1 leads to mitotic events in S phase and embryonic lethality. *Oncogene*, *38*(7). https://doi.org/10.1038/s41388-018-0464-0

Teixeira, L. K., Wang, X., Li, Y., Ekholm-Reed, S., Wu, X., Wang, P., & Reed, S. I. (2015). Cyclin e deregulation promotes loss of specific genomic regions. *Current Biology*, *25*(10), 1327–1333. https://doi.org/10.1016/j.cub.2015.03.022

Tort, F., Bartkova, J., Sehested, M., Ørntoft, T., Lukas, J., & Bartek, J. (2006). Retinoblastoma Pathway Defects Show Differential Ability to Activate the Constitutive DNA Damage Response in Human Tumorigenesis. *Cancer Research*, *66*(21). https://doi.org/10.1158/0008-5472.CAN-06-2178

Toy, G., Austin, W. R., Liao, H.-I., Cheng, D., Singh, A., Campbell, D. O., Ishikawa, T., Lehmann, L. W., Satyamurthy, N., Phelps, M. E., Herschman, H. R., Czernin, J., Witte, O. N., & Radu, C. G. (2010). Requirement for deoxycytidine kinase in T and B lymphocyte development. *Proceedings of the National Academy of Sciences*, *107*(12). https://doi.org/10.1073/pnas.0913900107

Trimarchi, J. M., & Lees, J. A. (2002a). Sibling rivalry in the E2F family. *Nature Reviews Molecular Cell Biology*, *3*(1). https://doi.org/10.1038/nrm714

Vaidyanathan, S., Cato, K., Tang, L., Pavey, S., Haass, N. K., Gabrielli, B. G., & Duijf, P. H. G. (2016). In vivo overexpression of Emi1 promotes chromosome instability and tumorigenesis. *Oncogene*, *35*(41). https://doi.org/10.1038/onc.2016.94

Varghese, B., Chen, F., Hwang, D., Palmer, S. L., de Castro Abreu, A. L., Ukimura, O., Aron, M., Aron, M., Gill, I., Duddalwar, V., & Pandey, G. (2019). Objective risk stratification of prostate cancer using machine learning and radiomics applied to multiparametric

magnetic resonance images. *Scientific Reports*, *9*(1). https://doi.org/10.1038/s41598-018-38381-x

Varghese, V., Magnani, L., Harada-Shoji, N., Mauri, F., Szydlo, R. M., Yao, S., Lam, E. W.-F., & Kenny, L. M. (2019). FOXM1 modulates 5-FU resistance in colorectal cancer through regulating TYMS expression. *Scientific Reports*, *9*(1). https://doi.org/10.1038/s41598-018-38017-0

Vassilev, A., Lee, C. Y., Vassilev, B., Zhu, W., Ormanoglu, P., Martin, S. E., & Depamphilis, M. L. (2016). Identification of genes that are essential to restrict genome duplication to once per cell division.,*Oncotarget 7*(23). https://doi.org/10.18632/oncotarget.9008

Vernell, R., Helin, K., & Müller, H. (2003). Identification of Target Genes of the p16INK4A-pRB-E2F Pathway. *Journal of Biological Chemistry*, *278*(46). https://doi.org/10.1074/jbc.M304930200

Villa, E., Ali, E., Sahu, U., & Ben-Sahra, I. (2019a). Cancer Cells Tune the Signaling Pathways to Empower de Novo Synthesis of Nucleotides. *Cancers*, *11*(5). https://doi.org/10.3390/cancers11050688

Virgo, K. S., Rumble, R. B., de Wit, R., Mendelson, D. S., Smith, T. J., Taplin, M.-E., Wade, J. L., Bennett, C. L., Scher, H. I., Nguyen, P. L., Gleave, M., Morgan, S. C., Loblaw, A., Sachdev, S., Graham, D. L., Vapiwala, N., Sion, A. M., Simons, V. H., & Talcott, J. (2021). Initial Management of Noncastrate Advanced, Recurrent, or Metastatic Prostate Cancer: ASCO Guideline Update. *Journal of Clinical Oncology*, *39*(11). https://doi.org/10.1200/JCO.20.03256

Wang, L.-M., Lu, F.-F., Zhang, S.-Y., Yao, R.-Y., Xing, X.-M., & Wei, Z.-M. (2012). Overexpression of catalytic subunit M2 in patients with ovarian cancer. *Chinese Medical Journal*, *125*(12). PMID: 22884145

Weinberg, R. A. (1995a). The retinoblastoma protein and cell cycle control. *Cell*, *81*(3). https://doi.org/10.1016/0092-8674(95)90385-2

Weinmann, A. S., Bartley, S. M., Zhang, T., Zhang, M. Q., & Farnham, P. J. (2001). Use of Chromatin Immunoprecipitation To Clone Novel E2F Target Promoters. *Molecular and Cellular Biology*, *21*(20). https://doi.org/10.1128/MCB.21.20.6820-6832.2001

Weinmann, A. S., Yan, P. S., Oberley, M. J., Huang, T. H.-M., & Farnham, P. J. (2002). Isolating human transcription factor targets by coupling chromatin immunoprecipitation and CpG island microarray analysis. *Genes & Development*, *16*(2). https://doi.org/10.1101/gad.943102

Woodman, P. W., Sarrif, A. M., & Heidelberger, C. (1980). Specificity of pyrimidine nucleoside phosphorylases and the phosphorolysis of 5-fluoro-2'-deoxyuridine. *Cancer Research*, *40(3):507-11.* PMID: 6451286

Xu, Y. Z., Huang, P., & Plunkett, W. (1995). Functional compartmentation of dCTP pools. Preferential utilization of salvaged deoxycytidine for DNA repair in human lymphoblasts. *The Journal of Biological Chemistry*, *270(2):631-7* PMID: 7822289

Yadav, M., Kumar, R., & Krishnamurthy, R. (2020). Chemistry of Abiotic Nucleotide Synthesis. *Chemical Reviews, 120*(11). https://doi.org/10.1021/acs.chemrev.9b00546

Yagoda, A., & Petrylak, D. (1993). Cytotoxic chemotherapy for advanced hormone-resistant prostate cancer. *Cancer*, *71*(3). https://doi.org/10.1002/1097-0142(19930201)71:3+<1098::aid-cncr2820711432>3.0.co;2-g

Yamasaki, L., Jacks, T., Bronson, R., Goillot, E., Harlow, E., & Dyson, N. J. (1996). Tumor Induction and Tissue Atrophy in Mice Lacking E2F-1. *Cell*, *85*(4). https://doi.org/10.1016/S0092-8674(00)81254-4

Yao, G., Lee, T. J., Mori, S., Nevins, J. R., & You, L. (2008). A bistable Rb-E2F switch underlies the restriction point. *Nature Cell Biology*, *10*(4). https://doi.org/10.1038/ncb1711

Yee, L. K., Chu, E., Pan, B., Chu, S.-H., Chen, T., Lipsky, M. H., Chu, M. Y. W., & Calabresi, P. (1998). Benzylacyclouridine Enhances 5-Fluorouracil Cytotoxicity against Human Prostate Cancer Cell Lines. *Pharmacology*, *56*(2). https://doi.org/10.1159/000028185

Young, A. P., Nagarajan, R., & Longmore, G. D. (2003). Mechanisms of transcriptional regulation by Rb-E2F segregate by biological pathway. *Oncogene*, *22*(46). https://doi.org/10.1038/sj.onc.1206804

Zeman, M. K., & Cimprich, K. A. (2014a). Causes and consequences of replication stress. In *Nature Cell Biology*, *16* (1). https://doi.org/10.1038/ncb2897

Zeng, Z., Cao, Z., & Tang, Y. (2020). Increased E2F2 predicts poor prognosis in patients with HCC based on TCGA data. *BMC Cancer*, *20*(1). https://doi.org/10.1186/s12885-020-07529-2

Zhang, Y.-W., Jones, T. L., Martin, S. E., Caplen, N. J., & Pommier, Y. (2009). Implication of Checkpoint Kinase-dependent Up-regulation of Ribonucleotide Reductase R2 in DNA Damage Response. *Journal of Biological Chemistry*, *284*(27). https://doi.org/10.1074/jbc.M109.003020

Zhao, F. J., Zhang, S., Yu, Z. M., Xia, S. J. & Li, H. (2009). Specific targeting of prostate cancer cells in vitro by the suicide gene/prodrug system, uracil phosphoribosyltransferase/5-fluorouracil, under the control of prostate-specific membrane antigen promoter/enhancer. *Prostate Cancer and Prostatic disease, 12*(2). https://doi.org/10.1038/pcan.2008.39

Zheng, C., Ren, Z., Wang, H., Zhang, W., Kalvakolanu, D. v., Tian, Z., & Xiao, W. (2009). E2F1 Induces Tumor Cell Survival via Nuclear Factor-κB–Dependent Induction of EGR1 Transcription in Prostate Cancer Cells. *Cancer Research*, *69*(6). https://doi.org/10.1158/0008-5472.CAN-08-4113

Zhou, B.-B. S., & Elledge, S. J. (2000). The DNA damage response: putting checkpoints in perspective. *Nature*, *408*(6811). https://doi.org/10.1038/35044005

Zhu, H., Guo, W., Zhang, L., Davis, J. J., Teraishi, F., Wu, S., Cao, X., Daniel, J., Smythe, W. R., & Fang, B. (2005). Bcl-XL small interfering RNA suppresses the proliferation of 5-fluorouracil-resistant human colon cancer cells. *Molecular Cancer Therapeutics*, *4*(3). https://doi.org/10.1158/1535-7163.MCT-04-0162

Zhu, J. W., Field, S. J., Gore, L., Thompson, M., Yang, H., Fujiwara, Y., Cardiff, R. D., Greenberg, M., Orkin, S. H., & DeGregori, J. (2001). E2F1 and E2F2 Determine Thresholds for Antigen-Induced T-Cell Proliferation and Suppress Tumorigenesis. *Molecular and Cellular Biology*, *21*(24). https://doi.org/10.1128/MCB.21.24.8547-8564.2001